CARBONIC ANHYDRASES AND BICARBONATE TRANSPORT IN LARVAL MOSQUITOES

By

THERESA J. SERON

A DISSERTATION PRESENTED TO THE GRADUATE SCHOOL
OF THE UNIVERSITY OF FLORIDA IN PARTIAL FULFILLMENT
OF THE REQUIREMENTS FOR THE DEGREE OF
DOCTOR OF PHILOSOPHY

UNIVERSITY OF FLORIDA

2004

Copyright 2004

by

Theresa J. Seron

DEDICATION

I wish to dedicate this dissertation to my incredible family, Mom, Dad, Grandparents, Tracey, and George. My family has witnessed my struggles and triumphs and has helped me through it all. I am so proud to call them my family. I cannot thank them enough for all of their support. This achievement is really a reflection of all of us.

I also want to dedicate this milestone to my soon to be husband, Dr. Peter Lovell. Coming home to his love, humor, and music, has given me true joy. My family would be incomplete if I did not mention our furry companions, Frodo and Princess, who remind us that a nap can solve most problems.

ACKNOWLEDGEMENTS

I would like to acknowledge my dissertation committee, Dr. Paul J. Linser, Dr. Edward J. Phlips, Dr. Leonid Moroz, Dr. Robert Greenberg, and Dr. Shirley Baker, for their suggestions and comments on the final rewriting of this document. I want to thank my project supervisor, Dr. Paul J. Linser, for allowing me to form my own project goals and the space to tackle them.

There are a number of people at The Whitney Laboratory who I would like to thank for their assistance with this dissertation project as well as their friendship. Dr. Judith Ochrietor devoted her time and energy to improving every aspect of this dissertation. Judy assisted me with experimental designs, introduced me to real time PCR, provided a wealth of knowledge about molecular biology, and was a great person with which to share a laboratory and office. Dr. Andrea Kohn provided molecular biology teaching and advice along with being a fantastic person to work with and be inspired by. Leslie vanEkeris taught me how to do mosquito dissections and provided many of the mosquito guts that I photographed for this document. Dr. Bill Harvey provided insight into the ionic transport mechanisms of the mosquito and the editing of this manuscript. Dr. Dmitri Boudko was instrumental in the expression of the anion exchanger and the production of amplified cDNA libraries. Jessica Roberts-Misterly and Dr. Robert Greenberg also provided teachings and suggestions in cloning cDNAs from the mosquito.

TABLE OF CONTENTS

page

LIST OF TABLES

LIST OF FIGURES

Abstract of Dissertation Presented to the Graduate School
of the University of Florida in Partial Fulfillment of the
Requirements for the Degree of Doctor of Philosophy

CARBONIC ANHYDRASES AND BICARBONATE TRANSPORT IN LARVAL MOSQUITOES

By

Theresa J. Seron

May 2004

Chair: Edward J. Phlips
Cochair: Paul J. Linser
Major Department: Fisheries and Aquatic Sciences

Carbonic anhydrase (CA) is an important enzyme due to its involvement in many pH-dependent, physiological processes. CA reversibly converts CO_2 and H_2O into bicarbonate and a proton. The anterior midgut lumen of the larval mosquito has an extremely alkaline pH; therefore, we hypothesized that an active CA within the epithelial cells surrounding this region would rapidly produce bicarbonate to buffer the high pH. A cDNA cloning strategy, followed by *in situ* hybridization, was employed to isolate and localize CA and anion exchanger (AE) transcripts within the mosquito gut. Localization of CA enzymatic activity was assessed via histochemical analyses. Enzymatic and electrophysiological analyses of recombinant CAs and AE were also performed. In this dissertation, cDNAs encoding three CA genes and an AE were cloned and localized within the larval mosquito gut. One isoform of mosquito CA, which was cloned from two different mosquito species, was localized to a specific subset of muscle fibers on the

basal side of the anterior midgut. This CA resembles the mammalian CA IV isozyme in that a glycosylphosphatidylinositol (GPI)-link tethers the enzyme to the extracellular membrane. The other CA isoform, an active cytosolic enzyme, was localized to the gastric caeca and posterior midgut regions. It was also determined that the AE transports chloride and is expressed in the gastric caeca, posterior midgut, and Malpighian tubules. We were unable to detect CA within the anterior midgut epithelial cells using a variety of assays. My studies have therefore led to an alternative hypothesis that one or more CAs within the mosquito gut, but located outside of the anterior midgut epithelial cells, contribute to buffering the alkaline pH of 11 within the anterior midgut lumen. The localization of two CA isoforms, one extracellular and the other cytosolic, and an AE possessing a putative CA binding sequence, to the regions flanking the anterior midgut, supports the prediction of a bicarbonate transport metabolon within the gastric caeca and posterior midgut regions. Such a metabolon has only been studied in mammals, however, the colocalization of CA and AE within the mosquito gut suggests a similar network of bicarbonate production and transport.

CHAPTER 1
INTRODUCTION

Insects represent one of the most numerous and diverse groups of animals on the planet. One particularly successful group of insects is the well-studied Pterogota (winged insect) group. This grouping includes the Lepidoptera (butterflies and moths) as well as the Diptera (flies). These insects have been extensively studied due to their huge impact on the lives of humans. For example, the Lepidopteran, *Manduca sexta,* is a great pest to tobacco companies that rely on abundant and healthy tobacco crops, on which *M. sexta* feeds. Also, mosquitoes (Dipterans) are responsible for transmitting a host of diseases to humans as well as other mammals by injecting pathogens, along with the anti-coagulants from their salivary glands, to aid in bloodletting. The pathogens that cause these diseases can be viruses or various parasites (eg. protozoans).

Mosquitoes belong to the order *Diptera,* family *Culicidae*. According to the American Mosquito Control Association, there are more than 2500 different species throughout the world, with 150 species in the United States (Darsie and Morris, 2000; Spielman and D'Antonio, 2001). Mosquitoes act as vectors for a wide variety of diseases such as malaria, yellow fever, west nile virus, and dengue fever. Recent reports estimate that fifty to one hundred million cases of dengue fever occur annually, along with several hundred thousand cases of the life-threatening form of the disease, dengue hemorrhagic fever (DHF; Halstead, 1997). The geographic range of dengue fever has expanded over the last two decades, primarily because of the spread of its principal vector, *Aedes aegypti*

(Gubler, 1997). Another mosquito example, *Anopheles gambiae* kills millions of people each year in Africa by infecting them with the deadly *Plasmodium* parasite that causes malaria. Many studies have therefore been undertaken to understand the life cycle and physiology of these insects that exert such a large socio-economic impact.

The mosquito's ability to acquire, harbor and transmit deadly pathogens has spurred research into the workings of the mosquito gut. Specific cells of the midgut, which express a proton pumping V-ATPase, have been found to be preferentially invaded by pathogens (Shahabuddin and Pimenta, 1998). Studies have also shown that the mosquito gut is not a static organ but is comprised of several different regions. Each region displays different characteristics and is made up of different cell types.

Alkaline Gut

Larval mosquitoes, as well as some caterpillars, are known to possess a highly alkaline digestive system (Dadd, 1975). The tobacco hornworm, *M. sexta,* has a gut lumen pH that can exceed 11, while the larval mosquito, *Aedes aegypti*, displays a pH greater than 10 in its anterior midgut region (Zhuang et al., 1999). These insects are not only unharmed by this caustic pH, but are able to generate this property while maintaining cellular homeostasis.

The larval midgut is involved in ionic and osmotic regulation as well as digestion, absorption, and excretion (Clements, 1992). It is subdivided into four structurally distinguishable regions: cardia, gastric caeca, anterior stomach, and posterior stomach (Fig. 1-1). Each of these regions consists of one cell layer of epithelial cells, composed of large columnar cells and much smaller cuboidal cells, which vary in character somewhat from region to region. Belying this simple architecture however, the epithelial

cells are capable of maintaining physiological homeostasis while facing a pH range of 7-11 along the length of the mosquito gut lumen (Dadd, 1975). This range in pH, along the length of the mosquito gut, is presumed to support digestive and assimilation functions (Clements, 1992). The epithelial cells of the anterior midgut (AMG) surround a highly alkaline lumen (pH 11) while those of the gastric caeca (GC) and posterior midgut (PMG) surround a neutral to mildly alkaline lumen (pH 7-8; Clements, 1992; Zhuang et al., 1999). The different pH values found along the midgut may support the various metabolic functions that are active in each gut region. The gastric caeca perform ion and water transport, the anterior midgut performs alkaline digestion, the posterior midgut performs nutrient absorption, and the Malpighian tubules (part of the hindgut) actively transport potassium and fluid (Clements, 1992).

The role of the alkaline pH in the anterior midgut is a point of some controversy. It has been suggested that the high pH contributes to the digestion of plant detritus and, in particular, to the dissociation of tannin-protein complexes (Martin et al., 1980). The high pH restricts the conglomeration of proteins within the anterior midgut that could interfere with the insects' normal physiology. These complexes could also interfere with insect digestion by blocking the active sites of many different digestive enzymes. Therefore, the alkaline gut serves as a proposed benefit to the insects by allowing ingested food to remain soluble. The alkalinity therefore keeps the gut free from attachable tannin-protein complexes and enhances the assimilation of proteins. Berenbaum's review (1980) of Lepidopteran insects correlated gut pH (range from 7.0–10.3) with diet. Caterpillars feeding on leaves containing tannins were found to display a more alkaline pH (average pH 8.76) than those feeding on low tannin diets (average pH 8.25; Berenbaum, 1980).

Although this alkaline digestive strategy is well documented in insects, the molecular processes involved have not been clearly defined.

Carbonic Anhydrase

Carbonic anhydrase (CA), a blood enzyme, first described by Meldrum and Roughton in 1933, catalyzes the reversible hydration of carbon dioxide to form bicarbonate and a proton ($CO_2 + H_2O \leftrightarrow HCO_3^- + H^+$; Meldrum and Roughton, 1933). Carbonic anhydrase was first characterized in erythrocytes as the result of a search for a catalytic factor that would enhance the transfer of bicarbonate from the erythrocyte to the pulmonary capillaries (Meldrum and Roughton, 1933). Since it was first described, CA has been shown to play an important role in most acid/base transporting epithelia. Fourteen different CA isoforms have been characterized to date in mammals (Hewett-Emmett and Tashian, 1996). These enzymes have been determined to function in pH regulation and ion balance, thereby performing a crucial role in many biological processes such as respiration, bone resorption, renal acidification, gluconeogenesis, aqueous humor production, gastric acid production, cerebrospinal fluid formation, and signal processing (Dodgson, 1991; Sly and Hu, 1995; Hewett-Emmett and Tashian, 1996; Lindskog, 1997; Sun and Alkon, 2002).

Various types of epithelial cells, such as those described in the mammalian kidney, contain CAs that can provide large quantities of bicarbonate for buffering cells and their microenvironment. Polarized epithelia play an important role in partitioning physiologically distinct compartments, and in maintaining cell and tissue homeostasis. The epithelial cells found in the larval mosquito midgut may serve a similar partitioning function. Like the mammalian kidney, different regions of the mosquito gut may play

differential roles in homeostasis and function. Elucidating the distribution of CAs along the mosquito midgut epithelium may uncover the mechanisms responsible for the unique alkaline physiology of the mosquito gut.

Mosquito Development and Control

Part of the success of insects can be attributed to the structural adaptation of their integument, which functions as skin, skeleton, sensory and respiratory organ, and food reserve (Rockstein, 1964). The advantage of having an extremely strong integument is offset by the disadvantage of not being able to grow significantly in size. Insects have overcome this growth-limiting problem by shedding their integument and rebuilding a new larger one. This process of ecdysis (molting) is used as a tool for marking the different stages of development in many insect species. While mosquito control can target different stages of mosquito development, this project focuses on the larval enzymes, specifically early fourth instar, which begins immediately after the third molt. Careful attention was paid to the stage of insect development in all experiments due to a previous study that showed insect enzymes to decrease or completely arrest prior to molting (Jungreis et al., 1981).

The mosquito life cycle begins at hatching from the egg (Fig.1-2). At this point the fully independent mosquito is called a first instar larva. Successive molts mark the transition to the next larval instar, four larval instars in all. In each instar, the larvae possess a series of morphological characteristics, some particular to that stage. However, there are only slight changes in internal organs such as the midgut. Within a day or two the late fourth instar larva changes into a pupa (Clements, 1992). Within twenty-four hours, the flying adult emerges from the pupa case. Adult females of most mosquito

species require a bloodmeal in order to nourish their developing eggs. However, the males do not ingest blood but instead feed on fruit or do not feed at all (Clements, 1992).

Mosquito control tactics use different methods for controlling mosquito larvae as compared to the flying adults. Mosquito larvae are confined to the water in which they develop, whereas the adults are free-flying and therefore highly mobile. Pesticide sprays are employed against the flying adult mosquitoes, but dragonflies and butterflies are also ill-affected. An arguably better strategy for mosquito control is to target the larvae before they are capable of biting and transmitting disease. Mosquito larvae are voracious eaters, incessantly consuming particulates in the water around them, taking in almost anything. Because of this non-discretional eating behavior, the wriggling larvae can potentially consume a larvacidal agent if placed in the water. Determining the physiological roles of larval mosquito gut enzymes and metabolic transporters may provide a lead for constructing mosquito larvacides.

Carbonic Anhydrase Inhibition

The focus of this project is to examine the distribution and expression of CAs within the fourth instar of larval development of two species of mosquito, *Ae. aegypti* and *An. gambiae*. A tangential result of characterizing mosquito CAs may be in the development of mosquito-specific inhibitors. If a CA is discovered to be essential for mosquito development or homeostasis, a specific inhibitor of precisely this mosquito CA isoform could be developed. Since virtually all organisms contain CA enzymes, an inhibitor that would compromise this mosquito CA while not affecting any other isozymes would be necessary for mosquito control so that non-target species would not be affected. Differentially specific CA inhibitors are already employed in the distinctive

characterization of mammalian CA isoforms. For example, the acidic sulfonamide benzolamide has been used for the preferential inhibition of extracellular CA while not compromising any intracellular CA activity (Tong et al., 2000). This occurs due to the inability of benzolamide to readily penetrate cell membranes (Tong et al., 2000). The wealth of information pertaining to mammalian CA isoforms and their specific inhibitors provides a basis for comparisons with CAs that are discovered in the mosquito midgut. Sulfonamide CA inhibitors are widely used to treat a number of conditions including glaucoma, gastro-duodenal ulcers, and cancer, by lowering the production of fluids and acids. Parkkila et al. (2000) showed that the invasion of renal cancer cells *in vitro* could be inhibited with CA inhibitors. If larval mosquito physiology is dependent upon the generation or maintenance of the alkaline gut, and CA is a necessary component, then the possibility exists for the use of CA inhibitors as mosquito larvacides.

Bicarbonate Transport

The site(s) of bicarbonate production by CA may not be as important as the translocation of the bicarbonate that is produced. Transporters can facilitate the passage of bicarbonate and other ions through otherwise impermeable cell membranes. Bicarbonate transporters compose a large family of membrane proteins that includes the anion exchangers (AEs), sodium bicarbonate cotransporters (NBCs), and members of the sulfate transporter group that can also transport bicarbonate (Alper et al., 2001). Most of the BT proteins consist of a cytosolic anchoring domain as well as a 10-14 membrane-spanning transporter domain (Alper et al., 2001). Also, evidence exists that some AEs are capable of physically binding CA enzymes. Thus, the fourth extracellular loop of AE1 contains a glycosyl-phosphatidyl-inositol (GPI)-linked CA IV binding site and the

intracellular carboxy terminus of AE1 was found to contain a cytosolic CA II binding site (Vince and Reithmeier, 2000; Sterling et al., 2002a). A metabolon, a complex of membrane proteins involved in regulation of bicarbonate metabolism and transport, defines the relationship between the CA and AE proteins (Sterling et al., 2001a). This bicarbonate transport metabolon, is thus capable of transporting bicarbonate as soon as it is available from the CA enzyme. Transport can be in either direction, into or out of the cell, and is therefore predictively capable of maintaining a tight hold on pH. The occurrence of such a tight bicarbonate control mechanism could be very advantageous to the mosquito. With such a large pH gradient across the membrane, a bicarbonate transport metabolon could ensure that the pH on either side of the membrane is strictly monitored. This bicarbonate transport metabolon has only been identified in a mammalian system. Despite this fact, an insect gut model that employs such a bicarbonate transport metabolon is easy to envision. Because of the strong pH gradient that is maintained in the mosquito gut, it is reasonable to propose that a bicarbonate transport metabolon could exist in this system as well.

Gut Alkalization Model

My first physiological model of the larval mosquito midgut was derived from the tobacco hornworm, *M. sexta,* which also uses an alkaline digestive strategy. In this model, several proteins contribute to the high alkalinity (Fig. 1-3). These are the CA, the H^+ V-ATPase, and the cation and anion exchangers. The H^+ V-ATPase is thought to be the energizer of the system by using ATP, and pumping protons out into the lumen of the anterior midgut. This sets up a potential difference across the membrane of about 210 mv (Harvey, 1992). In this model, the predicted cytosolic CA within the anterior midgut

combines carbon dioxide and water to produce bicarbonate and a proton ion. The bicarbonate is pushed from the epithelial cell, across to the lumen side by the anion exchanger, in trade for a chloride ion. The proton then gets stripped off of the bicarbonate and, along with the proton pumped across by the V-ATPase, is brought back into the cell in exchange for a potassium ion (Wieczorek et al., 2000). This potassium ion combines with the carbonate to produce potassium carbonate, which is hypothesized to be responsible for the high alkaline pH of the anterior gut region. This hypothesis stems from the fact that potassium ions are actively produced by the Malpighian tubules and are circulated throughout the gut via the hemolymph (Clements, 1992). Potassium carbonate also has a pKA greater than 10 and can therefore contribute to the gut alkalization.

The goal of this project was to expand and adapt this model to the larval mosquito by completing several clear objectives. These objectives are outlined within the following specific aims.

Specific Aims

1. Determine whether CA is involved in buffering the high alkalization of the larval mosquito gut.

   A. Determine if a CA enzyme is present within the mosquito gut. Determine which regions of the larval *Ae. aegypti* gut display CA activity using CA histochemistry and ^{18}O isotope exchange.

   B. Determine if CA-specific inhibitors, such as acetazolamide, can influence larval midgut alkalization.

2. Determine whether CA is expressed in the larval mosquito gut.

   A. Clone and characterize full length CA cDNAs from the larval midgut of *Ae. aegypti* and *An. gambiae*.

B. Use experimental and bioinformatical approaches to determine if CA expressed in the mosquito gut is similar to a characterized mammalian CA isoform. Furthermore, determine the subcellular location of mosquito CA isoforms as cytosolic, membrane-bound, mitochondrial, or GPI-linked.

C. Determine which regions of the mosquito gut express CA mRNA and protein using *in situ* hybridization, real time PCR, and immuno-localization.

3. Determine whether anion exchangers (AE) are involved in the pH regulation of the larval mosquito gut.

A. Clone and characterize an AE from the larval mosquito gut that uses the bicarbonate produced by CA as a substrate.

B. Determine whether the mosquito AE transports chloride using a *Xenopus* oocyte expression assay.

C. Determine if AE is expressed in the same regions of the mosquito gut as the CA. Co-localization of CA and AE would support the existence of a bicarbonate transport metabolon.

D. Determine if the AE contains the amino acid sequence predicted to be necessary for binding CA. If indeed the AE protein is predicted to bind CA, a bicarbonate transport metabolon within the larval mosquito gut could maximize bicarbonate production and transport.

4. Present a new larval mosquito model that reflects the studies in this dissertation. Bring together all localized components of mosquito gut physiology into one model.

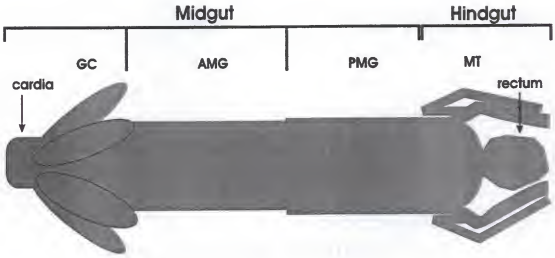

Figure 1-1. Illustration showing the regions of the larval mosquito gut. The midgut is composed of the cardia, gastric caeca (GC), anterior midgut (AMG), and the posterior midgut (PMG). The hindgut is composed of the Malpighian tubules (MT) and the rectum.

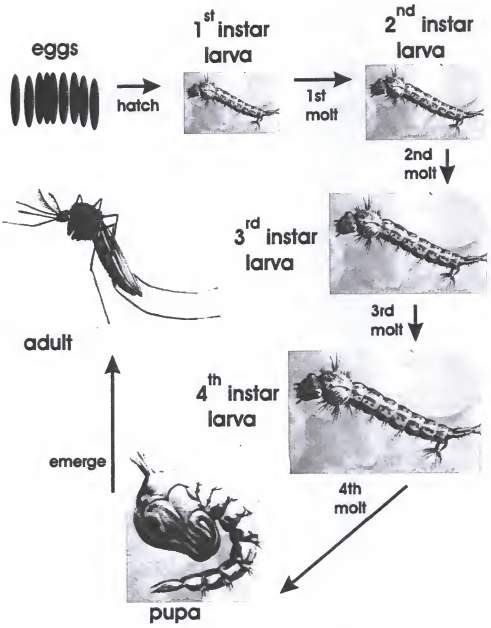

Figure 1-2. Illustration of the mosquito life cycle. The four life stages are egg, larva, pupa, and adult. The larval stage consists of four different instars. Early fourth instar larvae, following the third molt, were chosen for all experiments. The female mosquito continues the cycle by laying eggs, usually after a required blood meal.

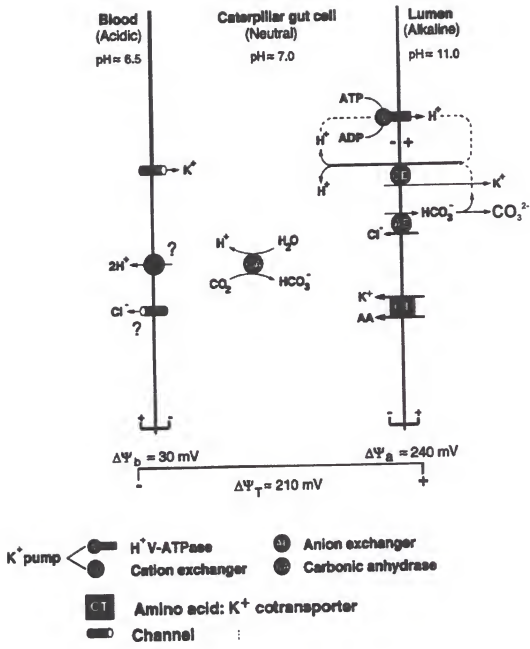

Figure 1-3. Preliminary mosquito anterior midgut model based on *M. sexta*. This theoretical model places a CA II-like isoform within the cell cytosol where it combines carbon dioxide and water to form bicarbonate and a proton. Alkalization is driven by a proton pumping V-ATPase that resides in the apical membrane and pumps protons into the lumen. A chloride/ bicarbonate exchanger, that is also located in the apical membrane, exchanges bicarbonate from the CA, for chloride from the lumen. A cation exchanger transfers potassium to the lumen while stripping protons from the bicarbonate for the exchange. The potassium ion combines with the de-protonated carbonate ion to form potassium carbonate, which brings the pH to highly alkaline levels.

CHAPTER 2
MATERIALS AND METHODS

Experimental Insects

Ae. aegypti eggs were obtained from a colony maintained by the United States Department of Agriculture (USDA) laboratory in Gainesville, Florida. The eggs were allowed to hatch in 20 ml of 2% artificial seawater (ASW; 8.4 mM NaCl, 1.7 mM KCl, 0.1 mM $CaCl_2$, 0.46 mM $MgCl_2$, 0.51 mM $MgSO_4$, and 0.04 mM $NaHCO_3$). The mosquito larvae were reared in 2% ASW at room temperature. The *Ae. aegypti* larvae were fed a mixture of yeast and liver powder (1:1.5 g respective dry weight; ICN Biomedicals Inc., Aurora, Ohio). Eight to ten days were required for this species to reach the early fourth instar.

An. gambiae eggs were obtained from the Centers for Disease Control and Prevention (CDC) in Atlanta, Georgia. Strict handling guidelines were followed with this particular species, which does not currently inhabit Florida, due to its inherent ability to acquire and transmit the *Plasmodium* protozoan, which causes malaria. This *Anopheles* species was therefore reared in deionized water inside of a locked incubator set at 30°C. A mesh screen served as a second barrier within the incubator while the sealed (but not airtight) containers harboring the *An. gambiae* larvae served as the third barrier against escape. The *An. gambiae* larvae were fed a Wardley tropical fish flake food (The Hartz Mountain Corp., Secaucus, New Jersey). Early fourth instar larvae were chosen for all experiments. Ten to twelve days from the hatch day were required for this species to

reach the early fourth instar. Late fourth instar larvae that went unused were sacrificed to prevent any chance of emerging adults.

Preparation and Fixation of Tissue

To dissect out the midgut, the heads of the cold-immobilized larvae were pinned down using fine stainless-steel pins to a Sylgard layer at the bottom of a Petri dish containing hemolymph substitute solution consisting of 42.5 mM NaCl, 3.0 mM KCl, 0.6 mM $MgSO_4$, 5.0 mM $CaCl_2$, 5.0 mM $NaHCO_3$, 5.0 mM L-succinic acid, 5.0 mM L-malic acid, 5.0 mM L-proline, 9.1 mM L-glutamine, 8.7 mM L-histidine, 3.3 mM L-arginine, 10.0 mM dextrose, 25 mM Hepes and adjusted to pH 7.0 with NaOH (Clark et al., 1999). The anal segment and the saddle papillae were removed using ultra-fine scissors and forceps, and an incision was made longitudinally along the thorax. The cuticle was gently pulled apart and the midgut and gastric caeca were removed. In some cases, the gut contents enclosed in the peritrophic membrane slid out, leaving behind the empty midgut. In other cases, it was necessary to remove the peritrophic membrane and its contents manually. For enzyme histochemistry, fixation was in 3% glutaraldehyde in 0.1 M phosphate buffer, pH 7.3, overnight at 4°C (Ridgway and Moffet, 1986). For *in situ* hybridization and immunohistochemistry, dissected tissues were fixed overnight in 4% paraformaldehyde in 0.1 M cacodylate buffer, pH 7.2 (0.1 M phosphate buffer, pH 7.2 was used for Ch 4 and 5 *in situ*). In some cases, the dissected larval midguts were photographed using a Nikon FX-35DX photographic camera mounted on a Nikon SMZ-10 dissecting microscope. In other cases, digital images were acquired using a Leica DMR microscope equipped with a Hammamatsu CCD camera. All images were assembled using Corel Draw-11 software.

Bromothymol Blue Qualitative Assay

A qualitative test to detect carbonic anhydrase activity in mosquito larval midgut homogenate was adapted from the test described by Tashian (1969). The procedure included immersing a piece of Whatman no.1 paper in a solution made with 0.15% Bromothymol Blue (BTB) in ice-cold 25 mM Tris HCl, 0.1 M Na_2SO_4, pH 8.0. The paper was allowed to soak completely in this blue solution and was placed on ice for 30 minutes. The colored filter was then transferred to a Petri dish with a hole in the lid. Samples of mosquito larval midgut homogenate were prepared by sonicating midguts of early fourth instar larvae in ice-cold 25 mM Tris HCl, 0.1 M Na_2SO_4 pH 8.0, with protease inhibitor cocktail (Sigma-Aldrich, St. Louis, MO; diluted 1:1000). An autopipette was used to spot exactly 4 µl samples on the paper. Controls were also spotted. The controls included a buffer with protease inhibitor and controls for the liver/yeast food added to the medium in which the mosquito larvae were reared. These food controls included a range of concentration from 1 to 100 µg/ml liver powder and yeast. Carbonic anhydrase from bovine erythrocytes (Sigma-Aldrich) dissolved in the same buffer described above was used as a positive control.

A steady stream of CO_2 at 34.5 KPa was blown for 3 seconds through the opening on the lid of the Petri dish, and the dish was sealed and kept on ice. The formation of yellow spots in a few seconds was indicative of carbonic anhydrase activity.

Effect of Methazolamide on the Alkalization of the Midgut of Live Larvae

The effect of a CA inhibitor, methazolamide, on gut alkalization and the capacity of whole larvae to alkalize their culture medium was examined. Flat-bottomed tissue culture plates (24 well, Sarstedt Inc., Newton, North Carolina) were filled with 1 ml of 25

mM Tris HCl, 0.1 M Na_2SO_4 buffer, pH 8.5. BTB solution was added to each well until a 0.003% solution was achieved. Five live early fourth-instar larvae that had been placed in BTB indicator solution for 2 hours were added to each of the wells, and the larvae were allowed to adjust to their new environment for 30 minutes. Methazolamide dissolved in Dimethyl Sulfoxide (DMSO; Sigma-Aldrich) at concentrations ranging from 10^{-6} M to $8x10^{-3}$ M was added to the wells. Controls included wells containing DMSO with BTB indicator but no inhibitor and wells containing BTB indicator but no DMSO. The plates were scanned using a Hewlett Packard ScanJet 6100C scanner before addition of the inhibitor and 5 hours later. In addition, the midguts were dissected and photographed to record the pH within the gut lumen as revealed by the color of ingested BTB.

^{18}O Exchange Method to Measure Carbonic Anhydrase Activity

Tissue homogenate carbonic anhydrase activity was measured using the ^{18}O exchange method (Silverman and Tu, 1986). Midguts were dissected, and the peritrophic membrane was removed together with its contents. Individual measurements of CA activity were performed with pooled samples of gastric caeca, anterior midgut, posterior midgut and Malpighian tubules. The method involved adding ^{18}O-labeled $NaHCO_3$ to 0.1 M Hepes buffer, pH 7.6, at 9.5°C. The disappearance of ^{18}O isotopes from CO_2 and/or HCO_3^- upon addition of the enzyme preparations was monitored. Measurements of ^{18}O in CO_2 were accomplished with a mass spectrometer, using a CO_2-permeable inlet that allowed very rapid, continuous measurement of the isotopic content of CO_2 in solution. All samples were centrifuged at 14,000 rpm at room temperature prior to the assay to remove food and insoluble material. Inhibition was accomplished by adding

methazolamide to a final concentration of 10^{-6} M. Recombinantly expressed and purified mosquito CAs were also tested for activity using this assay.

Isolation of RNA and Synthesis of cDNA

Total RNA was isolated from freshly dissected fourth instar mosquito larval midguts using TRI Reagent (Molecular Research Center Inc., Cincinnati, Ohio) according to the manufacturer's instructions. Briefly, 100 *Ae. aegypti* gut epithelial organs, including fore-, mid-, and hindgut (approximately 20 mg) were dissected in HSS and transferred to a sterile microcentrifuge tube containing TRI Reagent (600 µl). The tissue was homogenized and incubated for 5 min at room temperature. The homogenate was then extracted with chloroform (40 µL) and precipitated with isopropanol (100 µL). The RNA pellet was washed with 75% ethanol (200 µL), air-dried and resuspended in 50 µL diethylpyrocarbonate (DEPC; Sigma-Aldrich)-treated H_2O. RNA concentrations were calculated from the absorbance at 260 nm. Total RNA (10 µg) was reverse-transcribed for 2 hours at 42°C in a 20 µl reaction mixture using 5 pmol of oligo(dT)12-18, RNasin (1:40 dilution), 1X first strand buffer, 1 mM dNTPs, and 200 units (U) of Superscript II reverse transcriptase (Invitrogen Inc., Carlsbad, California). This cDNA was used to clone the first fragment of *Ae. aegypti* CA.

Bioinformatics

The National Center for Biotechnology Information (NCBI) website (www.ncbi.nlm.nih.gov) was used for the majority of the bioinformatical data presented in this study. The first mosquito genome, *An. gambiae,* was released in 2002 (Holt et al., 2002), and made accessible to the public on the NCBI website. The basic local alignment search tool (BLAST; Altschul et al., 1990) was employed for primer construction as well

as analyzing PCR products. The NCBI Blast Flies database (www.ncbi.nlm.nih.gov/BLAST/Genome/FlyBlast.html), together with the Ensembl database (www.ensembl.org/Anopheles gambiae/) were used to predict the number of CA genes in the *Drosophila melanogaster* and *An. gambiae* genomes by inputting the *Ae. aegypti* CA as the search sequence. These partial sequence results were then annotated to reflect the 2 full-length CA sequences that we have cloned from *An. gambiae* and presented within this manuscript.

Ensembl is a joint project between the European Bioinformatics Institute and the Sanger Institute to bring together genome sequences with annotated structural and functional information. The NCBI protein database (pdb) and the BLAST were used in conjunction with the 3-dimensional structure viewer (Cn3D; Hogue, 1997) for the prediction of antibody accessible peptide regions in mosquito proteins. BLAST analyses also confirmed that the chosen antigenic peptides were unique. The conserved domain database (CDD; Marchler-Bauer et al., 2002) and the conserved domain architecture retrieval tool (CDART; Geer et al., 2002) were used to predict the function of our newly cloned mosquito proteins. Alignments were produced using Clustal W (Thompson et al., 1994), as implemented in DNAman software (Lynnon Biosoft, Vaudreuil, Quebec, Canada).

Cloning of CA from *Aedes aegypti* Larval Midgut

Degenerate oligonucleotides were designed against the regions of conserved amino acids among CA proteins as determined by the BLAST analysis of several vertebrate and two putative, but annotated, CA proteins from the *D. melanogaster* sequence database.

The primer sequences used initially for *Ae. aegypti* CA were CA5F and CA3R (see Table 2-1). PCRs were performed in a total volume of 20 µl, and the reaction mixture contained 0.1 µg of cDNA as template, 0.2 µM of each primer, 200 µM each of dNTPs, 1X PCR buffer and 1 U of *Taq* polymerase (Promega; Madison, Wisconsin). The PCR cycling profile was: 94°C for 5 min, 55°C for 2 min and 72°C for 3 min, followed by six cycles of 94°C for 0.5 min, 53°C (in increments of 2°C/cycle) for 1 min and 72°C for 1 min and 35 cycles of 94°C for 0.5 min, 45°C for 1 min and 72°C for 2 min followed by a final extension at 72°C for 15 min. The PCR products were visualized on 1% agarose gels and specific products were isolated using a QIAquick gel extraction kit (Qiagen, Inc, Valencia, California), diluted 1:100 in water, and used as template for a second, identical PCR. The resulting 297 base-pair (bp) product was gel-purified, ligated into pGem-T (Promega) and transformed into JM109 *Escherichia coli* (Promega) for subcloning. This partial *Ae. aegypti* CA cDNA was completed using amplified cDNA pools from gastric caeca and posterior midgut.

Construction of Amplified cDNA Pools

Adapter-ligated, amplified cDNA pools ("libraries") were constructed from different regions of the fourth instar larval gut of both *Ae. aegypti* and *An. gambiae* using a technique optimized for invertebrate tissues (Matz et al., 1999). The gastric caeca, anterior midgut, posterior midgut, rectal salt gland, Malpighian tubules, and anal papillae of ten larvae were dissected in HSS and collected separately, resulting in six discreet tissue pools. The tissue was dissolved in Buffer D (500 µL; 4 M guanidine thiocyanate, 30 mM sodium citrate, and 30 mM beta-mercaptoethanol). The mixture was placed on ice and combined with phenol (500 µL, pH 7.0) and chloroform (100 µL). The mixture

was vortexed and centrifuged at 14,000 g for 30 seconds at 4°C. The upper, aqueous phase was transferred to a clean tube and 5 μL glycogen solution (Pharmacia Quick Prep Micro RNA purification kit, Piscataway, New Jersey). The RNA was precipitated by the addition of 100% ice-cold ethanol (550 μL) followed by centrifugation at 14,000 g for 6 minutes at room temperature. The supernatant was removed and 1 mL of ice-cold ethanol (80%) was added. The mixture was centrifuged at 14,000 g for 10 minutes at room temperature, the supernatant was removed, and the pellet was air-dried.

For first strand synthesis, the pellet was resuspended in DEPC-treated water (5 μL) and combined with the TRsa primer (1 μM; Table 2-1). This mixture was incubated at 50°C for 3 minutes and immediately placed on ice. Then 1X ligation buffer (Marathon cDNA Amplification kit, BD Biosciences, Palo Alto, California), 0.01 M DDT, 1 U Superscript II (Life Technologies; Rockville, Maryland), and 0.5 μL dNTP mix (10 mM each dNTP, Marathon cDNA Amplification kit) were added to a total volume of 10.5 μL. This reaction mixture was incubated at 42°C for 1 hour and immediately put on ice.

For second strand synthesis, DEPC-treated water (49 μL) was added to the first strand reaction mix. The mixture was then combined with 1.6 μL dNTP mix (10 mM each, Marathon cDNA Amplification kit), 1X reaction buffer (Marathon cDNA Amplification kit), and 4 μL second strand synthesis enzyme mix (Marathon cDNA Amplification kit) in 80 μL total volume. The reaction mix was then incubated at 16°C for 1.5 hours. T4 DNA polymerase (1 U; Marathon cDNA Amplification kit) was added to the reaction mixture and the entire mixture was incubated at 16°C for an additional 0.5 hour. The reaction was stopped by incubation at 65°C for 5 minutes.

The reaction mix (80 μL) was combined with 40 μL phenol and 40 μL chloroform and centrifuged at 14,000 g for 10 minutes. The upper, aqueous phase was removed and transferred to a clean tube. The cDNA was precipitated by the addition of 3 M sodium acetate (8 μL, pH 5.0) and 100% ethanol (160 μL). The mixture was centrifuged at 14,000 g for 15 minutes at room temperature. The supernatant was removed and the pellet was air-dried.

For adaptor ligation, the cDNA pellet was resuspended in DEPC-treated water (6 μL) and combined with 1 μM adaptor, 1X ligase buffer, and 1 U T4 ligase (Marathon cDNA Amplification kit) in 10 μL total volume. This mixture was stored overnight at 16°C. For cDNA amplification, the ligation mixture (10 μL) was combined with 40 μL DEPC-treated water. PCR amplification was then performed using the Advantage kit (BD Biosciences). The diluted cDNA (1 μL) was combined with 1X advantage buffer, 0.4 μL dNTP mixture (10 mM each), 0.1 μM DAP and TRsa primers (Table 2-1), and 0.4 μL advantage enzyme mix in 20 μL total volume. The cycling profile consisted of 94°C for 30 seconds, 66°C for 1 minute, and 72°C for 2.5 minutes. The reaction was analyzed on a 1% agarose gel after 12, 16, and 20 cycles. A final chase step was then performed to ensure that all cDNAs were completely double-stranded. Both 5' and 3' adaptor primers were added to the PCR reactions and two cycles of 77°C for 1 min, 65°C for 1 min, and 72°C for 2.5 min were performed. The resulting collections of amplified cDNA were then diluted 1:50 and used as template for subsequent PCR experiments.

Amplified cDNA pools from *An. gambiae* were used to clone two CA cDNAs and the AE cDNA. Exact primers were designed from conserved regions of the proteins as

determined by BLAST analysis using characterized proteins against the *An. gambiae* genome. See table 2-1 for all initial primer sequences.

3' and 5' Rapid Amplification of cDNA Ends and Sequencing

Full-length cDNAs were obtained by rapid amplification of cDNA ends (RACE), (Zhang and Frohman 1997, modified by Matz et al., 1999). Exact primers were defined according to the 5' adaptor (DAP primer) along with a reverse primer specific to the cloned fragment, and 3' TRsa adaptor (TRsa primer) along with a forward primer specific to the cloned fragment (see Table 2-1 for adaptor primer sequences). These ends, which included the 5' and 3' UTR sequences, were then used to design PCR primers to produce a single product with consensus start and stop codons.

Plasmid DNA from individual colonies was purified using a Qiaprep Plasmid Mini kit (Qiagen). The plasmid DNA (50 ng) was then sequenced using the ABI Prism Big Dye Terminator Cycle Sequencing Kit (PE Biosystems, Foster City, California) and the reaction products were analyzed on an ABI Prism 310 Genetic Analyzer (PE Biosystems).

Construction of *In Situ* Hybridization Probes

Sense and antisense digoxygenin (DIG)-labeled cRNA probes were generated by *in vitro* transcription using a DIG RNA labeling kit (Roche Molecular Biochemicals, Indianapolis, Indiana). The initial *in situ* hybridization experiment, presented in chapter 3, used a cRNA probe derived from the original 297 bp *Ae. aegypti* CA sequence. The *in situ* experiments presented in chapters 4 and 5 utilized the full-length CA and AE sequences. For the first CA antisense probe, the pGEM-T vector containing the 297 bp CA sequence was linearized by incubating 2 μg of plasmid with Pst I restriction enzyme

(New England Biolabs (NEB); Beverly, Massachusetts) and 1X buffer 3 (NEB) at a total volume of 20 µL for 1 hour at 37°C. For the sense probe, the pGEM-T vector containing the 297 bp CA sequence was linearized by incubating 2 µg of plasmid with Not I restriction enzyme and 1X buffer 3 (NEB) in a total volume of 20 µL for 1 hour at 37°C. After digestion, the volume was brought to 100 µL with the addition of 80 µL water. A phenol/ chloroform extraction was performed such that 100 µL of phenol/ chloroform-isoamyl alcohol was added to the linearized plasmid and the solution was centrifuged at 14,000 g for 1 minute. The upper aqueous phase was transferred to a new tube and 100 µL chloroform was added. After centrifugation at 14,000 g for 1 minute, the upper aqueous phase was transferred to a new tube and the chloroform step was repeated. The linearized plasmid DNA was precipitated by the addition of 10 µL sodium acetate (3 M, pH 2.5) and 200 µL cold ethanol (100%). The DNA was incubated at -80°C for 15 minutes and then centrifuged at 14,000 g for 10 minutes at 4°C. The supernatant was removed and the DNA pellet was washed by the addition of 500 µL ethanol (70%) followed by centrifugation at 14,000 g for 5 minutes at 4°C. The supernatant was removed and the pellet was air-dried and then resuspended in 13 µL DEPC-treated water.

The full-length *Ae. aegypti* CA was subcloned into pCR 4-TOPO plasmid using a PCR manufactured 5' Sal I restriction site and a 3' Xho I site. Therefore, the pCR 4-TOPO plasmid was linearized by incubating 2 µg of plasmid with either Sal I, 1X Sal I buffer, and BSA, or Xho I, 1X buffer 2, and BSA (NEB). The pCR 4-TOPO plasmid was also used for the generation of the *An. gambiae* CA and AE probes. For these probes, the unique restriction sites, Pme I and Not I, located within the pCR 4-TOPO plasmid were used for linearization with 1X buffer 4 and BSA, or 1X buffer 3 and BSA, respectively.

These mixtures were all incubated at 37°C for 2 hours to ensure complete linearization of the plasmids. After digestion the uncut pCR 4-TOPO plasmids were compared to the cut plasmids on a 1% agarose gel to confirm linearization. The cut plasmids (10 µL) were cleansed using a Qiaquick PCR Purification kit (Qiagen Inc, Valencia, California).

For *in vitro* translation, the resuspended pellet or purified plasmids were combined with 1X transcription buffer, 1X NTP labeling mixture, RNase inhibitor (20 U), and 40 U T3 RNA polymerase (or SP6 for pGEM-T plasmids) or 40 U T7 RNA polymerase. For the *Ae. aegypti* CA probes, T7 polymerase was used with the Sal I cut plasmid to produce the antisense probe, while T3 polymerase was used with the Xho I cut plasmid to produce the sense (control) probe. The pCR 4-TOPO plasmid used for the generation of the *An. gambiae* CA and AE probes contained the CA and AE sequences in the reverse configuration. Therefore, for these *An. gambiae* probes, T3 was used with the Not I linearized plasmids to produce the antisense probes, while T7 was used with the Pme I cut plasmids to produce the sense (control) probes. The mixtures were incubated at 37°C for 2 hours followed by the addition of 20 U DNase I and incubation at 37°C for 15 minutes. The DNase I reaction was stopped by the addition of 0.5 µL of EDTA (500 mM). The DIG-labeled cRNA was then precipitated by the addition of 2.5 µL of LiCl (4 M) and 75 µL cold ethanol (100%). The mixture was incubated overnight at -20°C and centrifuged at 14,000 g for 10 minutes at 4°C. The supernatant was removed and the pellet was washed with 50 µL cold ethanol (75%). The centrifugation step was repeated and the pellet was air-dried and resuspended in 100 µL DEPC-treated water. The probes were stored at -80°C.

In Situ Hybridization

The *in situ* hybridization experiments presented in chapters 4 and 5 added an additional fixation step due to a recommendation by Dr. Dmitri Boudko to increase the clarity of the *in situ* labeling. A glass electrode fitted to a micromanipulator was used to inject 4% paraformaldehyde into the thoracic cavity, just behind the head. Successful perfusion was easily identified by the cessation of the otherwise constant muscle twitching along the length of the body. This injection of fixative served to preserve the cellular integrity and protect against the many proteases that exist within the mosquito gut. For *in situ* hybridization, methods were adapted from Westerfield (1994). The midguts were washed with PBS at room temperature and then incubated in 100% methanol at -20°C for 30 minutes to ensure permeabilization of the gut tissue. The tissue was washed (5 min each wash) in 50% methanol in PBST (Dulbecco's phosphate buffered saline [Sigma-Aldrich] plus 0.1% Tween-20), followed by 30% methanol in PBST and then PBST alone. The tissue was fixed in 4% paraformaldehyde in 0.1 M sodium cacodylate buffer (or 0.1 M phosphate buffer) for 20 min. at room temperature and washed with PBST. The larval midguts were digested with proteinase K (10 µg/ml in PBST) at room temperature for 10 min, washed briefly with PBST and fixed again, as described previously.

Prehybridization of the tissue was accomplished by incubation in HYB solution (50% formamide, 5X SSC [1X SSC equals 0.15 M NaCl, 0.015 M Na-citrate buffer pH 7.0], 0.1% Tween-20) for 24 hours at 55°C. The larval midguts were transferred to HYB+ solution (HYB plus 5 mg/ml tRNA, 50 µg/ml heparin) containing 5 ng/ml DIG-labeled probe and incubated overnight at 55°C. Excess probe was removed by washing at

55°C with 50% formamide in 2X SSCT for 30 min (twice), 2X SSCT for 15 min and 0.2X SSCT for 30 min (twice). For detection, the tissue was incubated in PBST containing 1% blocking solution (Roche Molecular Biochemicals) for 1 h at room temperature. The tissue was incubated with anti-DIG-alkaline phosphatase (Roche Molecular Biochemicals) diluted 1:5000 in blocking solution for 4 hours at room temperature. The tissue was washed with PBST and incubated in alkaline phosphatase substrate solution (Bio Rad Laboratories, Hercules, CA, USA) until the desired intensity of staining was achieved (2-3 hours).

CA Histochemistry

Carbonic anhydrase activity was detected in isolated *Ae. aegypti* midguts using Hansson's method (Hansson, 1967), as modified by Ridgway and Moffet (1986). The procedure involved the incubation of isolated, 3% glutaraldehyde-fixed midguts in 1.75 mM $CoSO_4$, 53 mM H_2SO_4, 11.7 mM KH_2PO_4, and 15.7 mM $NaHCO_3$ (pH 6.8). The incubation medium contains a high concentration of bicarbonate, which stimulates the production of CO_2 and hence a decrease in pH in the presence of CA. The acidic pH then stimulates the formation of insoluble black cobalt salts which were visualized using 0.5% $(NH_4)_2S$ in distilled water. Therefore, micro-sites of active CA liberation of CO_2 from bicarbonate dehydration become apparent with this assay. Removal of the bicarbonate substrate ($NaHCO_3$) eliminated staining.

Real Time PCR

Region-specific cDNA was produced from dissected mosquito tissue using the Cells-to-cDNA standard protocol (Ambion INC, Austin, Texas). The gut regions used to make the amplified cDNA pools were incubated in 50 μL of hot cell lysis buffer for 10

minutes at 75°C. The lysed tissues were treated with 2 U of DNase I for 30 minutes at 37°C. The DNase I was then inactivated by heating to 75°C for 5 minutes. For the reverse transcription reaction, 10 µL of cell lysate was combined with 4 µL dNTP mix (contains 2.5 mM each dNTP) and 5 µM random decamer first strand primer in 16 µL total volume. The mixture was incubated at 70°C for 3 minutes and then chilled on ice for 1 minute. This mixture was then combined with 1X RT buffer, 1 U M-MLV reverse transcriptase, and 10 U RNase inhibitor, and incubated at 42°C for 1 hour. The reverse transcriptase was then inactivated by incubation at 95°C for 10 minutes. Primers (Table 2.1) were designed using Primer Express software (Applied Biosystems; Foster City, California). The SYBR Green PCR Master mix, which includes SYBR Green I dye, Amplitaq Gold DNA Polymerase, dNTPs, and buffer, was used for all real time PCR investigations. Each cycle of PCR was detected by measuring the increase in fluorescence caused by the binding of the SYBR Green dye to double-stranded DNA using an ABI Prism 7000 Sequence Detection System (Applied Biosystems). Initially, each primer set, including the control 18s ribosomal RNA (Genbank accession M95126), was assessed to determine the optimal concentration of primer to be used. All real time experiments used the same 2-step cycling profile: 50°C for 2 minutes followed by 95°C for 10 minutes and 40 cycles of 95°C for 15 seconds and 60°C for 1 minute. Whole gut cDNA (100 nM) was used as template with 500 nM, 300 nM, 100 nM, or 50 nM of each primer set and 1X SYBR green I master mix in 25 µL total volume. Each reaction was done in triplicate. The optimal concentration was then chosen based on the amplification plots and the dissociation curves generated. Once a concentration was chosen for each primer set, the efficiency of amplification of that set was determined. Serial dilutions of

whole gut cDNA were used as template with the appropriate concentration of primers and 1X SYBR green I master mix in 25 μL total volume. The threshold cycle number (Ct) was plotted versus the log of the template concentration and the slope (m) and intercept (b) were determined (Figure 2-1). These pre-determinations were then used in the standardized comparison of the amount of 18s transcript and CA transcript in each of the cDNA samples tested. For each analysis, a control containing all of the necessary PCR components except the cDNA template was run. To determine the relative expression level for each transcript analyzed, the following equation was used: (Ct-b)/m. The average log ng for each transcript was then compared to the average log ng of 18s RNA transcript to normalize the values. Then the expression levels were determined relative to the transcript with the greatest normalized log ng value and expressed in a bar graph using Microsoft Excel software.

Antibody Production

An antigenic peptide consisting of eighteen amino acids was chosen from the *Ae. aegypti* CA sequence for antibody production. In order to increase the probability that this antibody would be specific for this particular CA sequence (in the event that other CA isoforms were isolated from the mosquito gut), attempts were made to synthesize an antigenic peptide that would be specific to this isoform. The well-characterized mammalian CA isoforms served as a model in trying to choose a unique CA peptide sequence. The comparison of the mosquito CA with the mammalian isoforms yielded a peptide sequence from the amino (N) terminus, where CA isoforms showed the most diversity, and least conservation. The N terminus of our mosquito CA was predicted to have an extended loop secondary structure. Unlike an alpha helix, an extended loop is

more accessible to antibody probing. Furthermore, three-dimensional analyses (Cn3D v4.1 NCBI) of predicted CA IV structures (human 1ZNC and mouse 2ZNC) predicted that the N terminus is exposed and accessible (Figure 2-2). An antigenic peptide was therefore chosen from the N terminus of the *Ae. aegypti* CA sequence. This peptide sequence (GVINEPERWGGQCETGRR) was sent to Sigma-Genosys (Woodlands, Texas), where it was synthesized and conjugated to bovine serum albumin (BSA). The synthetic peptide-BSA construct and Freund's incomplete adjuvant were injected into two rabbits to elicit an immune response. Prior to injection, a blood sample from each rabbit was collected to serve as the control pre-immune serum. Every two weeks a blood sample was collected from the rabbits, the fraction of immunoglobulin G (IgG) pooled, and another dose of the peptide-BSA construct administered. Three months after the initial injections, the final bleeds were collected and used for all immunohistochemical analyses.

We also raised antibodies against an *An. gambiae* cytosolic CA peptide and an anion exchanger (AE) peptide. These antibodies were produced by the Aves Labs, Inc., (Tigard, Oregon), using a similar strategy to that described above. However, these antibodies were produced in hens. The synthesized peptides were conjugated to BSA and injected into two hens each. The immunoglobulin Y (IgY) antibodies were collected from the hens' eggs, pooled, and purified.

Immunohistochemistry

The specificity of the antibodies in the resultant antisera was determined. The antisera were then used to localize the larval mosquito proteins. Dissected and fixed whole mount mosquito guts were washed 6 times in tris-buffered saline (TBS), placed in

pre-incubation medium (pre-inc) for a minimum of 1 hour, and then incubated in primary antibody (1:1000) overnight at 4°C. The guts were then washed in pre-inc and incubated in FITC-conjugated goat anti-rabbit (GAR) or Alexa-GAR secondary antibody (Jackson ImmunoResearch, West Grove, Pennsylvania, 1:250 dilution) overnight at 4°C. The whole mount preparations were rinsed in pre-inc and mounted onto slides using p-phenylenediamine (PPD, Sigma-Aldrich) in 60% glycerol. In some cases Draq 5 (Jackson ImmunoResearch, 1:1000 dilution) was applied before mounting to visualize nuclear DNA. The samples were examined and images captured using the Leica scanning confocal microscope.

Live preparations were examined, following a similar procedure, to ensure that antibodies were capable of localizing extracellular proteins only. In this case, the primary antibody was applied to the live guts for four hours. The samples were washed in TBS, and fixed as described previously, before the secondary antibody was applied. The samples were mounted on slides as described above.

The live gut assays were also performed to determine whether this specific CA is tethered to the cell membrane via a GPI linkage. Ten live gut preparations were incubated with phosphoinositol-specific phospholipase C (PI-PLC, 1:100 in HSS; Sigma-Aldrich) for 90 minutes at 37°C. PI-PLC was used as a tool in determining the presence of a GPI link. Controls in which the guts were incubated in HSS alone were also performed. The guts were then washed in HSS, fixed, and treated with primary and secondary antibodies as described above.

CA Protein Expression

Recombinant *Ae. aegypti* and *An. gambiae* CAs were produced using the pET100 vector (Invitrogen). Specific primers were designed to amplify each cDNA. The 3' primers included the sequence 5' to and including the native stop codon. The 5' primers contain the sequence CACC preceeding the native start codon for correct frame insertion (See Table 2-1 for primer sequences). PCRs were performed using 1 U of Platinum *Pfx* polymerase (Invitrogen), the gastric caeca cDNA collections as template (200 ng), 1X Pfx amplification buffer, 1.2 mM dNTP mixture, 1 mM MgSO4, and 0.3 μM of each primer in a total volume of 50 μL. A three-step PCR protocol was used consisting of 94°C for 2 minutes followed by 30 cycles of 94°C for 30 seconds, 55°C for 30 seconds, and 68°C for 1 minute.

The resultant blunt-ended cDNAs (4 μL from PCR mix) were ligated with the pET100 directional Topo vector (1 μL and 1 μL salt solution; Invitrogen) for 10 minutes at room temperature. Top 10 chemically competent *E. coli* (50 μL; Invitrogen) were transformed by incubating 3 μL of ligation mix with the cells for 30 minutes on ice, followed by a heat shock of 42°C for 30 seconds. SOC (250 μL) was added to the cells and they were then incubated at 37°C for 30 minutes with shaking. The transformation mix (100 μL) was then plated on a LB-carbenicillin plate (50 μg/mL) and incubated overnight at 37°C. Colonies were sequenced using Big Dye version 1.1 as described previously. The purified plasmids (10 ng each) were transformed into BL21 Star (DE3) cells (Invitrogen) for CA expression as described above. However, after SOC addition and incubation, the culture was transferred to fresh LB-carb (10 mL) and grown overnight at 37°C with shaking. The next day, 1 mL of culture was transferred to 100

mL of fresh LB-carb and was grown at 37°C with shaking. Optimization experiments were performed in order to facilitate the production of the greatest quantity of CA protein. For production of CA protein, isopropylthio-β-galactoside (IPTG, 1 mM final concentration; Stratagene, La Jolla, California) was added when the culture had attained an optical density of 0.5 at a 600 nm wavelength. Achieving this density took about 1.5 hours of growth at 37°C and 200 rpm. Zinc, in the form of zinc sulfate (0.5 mM final concentration), was added along with the IPTG to facilitate the proper conformation of an active CA protein. In order to optimize the duration of the induced growth phase, samples were collected every hour for six hours. These samples were analyzed on an SDS-Page 4-12% Bis-Tris gel to compare CA protein content. Four hours of growth was determined to be ideal for the production of the truncated *Ae. aegypti* CA IV-like and full-length *An. gambiae* CA II-like proteins.

Total protein was collected using the Probond Purification System according to the manufacturers instructions for soluble proteins (Invitrogen). The cells were harvested by centrifugation, sonicated in native buffer (250 mM $NaPO_4$, 2.5 M NaCl; Invitrogen) with lysozyme (1 mg/mL; Sigma-Aldrich), and centrifuged again to collect a crude protein extract. The supernatant was applied to a Probond nickel column (Invitrogen) and washed free of non-specific binding contaminants. The nickel column binds the CA protein due to the added histidine tag, a repeat of six histidine residues within the pET100 expression vector that is inserted after the carboxy-terminus of the CA protein. CA was eluted by adding imidazole (250 mM; Invitrogen) to the column, which competes with and displaces the histidine tag. Eluted fractions were separated on an SDS-Page 4-12% Bis-Tris gel (Invitrogen).

Anion Exchanger Oocyte Expression

The full-length anion exchanger (AE) sequence was subcloned into the pXOOM vector, which is optimized for both oocyte and mammalian expression (Jespersen et al., 2002; a generous gift from Dr. T. Jespersen). In addition to a T7 RNA polymerase promoter, this vector contains *Xenopus*-specific 5' and 3' UTR sequences flanking the insert in both directions. cRNA synthesis was performed using the T7 mMessage mMachine kit (Ambion, Austin, Texas), after the cDNA was linearized using PMEI.

One day after surgical removal of the eggs from the frog, the eggs were injected with either AE cRNA or water (control). After injection the eggs were incubated at 16°C for 4 days, long enough for measurable protein production and expression. The oocytes were maintained in ND96 (96 mM NaCl, 2 mM KCl, 1 mM $MgCl_2$, 10 mM HEPES, pH 7.4 with NaOH). The medium was changed daily and dead oocytes were removed.

Anion Exchanger Physiology

Expression of the *An. gambiae* AE was examined using 2-electrode voltage clamp electrodes. The voltage electrodes were pulled using 1.2 mm glass (M1B120F-3, World Precision Instruments), and showed resistances between 1-2 MΩ. Oocytes were clamped to –50 mV and stepped from –90 mV to +70 mV in 10 mV increments. The water injected eggs served as the control in evaluating any activity exerted by endogenous proteins found in the *Xenopus* oocytes. Several different solutions were used to determine the exchanger's functional activities (refer to table 2-2). The transporter blockers, 4,4'-diisothiocyanodihydrostilbene-2,2'-disulfonate (DIDS, Calbiochem, La Jolla, California) and niflumic acid (Sigma-Aldrich) were used to inhibit the transporter capabilities of the expressed AE1 protein.

***Aedes* degenerate CA primers:**										
CA5F:	5'	GAR	CAR	TTY	CAY	TKY	CAY	TGG	GG	
CA3R:	5'	GTI	ARI	SWN	CCY	TCR	TA			
N=G,A,T,C; K=G,T; S=G,C; W=A,T; Y=C,T; R=A,G										
Amplified cDNA adaptor primers:										
DAP:	5'	CGA	CGT	GGA	CTA	TCC	ATG	AAC	GCA	
TRsa:	5'	CGC	AGT	CGG	TAC	TTT	TTT	TTT	TTT	T
***Anopheles* exact CA primers:**										
Ag1CA2F:	5'	CAG	TCA	CCT	ATC	GAC	CTA	AC		
Ag1CA4R:	5'	CTC	GCG	TGT	TCA	ATG	GTT	G		
Ag4CA11F:	5'	GGA	GGC	GTC	CTT	GGC	AAC			
Ag4CA12R:	5'	CTG	CAC	TGA	CCG	GAA	GTT	G		
***Anopheles* exact AE primers:**										
AgAE1F:	5'	CCT	GGA	AGG	AAA	CGG	CAC	G		
AgAE4R:	5'	CCT	CGA	GCT	GGT	GCA	GAT	C		
***Aedes* CA Real time PCR primers:**										
5SPCAF1:	5'	GCA	ACA	CTG	CTT	CCG	TCT	ACA	A	
5SPCAR1:	5'	CCG	GTT	CGT	TAA	TAA	CTC	CAT	TG	
18s RIBF:	5'	CGC	TAC	TAC	CGA	TGG	ATT	ATT	TAG	TG
18s RIBR:	5'	GTC	AAC	TTC	AGC	GAT	TCA	AAT	GTA	A
***Aedes* CA expression primers:**										
ExCAshortF:	5'	CACC	ATG	GAC	GAA	TGG	CAC	T		
ExCAshortR:	5'	TTA	GTA	ATC	CAT	ATC	GGT	GTG	GT	
***Anopheles* CA expression primers:**										
ExCA4F:	5'	CACC	ATG	GCA	TCA	AAA	ACA	ACA	AAG	
CA4end:	5'	TTA	CAG	CTT	CGA	AAG	CAC	AAC	GG	

Table 2-1. PCR primer sequences.

Salt for 98mM value	mW	#1			#2			#3			#4		
		98N			98K			98N-Cl			98K-CL		
		mM	g/l	g/l	mM	g/l	g/l	mM	g/l	g/l	mM	g/l	g/l
Solution:			1x	4x		1x	4x		1x	4x		1x	4x
NaCl	58.44	**98**	5.73	22.91	**2**	0.12	0.47		0	0		0	0
KCl	74.55	**2**	0.15	0.60	**98**	7.31	29.22		0	0		0	0
Na Gluconate	218.1		0	0		0	0	**98**	21.37	85.50	**2**	0.44	1.74
K Gluconate	234.2		0	0		0	0	**2**	0.47	1.87	**98**	22.95	91.81
Choline Cl	139.6		0	0		0	0		0	0		0	0
$MgSO_4 7H_2O$ (120.36)	246.5		0	0		0	0	**0.5**	0.12	0.49	**0.5**	0.12	0.49
$MgCl_2 6H_2O$ (59.7)	203	**0.5**	0.10	0.41	**0.5**	0.10	0.41		0	0		0	0
$CaCl_2 2H_2O$ (110.98)	147.02	**0.5**	0.07	0.29	**0.5**	0.07	0.29		0	0		0	0
Ca Gluconate	430.38		0	0		0	0	**0.5**	0.22	0.86	**0.5**	0.22	0.86
HEPES (free base)	238.3	**10**	2.38	9.53	**10**	2.38	9.53	**10**	2.38	9.53	**10**	2.38	9.53
EGTA for Inside0out	380.4		0	0		0	0		0	0		0	0
	pH	7.2 (4M NaOH)			7.2 (4M KOH)			7.2 (4M NaOH)			7.2 (4M KOH)		

Table 2-2. Composition of all solutions used in *Xenopus* oocyte expression of *An. gambiae* AE. Total molarity and pH were kept constant in all solutions. Expression profiles were recorded in high sodium (#1), high sodium minus chloride (#3), high potassium (#2), and high potassium minus chloride (#4).

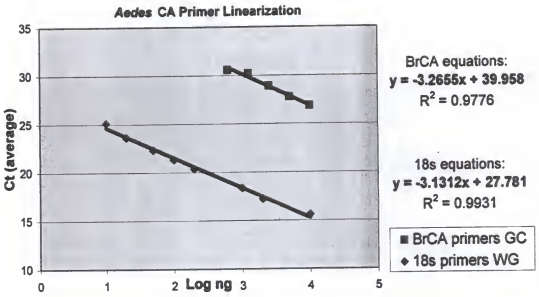

Figure 2-1. Efficiency plots for real-time PCR primers. Serially diluted cDNA samples were tested with each primer set to determine the efficiency of amplification. A linear regression was performed to determine the slope and intercept for each primer set. These values were then used in an algorithm to compare cDNA concentrations within the samples.

Figure 2-2. Three-dimensional (Cn3D) depiction of human CA IV (1ZNC). The green barrel represents an alpha helix structure, the tan arrows represent beta sheets, and the colored strings represent extended loop structures. The yellow coloring represents the accessible, extended loop peptide region against which the homologous *Ae. aegypti* CA antibody was raised.

CHAPTER 3
CARBONIC ANHYDRASE IN THE MIDGUT OF LARVAL *AEDES AEGYPTI*: CLONING, LOCALIZATION, AND INHIBITION[1]

Introduction

Bicarbonate (and ultimately carbonate) ions are produced *in vivo* primarily by the enzymatic action of carbonic anhydrase (CA). Its activity contributes to the transfer and accumulation of H^+ or HCO_3^- in bacteria, plants, vertebrates and invertebrates. Although there are innumerable reports related to the isolation of CA from vertebrates, studies involving CA from invertebrates are very rare and there are no reports of the isolation of CA from adult or larval mosquitoes.

There is strong immunohistochemical (Zhuang et al., 1999) and physiological (Clark et al., 1999; Boudko et al., 2001b) evidence that an electrogenic, basal H^+ V-ATPase energizes luminal alkalinization in the anterior midgut of the larval mosquito by producing a net extrusion of protons out of the lumen and a hyperpolarization of the basal membrane. In contrast, H^+ V-ATPase appears to be localized in the apical membrane of the posterior midgut and gastric caeca providing a reversed H^+- pumping capacity relative to the anterior midgut (Zhuang et al., 1999). A system capable of generating a high luminal pH is likely to be buffered by carbonate (CO_3^{-2}), which has a pKa of approximately 10.5.

---

[1]This chapter was slightly modified and reprinted with permission from The Company of Biologists LTD. **Corena, M. P., Seron, T. J., Lehman, H. K., Ochrietor, J. D., Kohn, A., Tu, C. and Linser, P. J.** (2002). Carbonic anhydrase in the midgut of larval Aedes aegypti: cloning, localization and inhibition. *J. Exp. Biol.* **205**, 591-602.

The purpose of this study was to determine the presence and location of CA in the midgut of larval *Ae. aegypti* and to clone and characterize the enzyme. To investigate the role of CA in the alkalization of the larval midgut, the effects of CA inhibitors were tested. Here, we report the cloning and localization of the first CA from mosquito larvae and, in particular, from the midgut epithelium of larval *Ae. aegypti*. A cDNA clone isolated from fourth-instar *Ae. aegypti* midgut (termed A-CA) revealed sequence homology to the α-carbonic anhydrases (Hewett-Emmett, 2000). Histochemistry and *in situ* hybridization showed that the enzyme appears to be localized throughout the midgut, although preferentially in the gastric caeca and posterior regions. In addition, classic carbonic anhydrase inhibitors such as acetazolamide and methazolamide inhibit the mosquito enzyme in the midgut.

Results

Bromothymol Blue Qualitative Assay

This assay allowed the identification of samples of solubilized midgut tissue containing CA activity by spotting them onto a filter paper soaked in a basic buffered solution containing a pH indicator, bromothymol blue (BTB). As stated previously, BTB changes color from yellow (at pH<7.6) to blue when the pH increases above this value. The principle behind the assay is based on the fact that CA catalyzes the conversion of CO_2 into bicarbonate with the concomitant release of protons (Donaldson and Quinn, 1974). The presence of protons lowers the pH in those regions of the paper where the spotted samples contain the enzyme. As the pH falls below 7.6, these spots rapidly change color from blue to yellow. This assay is not effective for samples in acidic solution, and the tissue homogenization must be accomplished in alkaline buffer. The

enzymatic reaction takes only a few seconds, and it can be delayed if the solutions, the paper and the samples are kept cold on ice. However, a few seconds is usually sufficient to discriminate the samples that contain CA from those lacking enzymatic activity. The assay must be performed quickly since, after approximately one minute the entire filter paper turns yellow, probably as a result of the uncatalyzed hydration of carbon dioxide absorbed by the solution at this basic pH.

The test has proved useful in determining the presence of small amounts of CA in homogenates of mosquito larvae. The assay was also used to detect CA activity qualitatively, in fractions obtained from affinity chromatography (Osborne and Tashian, 1975) of larval homogenates. The affinity chromatographic procedure, which employs a bound CA inhibitor (*p*-aminomethyl benzyl sulfonamide (*p*-AMBS); Sigma), produced two peaks of CA activity upon exposure to the standard elution buffers. The amount of protein that we were able to produce by this technique was, however, very small and resisted several efforts at direct microsequencing. This change in color was inhibited by acetazolamide and methazolamide when these inhibitors (10^{-5} M) were added to the samples prior to spotting on the dye-impregnated filter papers. Inhibition of the reaction resulted in blue spots that did not change color upon addition of CO_2. The positive control containing commercial CA turned yellow when carbon dioxide was added, and this color change was also inhibited by acetazolamide and methazolamide. This finding confirmed that the yellow color of the spots was due to the action of CA and that the mosquito larva contains active CA.

Carbonic Anhydrase Activity and Alkalization

A classic CA inhibitor methazolamide, was tested in live fourth instar larvae to examine the influence of CA on the maintenance of the pH extremes inside the midgut, and the effect of the enzyme on the net alkalinization of the growth medium by the intact animals. Previous investigations have shown that living mosquito larvae excrete bicarbonate, which results in the net alkalization of their surrounding aqueous medium (Stobbart, 1971). Equal numbers of living larvae of equivalent age and size were placed in culture plate wells containing lightly buffered medium and the pH indicator BTB. The tissue culture plates used in this assay were scanned before and after addition of various concentrations of methazolamide. In the absence of methazolamide, the blue color of the medium, indicating a pH of at least 7.6, was maintained (Stobbart, 1971). Actual measurement of the pH in each well showed a slow increase over time (data not shown). Upon addition of methazolamide, the culture medium slowly became acidic, with a resulting change in color to yellow as the pH dropped below 7.6 (Figure 3-1). All of the controls that did not contain methazolamide remained blue. Addition of methazolamide, at various concentrations, to wells containing only medium with BTB (no mosquito larva control) remained blue. These data show that CA activity is present in the living larvae and that it plays some role in acid/base excretion.

Moreover, fourth instar larvae cultured in BTB-containing medium ingest the dye, which can then be used as a visible indicator of the pH in the gut lumen. Treatment of the cultured larvae with methazolamide showed a direct impact of inhibited CA activity on gut luminal pH. Figure 3-2 compares the luminal pH of dissected larval midguts with and without a 5 hour exposure to methazolamide. The micrographs reveal that

alkalinization of the midgut was inhibited by methazolamide as shown by the color change of the BTB indicator. Interestingly, the effect was most pronounced in the anterior midgut, where the pH indicator changed from blue in the midgut of larvae reared in the absence of inhibitor to yellow in as little as 30 minutes when methazolamide (10^{-6} M) was added to the culture. The indicator also changed color progressively from blue through green to yellow in the gastric caeca (Figure 3-2). No apparent change was observed in the posterior midgut. The color of the midgut in this region was yellow both in the untreated larvae and in the larvae treated with methazolamide. Since the pH of the posterior midgut has been associated with values close to 7.6, no change in color was evident using this qualitative method.

^{18}O Isotope-Exchange Experiments

The relative activity of CA, normalized to total protein content, was calculated as described by Silverman and Tu (1986). The relative activity of CA was highest in the gastric caeca, followed by the posterior midgut and Malpighian tubules (Figure 3-3). The relative activity of CA in the anterior midgut was either extremely low or non-existent, falling at or below that of the buffer blank. The specificity of the reaction was confirmed by complete inhibition with the addition of 10^{-6} M methazolamide (results not shown).

Cloning of Carbonic Anhydrase from *Aedes Aegypti* Larvae

We utilized a cDNA cloning strategy to obtain a specific carbonic anhydrase cDNA from the midgut epithelial cells of the larval *Ae. aegypti*. A comparison of twelve CA sequences, including two putative CA sequences that had been annotated but not characterized in the *Drosophila melanogaster* databases, was made. We then produced degenerate PCR primers from consensus regions of the CA gene family. The initial 297

bp partial sequence was used to derive exact PCR primers for a modified 3'- and 5'-RACE (Frohman and Zhang, 1997, modified by Matz, 1999). Amplified cDNA pools from each region of the isolated gut, facilitated the eventual cloning of a single contiguous cDNA (Matz, 1999). The final contiguous region spanned both start and stop codons, and encoded a polypeptide of 298 residues (GenBank accession number AF395662). Figure 3-4A shows an alignment of the *Ae. aegypti* carbonic anhydrase (A-CA) amino acid sequence with several other, previously characterized members of this extensive α gene family. Figure 3-4B shows a homology tree depicting the percentage of identical amino acids between sequences, generated using DNAman software. Figure 3-5A shows the alignment between A-CA and six putative CA gene sequences from the *D. melanogaster* genome that our homology search (BLAST) revealed. Four of the *D. melanogaster* genes (AAF54494, AAF56666, AAF57140, AAF57141) had not previously been annotated. Figure 3-5B shows the homology tree generated with these sequences. A-CA has a putative molecular mass of 32.7 kDa. The translated A-CA protein sequence possesses a characteristic eukaryotic-type CA signature sequence within the polypeptide (amino acid residues 99-115; Fernley, 1988).

To examine the possibility of regionalized expression of the A-CA, PCR using exact primers was performed on amplified cDNA pools from the various sections of the gut. Figure 3-6 shows an ethidium-bromide-stained agarose gel. PCR products of the expected, 894 nucleotide length, are readily seen in the gastric caeca and the posterior midgut regions. Anal papillae (not shown), anterior midgut, Malpighian tubules and rectal salt gland showed little or no PCR product. When the PCR products were subjected to a second round of PCR using the same primers, an appropriately sized

product was also discernible in the anterior midgut. This PCR analysis also revealed higher molecular mass products in the anterior midgut and Malpighian tubules that may represent additional carbonic anhydrases specific to larval *Ae. aegypti* (Figure 3-6). This result is shown only to display the gut regions in which the A-CA clone was derived. The lack of an 894 bp product in the other gut regions may simply be due to poor quality cDNA pools from those regions. However, the cloning of A-CA from both the gastric caeca and posterior midgut regions is consistent with the location of enzyme activities described above.

Localization of the Enzyme in the Midgut Epithelium: Carbonic Anhydrase Enzyme Histochemistry

To further analyze the regional and cellular expression of CA in the midgut epithelium of larval mosquitoes, a modified Hansson's histochemical reaction was performed on whole mount preparations of the gut (Hansson, 1967). Figure 3-7 summarizes the results of this analysis. Carbonic anhydrase activity was detected in a non-uniform pattern along the length of the gut. The most intense staining was evident in the gastric caeca and the posterior midgut. Staining was less intense in the anterior midgut. At higher magnification, it was obvious that cellular heterogeneity with regard to CA activity also exists. This is particularly evident in the posterior midgut, where very large and regularly spaced cells appear nearly white on a background of dark CA reaction product. The larger cells have been characterized as "columnar" or ion-transporting cells (Volkman and Peters, 1989b). Surrounding these large cells are more numerous smaller cells termed "cuboidal" or resorbing/secreting cells (Zhuang et al., 1999). The CA histochemical stain clearly distinguishes these cells from one another and indicates that the large columnar cells contain relatively very little CA in comparison with the smaller

cuboidal cells. In addition, the distal cells of each lobe of the gastric caeca, termed Cap cells, show little or no histochemical staining, suggesting further cellular heterogeneity with respect to CA distribution in the gut (Figure 3-7).

***In Situ* Hybridization**

To further characterize the localization of A-CA expression, *in situ* hybridization was performed using a portion (approximately 300 bp) of the central coding region of the cDNA. Figure 3-8 shows typical results of this type of analysis. A strong hybridization signal was evident in the gastric caeca and the posterior midgut. Lower levels of hybridization were evident in other gut regions. As with the CA histochemical stain, higher magnification revealed that the relatively small cuboidal cells exhibit more intense labeling than do the large columnar cells (Figure 3-8B).

Discussion

The search for the enzyme in the midgut of the larval mosquito was triggered by the observations of a pH value around 11 in the anterior midgut lumen and a high bicarbonate concentration (Zhuang et al., 1999; Boudko et al., 2001b). The presence of CA in the midgut of the larval mosquito has been suggested before by investigations of the epithelium of larval lepidopteran midgut. Carbonic anhydrase has been studied in *Manduca sexta,* where the enzyme has been associated with the fat body, midgut and integumentary epithelium (Jungreis et al., 1981). The enzyme has also been localized in the goblet cells of the epithelium of *Hyalophora cecropia* using Hansson's histochemical stain. The same procedure showed that the columnar cells were devoid of activity (Turbeck and Foder, 1970).

Even though a number of genes and their products have been isolated from the midgut of *Ae. aegypti*, and the role of CA in the alkalization of the midgut has been suggested (Turbeck and Foder, 1970; Haskell et al., 1965; Ridgway and Moffett, 1986; Boudko et al., 2001b), there have been no reports of the isolation or cloning of CA or of the localization of the enzyme within the midgut of larval mosquitoes. This is the first recorded cloning of a CA from a mosquito, and is also the first to be cloned from any arthropod. Our results show that at least one (and perhaps more) CA is present in the midgut of larval *Ae. aegypti.* The CA of larval *Ae. aegypti* (A-CA) is inhibited by classical carbonic anhydrase inhibitors such as methazolamide and acetazolamide. Methazolamide has the most potent effect on A-CA. Direct physiological measurements of ion fluxes from living larval mosquito midgut epithelial cells also show methazolamide to be a very potent inhibitor of ion movements and balance (Boudko et al., 2001a).

To investigate the distribution of CA in the midgut of the larval mosquito, we employed both *in situ* hybridization and enzyme histochemistry. Our results indicate that enzymatic activity is greatest in the gastric caeca and the posterior midgut, as demonstrated by the intense staining obtained using Hansson's method and by *in situ* hybridization using cRNA probes. Measurements of activity using the ^{18}O exchange method in pools of dissected regions of the gut corroborate these findings. In addition, the enzyme seems to be preferentially associated with the small cuboidal cells in the midgut epithelium, as determined both by enzyme histochemistry and by *in situ* hybridization.

As reviewed in Clements (1992), two major cell types have been defined in the gastric caeca by inferring functional states from cytological findings. These two major cell types have been called ion-transporting cells and resorbing/secreting cells (Volkman and Peters, 1989a,b) and they correspond to the columnar and cuboidal cells mentioned above with the ion-transporting cells being equivalent to the columnar cells and the resorbing/secreting cells being the cuboidal cells (Zhuang et al., 1999). Neither of these cell types, as characterized in the larval mosquito gut, parallels the structurally unique qualities of the lepidopteran goblet cell. Nonetheless, our results indicate that, as in lepidopterans, CA activity is preferentially associated with one of two distinct cell types whose functional complementation must produce the alkalization and ionic balances regulated by the gut. These results are consistent with the observations of lepidopteran midgut by Turbeck and Foder (1970). In the larval lepidopteran midgut, two morphologically distinct cell types have been long recognized: goblet cells and columnar cells. Goblet cells posses both the proton-pumping V-ATPase and CA activity (Harvey, 1992; Ridgway and Moffet, 1986; Wieczorek et al., 1999). One of the enigmas of using the pioneering analyses of insect model systems such as *M. sexta* to produce testable hypotheses for gut alkalinization in mosquito larvae has been the apparent absence of goblet cells from mosquitoes. Previous investigations have inferred different functional cell types in the larval mosquito gut epithelium. We are currently developing antibody probes for A-CA. Immunocytochemical analyses of A-CA distribution in comparison with other key components of gut function, such as V-ATPase (Zhuang et al., 1999), should provide new insights into the cell biology of this intriguing epithelial system.

It is interesting to note that the lowest concentration of CA in the midgut epithelium occurs in the region that surrounds and probably regulates the region of highest luminal pH, the anterior midgut. The pKa of CO_3^{-2} is approximately 10.5 and, hence, this anion is likely to be the primary buffer of the pH 10.5-11 gut contents within the anterior midgut. Our results therefore suggest that the major buffering anion in this area of the midgut is probably not produced by local CA but instead either upstream, in the gastric caeca, or downstream, in the posterior midgut, where CA levels are very high. This result, and results presented elsewhere (Boudko et al., 2001a), are consistent with a model in which a major function of the anterior midgut is to pump protons out of this region of the gut lumen, promoting the conversion of HCO_3^- to CO_3^{-2}. A comprehensive model of the regulation of ion homeostasis and gut alkalization in the larval mosquito awaits the characterization and localization of other major components of the system in addition to CA. It will also be very important to resolve the question of whether multiple CAs are expressed in the midgut and how each is distributed in this dynamic tissue.

Quantitative evidence corroborating the distribution of CA within the midgut and supporting the histochemical and *in situ* observations was obtained using the ^{18}O-exchange mass spectrometric method. The results obtained with this method indicate that the gastric caeca exhibit the highest level of carbonic anhydrase, relative to total protein content, followed by the posterior midgut and the Malpighian tubules. The anterior midgut showed levels of activity so low that two possibilities could be considered: either the method could not detect the enzyme or it is absent from the anterior midgut. The presence of faint staining using the histochemical and *in situ* methods suggests that the

levels of activity in the anterior midgut might be too low to be detected using the ^{18}O method, but that the enzyme is present throughout the entire length of the midgut.

In summary, our evidence demonstrates the existence of CA in *Ae. aegypti* larvae and it also suggests that the gastric caeca and posterior midgut exhibit the highest levels of CA activity. In addition, the enzyme seems to be associated with the small cuboidal cells of the midgut epithelium. Furthermore, enzyme activity has also been detected in membrane preparations isolated from whole midguts and could be due to the presence of more than one isoenzyme. Carbonic anhydrase activity has previously been demonstrated in the epithelium of the larval midgut of six species of lepidopterans, in which it has been associated with the particulate fractions of the homogenate (Turbeck and Foder, 1970). This is consistent with our hypothesis that there might be more than one CA and that one of these enzymes may be associated with the plasma membrane.

What is the role of CA in the alkalization mechanism? BTB proved useful in monitoring the impact of CA inhibition on the maintenance of gut luminal pH and the excretion of acid/base. As mentioned earlier, *Ae. aegypti* larvae typically alkalize the medium in which they are reared by secreting bicarbonate ions (Stobbart, 1971). The ingestion of CA inhibitors altered the metabolism of the larvae to the point that the metabolic products secreted into the medium change the pH of the environment, shifting it towards more acidic values than those observed in the absence of inhibitors. The lowering of the pH of the medium might be related to a decrease in the rate of secretion of HCO_3^-. The effect of the ingestion of CA inhibitors on the secretion of bicarbonate into the medium remains to be explored. However, as indicated by measurements with ion-selective microelectrodes, inhibition of CA in the midgut has an extreme effect on the

maintenance of an alkaline pH within the midgut lumen (Boudko et al., 2001a). It is plausible that a decrease in the rate of secretion of bicarbonate is elicited by inhibiting the CA enzyme.

A simple model of bicarbonate transport fails to explain how the high pH is achieved within the anterior midgut of the larval mosquito. At a pH of approximately 11, similar to that observed within the anterior midgut, the majority of bicarbonate is present as carbonate. In fact, measurements of lepidopteran midgut fluid have shown that it contains 37 mM carbonate and 17 mM bicarbonate (Turbeck and Foder, 1970). Since the pH of a 0.1 M solution of sodium bicarbonate is only approximately 8.3, secretion of bicarbonate alone cannot be responsible for the high pH observed in the anterior midgut (Dow, 1984). It could, however, explain the pH values at the gastric caeca and posterior midgut. The mechanism for maintenance of an alkaline pH within the anterior midgut must be more complex than just a simple buffering of a physiological solution with bicarbonate. Although this mechanism has been investigated (Wieczorek et al., 1999; Zhuang et al., 1999; Boudko et al., 2001a), its details remain unclear. However, the evidence suggests that a basal, electrogenic H^+ V-ATPase energizes luminal alkalization in the midgut of larval mosquitoes (Zhuang et al., 1999; Boudko et al., 2001b). Although the electrogenic transport of K^+ drives the pH gradient, there must also be flux of one or more weak anions in the opposite direction to maintain homeostasis. Several transporters are thought to participate in this mechanism.

Another line of evidence suggests that the levels of carbon dioxide in the hemolymph of lepidopterans are lower than those within the midgut lumen. The concentration of CO_2 has been determined to be near 5 mM in the hemolymph and 50

mM in the midgut lumen in larval *Hyalophora cecropia* (Turbeck and Foder, 1970). Recent measurements using capillary zone electrophoresis of larval *Ae. aegypti* fluids have revealed a bicarbonate/carbonate level as high as 50.8±4.21 mM in the midgut lumen compared with 3.96±2.89 mM in the hemolymph (Boudko et al., 2001a). These values correlate with those observed by Turbeck and Foder (1970). This combined evidence suggests that the CO_2 that reaches the midgut lumen in the larvae of lepidopterans is rapidly converted to a mixture of bicarbonate and carbonate. The role of CA in the alkalization process would be of great significance. The generation of antibodies against A-CA will facilitate a detailed analysis of the cellular and subcellular distribution of this key enzyme in this system.

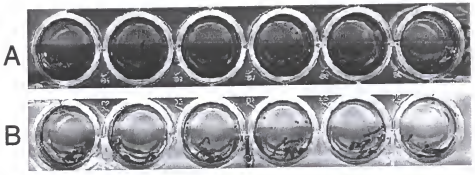

Figure 3-1. Effect of CA inhibition on culture medium pH with fourth-instar *Ae. aegypti* larvae. Mosquito larvae typically alkalize the medium in which they are reared (Stobbart, 1971). (A) Six culture wells each containing five fourth-instar larvae incubated for 5 hours in medium containing 0.003% Bromothymol blue (BTB). The blue color is retained, indicating a pH greater than 7.6. (B) The same as A, except that each well also contains a different concentration of the CA inhibitor methazolamide ranging from 10^{-6} to 10^{-3} M from left to right. A yellow color indicates a pH below 7.6.

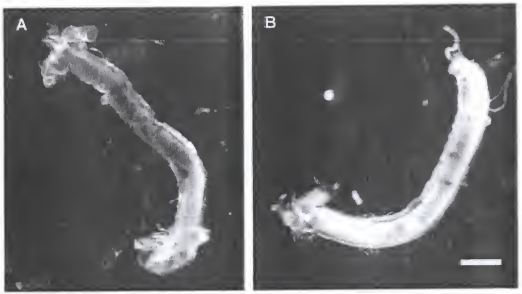

Figure 3-2. Effect of methazolamide on the alkalization of the midgut using Bromothymol Blue (BTB) assay of pH within living, but isolated, gut tissue. Gut tubes were dissected after pre-loading with BTB and then incubated for 5 hours in hemolymph substitute (Clark et al., 1999) in the absence (A) or presence (B) of 10^{-6} M methazolamide. The loss of blue coloration in B shows that the internal pH of the gut lumen has dropped below 7.6. Scale bar represents 300 μm.

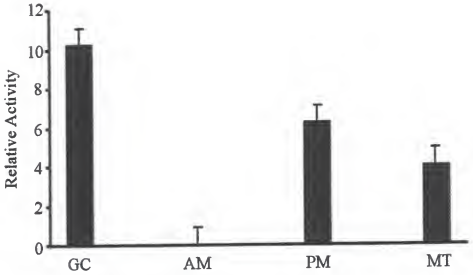

Figure 3-3. Relative activity of CA in different pooled segments of the midgut of larval *Ae. aegypti*. Midguts were dissected from early fourth-instar larvae and separated into gastric caeca (GC), anterior midgut (AM), posterior midgut (PM) and Malpighian tubules (MT). The relative activity of CA was measured using the ^{18}O mass spectrometry method (Silverman and Tu, 1986), normalized to total protein content. The activity of the anterior midgut was lower than that of the water blank and, thus, is set as "zero" activity.

A

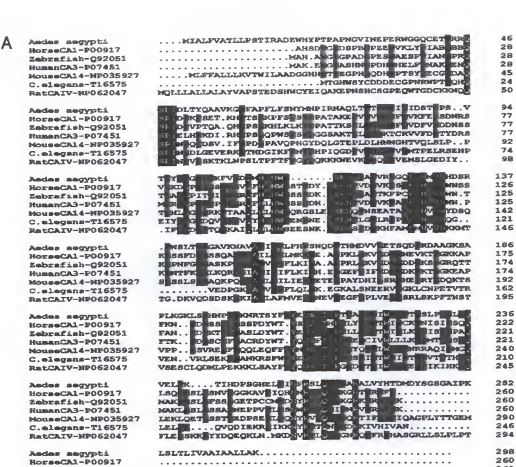

B

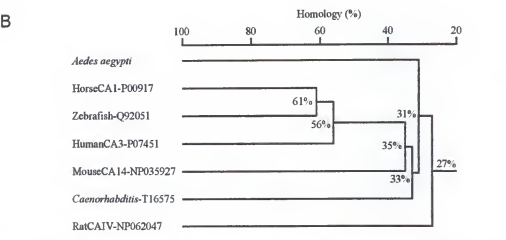

Figure 3-4. Carbonic anhydrase from the midgut of larval *Ae. aegypti*. (A) Alignment (BLAST) of the predicted amino acid sequence of *Ae. aegypti* cDNA with several known α-carbonic anhydrases. Regions of exact homology across all species are highlighted in blue (100%); regions with less homology are highlighted in red (>75%) and green (>50%). (B) A homology tree comparing A-CA and several other α-CAs (DNAman software).

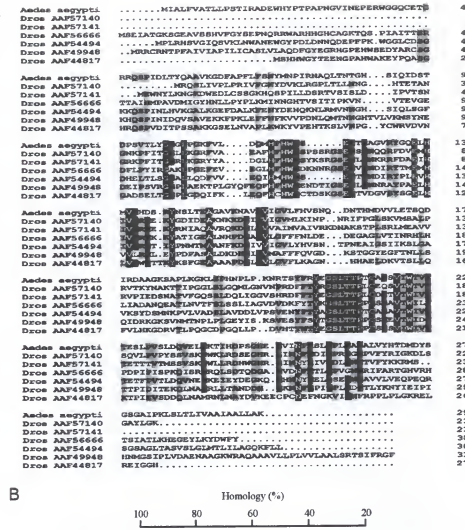

Figure 3-5. Comparison of the extrapolated amino acid sequences of A-CA with six putative dipteran CA genes identified in the *D. melanogaster* gene databases. (A) An alignment of A-CA with the amino acid sequences of the six *D. melanogaster* genes (accession numbers listed) identified through bioinformatics searching. Regions of exact homology across all species are highlighted in blue (100%); regions with less homology are highlighted in red (>75%) and green (>50%). (B) A homology tree comparison of these seven Dipteran CAs.

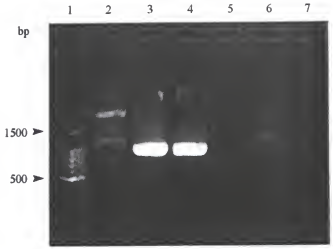

Figure 3-6. Polymerase chain reaction (PCR) analysis of *Ae. aegypti* amplified cDNA from different gut regions. PCR was performed using exact primers for the cloned A-CA. Anterior midgut (lane 2), gastric caeca (lane 3), posterior midgut (lane 4), whole gut RNA control (lane 5), Malpighian tubules (lane 6) and a water template control (lane 7) are shown. Note the primary product in gastric caeca and posterior midgut samples at the expected size of approximately 894 nucleotides. Also note the absence of this band from other gut regions but the appearance of bands of higher molecular masses. Lane 1 is a 100 bp molecular mass ladder (Promega).

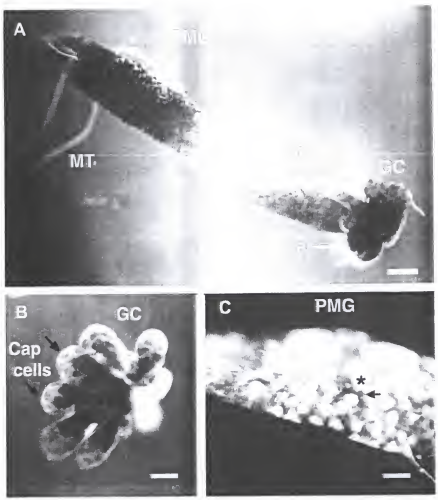

Figure 3-7. Hansson's histochemistry of whole mount *Ae. aegypti* gut. A. Intense dark staining is observed in the cardia, gastric caeca (GC) and posterior midgut (PMG), indicating CA activity. B. Higher magnification of the gastric caeca. The distal lobes of the gastric caeca (Cap cells) exhibit relatively low levels of reaction product, indicating lower levels of enzyme activity in these cells relative to other cells of the gastric caeca. C. Higher magnification of the PMG shows large, relatively unstained columnar cells (*) contrasted with the smaller stained cuboidal cells (arrow). Scale bars represent 150 μm in A and B, and 75 μm in C.

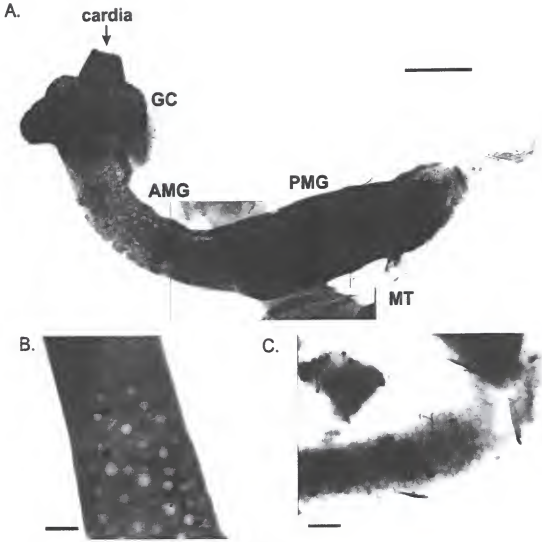

Figure 3-8. Localization of CA mRNA expression in larval *Ae. aegypti*. A. An isolated whole mount gut probed with DIG-labeled cRNA for A-CA. Abundant hybridization is observed in the cardia, gastric caeca (GC), and posterior midgut (PMG). B. The smaller cuboidal cells (arrow) display stronger hybridization than the larger columnar cells (*). C. Isolated midgut reacted with the sense (control) cRNA for A-CA. Scale bars represent 300 μm in A, 75 μm in B and C.

CHAPTER 4
A GPI-LINKED CARBONIC ANHYDRASE EXPRESSED IN THE LARVAL MOSQUITO MIDGUT

Introduction

The CA enzyme expressed in the midgut of larval mosquitoes shares some characteristics with the mammalian CA IV isozyme, including a glycosyl-phosphatidyl-inositol (GPI) link to the plasma membrane. Mammalian CA IV enzymes have been found in dynamic organs such as kidney, lung, gut, brain, eye, and capillary endothelium (Chegwidden and Carter, 2000). The human CA IV isoform was found to be as active as the CA II isoform in carbon dioxide hydration and even more active in bicarbonate dehydration (Baird et al., 1997). Studies of larval mosquito CAs are being pursued to better understand the alkaline gut system. As the anterior midgut of the larval mosquito lacks a highly active cytosolic CA II-like isozyme (previous chapter; Corena et al., 2002), the presence of a highly active CA IV-like isozyme within the mosquito gut may be able to provide the buffering capacity that is needed within the highly alkaline anterior midgut. A more detailed characterization of larval *Aedes aegypti* CA is presented in this study as well as the sequence of a homologous CA isoform from *Anopheles gambiae*. New tools and techniques, such as the generation of a mosquito-specific CA antibody and real time PCR, as well as improved methodology for *in situ* hybridization, have enabled this further analysis.

Results

Bioinformatics of *Aedes Aegypti* CA

We have previously cloned a CA cDNA from the *Ae. aegypti* midgut (accession number AF395662; Corena et al., 2002). Our initial structure prediction indicated that the protein was cytosolic. However, further characterization has indicated that this CA is actually membrane associated via a GPI-link. We have determined that the CA propeptide sequence encodes an extracellular protein with a hydrophobic tail region. The first 17 amino acids of the propeptide are predicted by the Simple Modular Architecture Research Tool (SMART) program to be the signal sequence (Letunic et al., 2002). This sequence "flags" the message for transport to the endoplasmic reticulum (ER). Using the PSORT II server, the prediction of membrane topology (MTOP) indicates that the *Ae. aegypti* CA sequence is GPI anchored. Amino acid G-276, is predicted by the GPI prediction server (Eisenhaber et al., 1999) to be the site for GPI attachment. The hydrophobic tail (L278-A289) allows translocation of the transcript through the ER plasma membrane and is also predicted to stabilize the protein with the membrane until the pre-formed GPI anchor is transferred to the protein. The hydrophobic tail is then cleaved to produce a completely extracellular protein that is tethered to the cell by the GPI link (for a review of GPI-linked proteins see Brown and Waneck, 1992).

Sequence Comparisons of CA IV-like Isoforms

I also cloned a CA IV-like cDNA from the gut of *An. gambiae*, an important vector in the spread of malaria. This CA isoform (Ensembl gene ID: ENSANGG00000018824, chromosome 2L) is partially predicted by the Ensembl CA protein family (ENSF00000000228) as 1 of the 14 gene members found in the *An.*

gambiae genome. These cloned mosquito cDNAs from *Ae. aegypti* and *An. gambiae* are 61% identical to each other in amino acid residues and show similarities to the mammalian CA IV isozyme. However, in contrast to the mammalian CA IV, which is encoded by 7 exons (Sly and Hu, 1995), only 3 exons make up the *An. gambiae* CA isoform. Alignment of the mosquito CA IV-like isoforms from *Ae. aegypti* and *An. gambiae* with various mammalian CA IV isozymes reveals conserved features within this CA isoform (Fig. 4-1). For example, the multiple leucine (L) residues within the amino terminus of the mammalian CA IV propeptides that comprise the signal sequence are found in the *Ae. aegypti* and *An. gambiae* CA IV-like isoforms. One important feature of the mosquito CA IV-like sequences is the conserved alignment of G-69 (human CA IV numbering) with the human, bovine, and rabbit CA IV sequences. This particular amino acid residue has been changed to glutamine (Q) in rat and mouse CA IV, which results in reduced enzyme activity (Tamai et al., 1996b). Additionally, all of the CA IV sequences, including the mosquito isoforms, display a hydrophobic tail region. In addition to the conserved CA IV-like features of GPI-linked proteins, there are also conserved cysteine residues (C28 and C211, human CA IV numbering) between all of these CAs (Fig. 4-1). It has been determined via cysteine labeling, proteolytic cleavage and sequencing that these two cysteine residues, in the human CA IV, form a disulfide bond (Waheed et al., 1996). A second disulfide bond is present in the mammalian CA IVs between residues C6 and C18 (human CA IV numbering; Waheed et al., 1996). This second pair of cysteine residues, and hence the resultant disulfide bond, is not present in either of the mosquito isoforms.

Although the mosquito CA isoforms display features similar to mammalian CA IVs, such as a 5' signal sequence, a hydrophobic 3' tail, and extracellular GPI expression, there is one striking difference in the amino acid composition of the mosquito CAs' active sites. The active site within all of the 14 characterized mammalian CA isoforms is tightly conserved. Three histidine residues (His-94, His-96, and His-119) are essential for CA activity through their coordinated binding of a required zinc molecule. The absence of one or more of these histidine residues results in inactive proteins called CA-related proteins (CARPs), as found in mammalian CA isoforms VIII, X, and XI (Tashian et al., 2000). The mosquito CA IV-like isoforms contain all three of the required histidine residues along with all of the other 13 highly conserved residues found in most other CAs (refer to Fig 4-1; Tashian, 1992; Sly and Hu, 1995; Tamai et al., 1996a). However, as the alignment shows in Figure 4-1, there is a conserved gap within the active site of the mosquito CAs that is not present in any of the mammalian active sites. Because this shortened active site was found in mosquitoes but was not found in any mammalian CA isoform, I searched the *Drosophila melanogaster* genome for potential CA homologs. The *D. melanogaster* genome was found to contain 14 putative CA genes (ENSF00000000228), the same number found in *An. gambiae*. One out of the fourteen *D. melanogaster* CA isoforms was found to contain the identical number of deleted amino acids as the mosquito forms within the active site region. This *D. melanogaster* CA sequence (accession number CG3940-PA) may also be a GPI-linked isoform due to the presence of a lysine-rich 5' signal sequence and hydrophobic tail region. Figure 4-2 shows an alignment of the three Dipteran CAs with shortened active site regions and all

of the human CAs, which show several additional amino acids within the conserved active site region.

Localization of CA IV-like Isoform in the Mosquito Midgut

In situ hybridization analyses indicate that the *Ae. aegypti* CA message is expressed most heavily within the epithelial cells of the gastric caeca and posterior midgut (Fig. 4-3). An antisense cRNA probe corresponding to the entire cDNA sequence generated strong cytoplasmic staining of the proximal gastric caeca, while the distal Cap cells showed no detectable hybridization (Fig. 4-3B). Rostral to the gastric caeca, a strong localization was evident in a small subset of cardia cells that encircle the tissue, forming a collar (Fig 4-3B). These "collar cells" are clearly different from the surrounding cells in this same area. This technique also highlighted a set of specific epithelial cells that are found only in a subset of the posterior midgut. These CA-positive cells form a ring of about 5 cells in width that circumscribe the lower-posterior gut region (Fig. 4-3C). The CA message was also localized to longitudinal and circular muscle fibers of the anterior and posterior midgut (Fig. 4-4). Following the longitudinal muscle fibers, in close association, are distinct nerve fibers that also show strong CA mRNA expression (Fig. 4-4). Epithelial cells of the anterior midgut were clearly void of signal beneath the labeled muscle and nerve cells. Specific staining was also evident however within the abdominal ganglia central nervous system (CNS) and peripheral nerve tissue (Fig. 4-5). No labeling was seen in the Malpighian tubules.

Real Time PCR Analysis of *Aedes aegypti* CA IV-like Transcripts

Real time PCR was used to compare the levels of *Ae. aegypti* CA mRNA within specific tissue regions of the larvae. The guts of 20 fourth instar *Ae. aegypti* larvae were

dissected and the head, gastric caeca (GC), anterior midgut (AMG), posterior midgut (PMG), and Malpighian tubules (MT) were pooled. RNA was isolated from each tissue sample for subsequent real time PCR analysis. *Ae. aegypti* ribosomal RNA (Genbank accession number M95126) was used to normalize the quantity of transcript from each sample. The results are presented in graph format in figure 4-6. Gastric caeca contain the greatest quantity of CA message within the gut sections (Fig. 4-6). The head tissue contained roughly half as much message as the gastric caeca (Fig. 4-6). The localization of CA IV-like message within the larval head is consistent with the localization of CA message to CNS tissue by *in situ* hybridization. The anterior midgut, posterior midgut, and Malpighian tubule collections showed CA message only marginally greater than zero (Fig. 4-6).

Immunolocalization of CA IV-like Protein in the Mosquito Gut

The amino terminal peptide sequence (GVINEPERWGGQCETGRR) was chosen from the *Ae. aegypti* CA sequence as an antigen for antibody production. The resultant antiserum was used to immunolocalize the CA IV-like isoform within the mosquito gut. The pre-immune serum was used as a control for all experiments. Immunoreactivity was found within the gastric caeca region of the gut as well as on muscle fibers along the anterior midgut (Fig. 4-7A). A subset of anterior muscle fibers displays the strongest and most striking labeling on their extracellular surface, while other muscle fibers show little or none. Immunoreactivity was also found within the CNS ganglia and immunoreactive nerve fibers that traverse the gut (Fig. 4-8). There was no immunoreactivity detected in the Malpighian tubules.

Antibody Cross-Reactivity with Other Mosquito Species

The 18 amino acid sequence from the *Ae. aegypti* CA, used to elicit the antibody response, shares 14 identical residues with the homologous *An. gambiae* CA protein (refer to Fig. 4-1), and therefore, the antiserum recognizes the CA IV-like isoform present in *An. gambiae* as well. The immunoreactivity within the *An. gambiae* gut displays a strikingly similar, yet species-distinctive pattern of CA IV-like protein expression (Fig. 4-7B). Similar to *Ae. aegypti* (Fig. 4-7A), not all of the muscle fibers were localized in the *An. gambiae* gut. However, in *An. gambiae* the immunolabeled muscle fiber network runs down the lateral sides of the midgut, while the dorsal and ventral muscle fibers are not immunoreactive (compare Fig. 4-7A to 4-7B).

The high sequence conservation between the chosen antigenic peptide from *Ae. aegypti* and the *An. gambiae* CA, prompted us to check other mosquito species for immunoreactivity. The other species tested also displayed the same strong labeling on a subset of anterior gut muscle fibers that included both circular and longitudinal muscle fibers. Figures 4-9 and 4-10 display the immunoreactive results obtained from *Aedes albopictus* and are representative of the results from the other mosquito species including *Ae. aegypti* and *An. gambiae*. The CA IV-like immunolabeling is clearly confined to only a subset of actin-containing muscle fibers (Fig. 4-9D). Labeled phalloidin, which binds to actin, labeled all of the muscle fibers within the gut, while the antibody for CA IV-like mosquito CA only recognized a subset of the anterior muscle fibers. The CA antibody is also specific for the extracellular plasma membrane of these muscle cells, which is clearly shown by cross-sectional analysis (Fig. 4-10). Thus, there appear to be two different sets of muscle fibers within the anterior mosquito midgut is an intriguing

discovery. This immunoreactive subset of CA-containing muscle fibers traverses the cells that surround the highly alkaline anterior gut lumen. Determining the role of these CA-specific muscle fibers holds promise for deciphering the necessary CA component of mosquito gut alkalization.

Phospholipase C Treatment

In order to validate the CA IV-like isoform cloned from *Ae. aegypti* is indeed GPI linked to the membrane, live fourth instar *Ae. aegypti* larvae were subjected to phosphoinositol-specific phospholipase C (PI-PLC) treatment and subsequent immunohistochemistry. This compound is capable of breaking the GPI-anchor and therefore severs GPI-linked proteins from the plasma membrane. Larvae subjected to PI-PLC treatment showed a decrease in CA immunoreactivity along the midgut muscle fibers, as compared to the non PI-PLC treated controls (Fig. 4-11). This evidence supports the prediction that the mosquito CA IV-like isoform is in fact GPI-linked to the outer plasma membrane.

Discussion

In this study, we show that two GPI-linked CAs are expressed in the midguts of two different mosquito species that rely on an alkaline digestive strategy. These mosquito CAs share characteristics with the mammalian CA IV isozyme, including the GPI link to the membrane. *In situ* hybridization localized CA message predominantly to the gastric caeca and posterior midgut epithelial cells, as well as muscle and nerve fibers along the anterior midgut, and CNS ventral ganglia. Real time PCR analyses confirmed the presence of CA message within the *Ae. aegypti* gut and CNS. The gastric caeca were found to contain the greatest amount of CA message in relation to the other gut samples

while the head sample contained roughly half of the gastric caeca concentration. CA immunoreactivity was most striking on specific muscle fibers of the anterior midgut, along with labeling of the gastric caeca and CNS ganglia. The localization of CA protein in a distinct subset of muscle fibers was found in several different mosquito species. This finding suggests that many mosquito species express a similar CA IV-like protein as well as confirms the immunoreactivity by only a subset of muscles. Immunolocalization of the CA IV-like isozyme within the mosquito gut and CNS also demonstrates that the CA message is being translated into protein and agrees with the localization of CA mRNA in the gastric caeca and muscle fibers. Interestingly, not all of the muscle fibers that show CA mRNA expression also show CA protein. Therefore, only a fraction of the muscle fibers that contain the CA mRNA are translating the message into protein. This may represent a form of regulation, in which the muscle fibers not expressing the CA protein could be "turned on" to translate the CA message if needed. This ability would be very advantageous if indeed this particular CA isoform is involved in buffering the alkaline gut.

The posterior midgut was also found by *in situ* hybridization to express the CA mRNA. However, both the real time PCR analysis of CA mRNA expression and the immunolocalization of CA protein failed to determine the presence of this particular CA within the posterior midgut. One explanation for this may be the inability of our CA antibody to permeate the posterior midgut tissue. However, the real time analysis, which is very specific for a region of mRNA, also did not find this particular CA message in that region. The most likely cause for the *in situ* hybridization showing a positive CA result in the posterior midgut, is the existence of a very similar CA isoform within that

region. Evidence for this is supported by genome data showing 14 different CA isoforms, all with regions of high nucleotide identity. The posterior midgut region does display CA activity, but apparently not as a result of the GPI-linked CA isoform presented here. The specific isoform or number of CAs contributing to the activity of the posterior midgut is still unknown.

We have previously shown that the application of CA-specific inhibitors dramatically decreases the alkaline gut pH, and in fact is lethal to the larval mosquitoes (Corena et al., 2002). We now present evidence that a CA found in the mosquito gut is most similar to the mammalian CA IV isozyme but contains a novel active site motif unlike any of the mammalian CA IV isoforms (Fig. 4-1). The finding of a novel CA active site within the mosquito may facilitate the construction of a mosquito-specific CA inhibitor for use in larval mosquito control. We are hopeful that the ongoing mosquito CA crystallization project will yield further significant structural differences from the mammalian CA IV structure. These differences may be useful in the design of a mosquito-specific CA inhibitor.

Out of the 14 mammalian CAs identified thus far as cytosolic, membrane-bound, secreted, and mitochondrial, only CA IV has a GPI link to the cell membrane. The localization of this highly active mammalian isozyme to dynamic tissues such as the gut, brain, kidney, and lung supports the important catalyst role of CA. It should not be surprising that the gut of a mosquito, a highly alkaline and fluctuating system, has been found to contain a presumably active CA IV-like isoform as well. The single amino acid substitution of glycine-63 to glutamine is unique to rodents (rat and mouse) CA IV, and was found to be responsible for their reduced activity rate of only 10-20% of the human

CA IV enzyme (Tamai et al., 1996b). Mutating glutamine-63 to glycine within the rodent sequence resulted in almost three times greater CA activity (Tamai et al., 1996b). Unlike the rodent sequences, both of the mosquito CA IV-like sequences display the high activity glycine residue adjacent to histidine-69 (Human CA IV numbering, refer to Fig. 4-1).

The task ahead is to decipher if a GPI-linked CA is better equipped to function in a highly dynamic system than other CA isoforms. Perhaps the GPI link affords the mosquito CA enzyme a characteristic advantage in buffering such an alkaline pH through its exclusively extracellular expression. Residing at the plasma membrane intrinsically affords this isozyme the best location for monitoring CO_2 and HCO_3^- flux. Indeed, mammalian CA IVs are expressed on membrane surfaces where large fluxes of CO_2 and /or HCO_3^- are expected (Sly, 2000). The most compelling ability of GPI-linked proteins is that they are known to elicit second messengers for signal transduction (Brown and Waneck, 1992). The alkaline pH of the larval mosquito gut was found to drop within two to three minutes after being narcotized or just simply handled (Dadd, 1975). This "handling effect" lends itself to our prediction that larval mosquitoes may exert neuronal control over the generation of the gut lumen's pH. Since a GPI-linked CA was localized within the mosquito gut and CNS tissue we propose that a GPI-linked CA may regulate the pH of the mosquito gut by severing the GPI-link and starting a signal cascade.

Further studies are being pursued within the mosquito gut to encompass the localization and characteristics of other CA isoforms as well as bicarbonate exchangers.

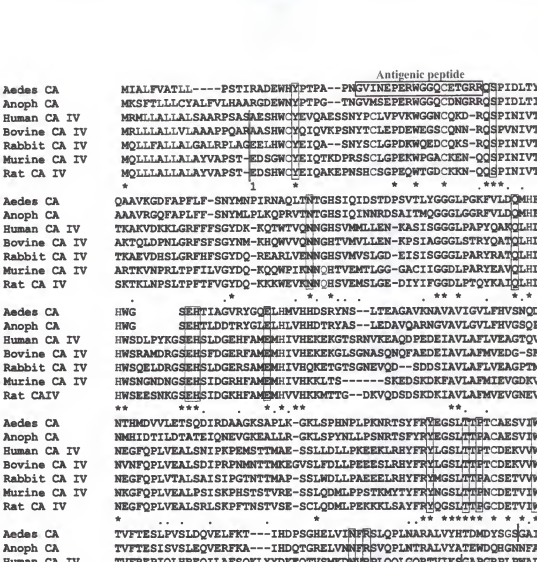

Figure 4-1. Alignment of several mammalian CA IV enzymes with two mosquito CA isoforms. The leucine-rich signal sequences are found in all aligned isoforms, along with the 3 essential zinc-binding histidines (red), and cysteine residues (green) that form disulfide bonds. The reduced activity in rodent CA IVs is caused by the glycine-69 mutation to glutamine (orange; Tamai et al., 1996b), which the mosquito CAs do not display. Important conserved residues are boxed. The position of mammalian signal sequence cleavage is shown and the following amino acid is residue #1 in the functional protein. Antigenic peptide sequence is also displayed.

```
AAL72625 Aedes CA       FVLDQMHFHWG--------SEHTIAGVRYGQELHMVHHDS
AAQ21365 Anoph CA       FVLDQMHFHWG--------SEHTLDDTRYGLELHLVHHDT
CG3940-PA Dros CA       FVVEQIHMHWW--------SEHTINDIRYPLEVHIVHRNT
P00915 Human CA I       YRLFQFHFHWG--STNEHGSEHTVDGVKYSAELHVAHWNS
P00918 Human CA II      YRLIQFHFHWG--SLDGQGSEHTVDKKKYAAELHLVHWNT
P07451 Human CA III     YRLRQFHLHWG--SSDDHGSEHTVDGVKYAAELHLVHWNP
P22748 Human CA IV      YQAKQLHLHWS--DLPYKGSEHSLDGEHFAMEMHIVHEKE
AAB47048 Human CA V     YRLKQFHFHWG--AVNEGGSEHTVDGHAYPAELHLVHWNS
CAC42429 Human CA VI    YIAQQMHFHWGGASSEISGSEHTVDGIRHVIEIHIVHYNS
P43166 Human CA VII     YRLKQFHFHWG--KKHDVGSEHTVDGKSFPSELHLVHWNA
JN0576 Human CA VIII    FELYEVRFHWG--RENQRGSEHTVNFKAFPMELHLIHWNS
AAH14950 Human CA IX    YRALQLHLHWG--AAGRPGSEHTVEGHRFPAEIHVVHLST
Q9NS85 Human CA X       HRLEEIRLHFG--SEDSQGSEHLLNGQAFSGEVQLIHYNH
AAH02662 Human CA XI    HRLSELRLLFG--ARDGAGSEHQINHQGFSAEVQLIHFNQ
AAH23981 Human CA XII   YSATQLHLHWG-NPNDPHGSEHTVSGQHFAAELHIVHYNS
BAA85002 Human CA XIV   YVAAQLHLHWG-QKGSPGGSEHQINSEATFAELHIVHYDS
                          . .          *** .        *... *
```

Figure 4-2. Clustal alignment of CA protein sequences. All characterized human CA isoforms are presented along with putative GPI-linked isoforms from *Ae. aegypti*, *An. gambiae*, and *D. melanogaster*. Three histidine residues that are required for the essential binding of zinc are shaded in blue. Note that 1 or more of these histidine residues are missing from the inactive human CA-related proteins VIII, X, and XI while all three histidines are present within the Dipteran sequences. The three CAs from Dipterans contain a shortened active site region (marked by red dashes) when compared to any of the human or other mammalian CA sequences. This difference may provide a potential target for mosquito-specific CA inhibitors, for use as larvacides.

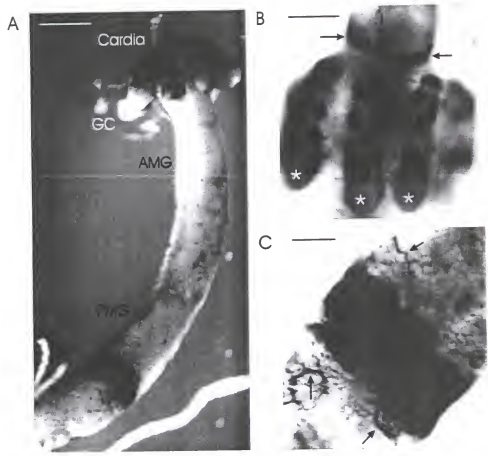

Figure 4-3. Localization of CA mRNA in a wholemount preparation of early 4th instar *Ae. aegypti*. A. The wholemount gut preparation localizes CA message to specific cells of the gastric caeca (GC) and posterior midgut (PMG). B. A subset of cardia (arrows) and gastric caeca cells display the CA message. The distal lobes of the caeca, called Cap cells, display no staining (*). C. There is a distinctive labeling pattern of CA message within a specific band of posterior epithelial cells. In addition, numerous trachea (arrows) are heavily labeled along the length of the midgut. Scale bar represents 300 μm in A, 150 μm in B, 75 μm in C.

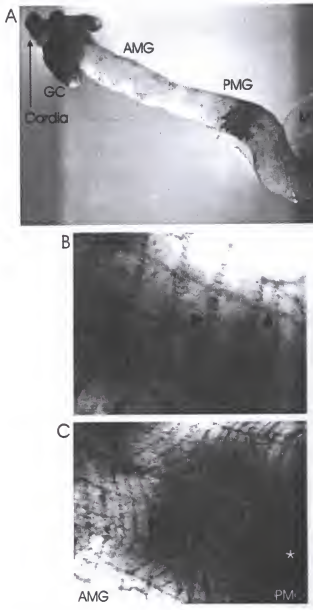

Figure 4-4. Expression of CA mRNA in *Ae. aegypti* anterior midgut. While the cardia, gastric caeca and posterior midgut display heavy epithelial hybridization, there is also specific CA mRNA expression seen in muscle and nerve cells. A. A representative whole mount *Ae. aegypti* larvae displaying the strong CA expression in epithelia, along with muscle fiber staining that can be overlooked at low magnification. B. The beginning of the anterior midgut shows hybridization to both muscle (arrowheads) and nerve fibers (arrows). The labeled fibers reveal striated muscle running longitudinally down the length of the anterior gut and circularly around the girth of the gut. C. The anterior midgut (AMG) displayed strong hybridization in muscle (arrowheads) and nerve fibers (arrows) while displaying no epithelial cell labeling. The posterior midgut (PMG) shows intense fiber labeling as well as epithelial cell labeling (*). The scale bar represents 300 μm in A, 25 μm in B, 50 μm in C.

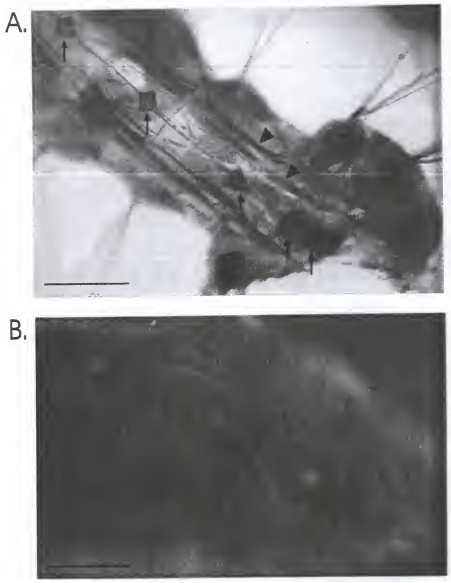

Figure 4-5. Localization of CA IV-like message within *Ae. aegypti* CNS tissue. A. *In situ* hybridization localized the CA IV-like mRNA within all ventral ganglia CNS clusters (arrows) as well as hair sensory cells (*) and longitudinal nerve fibers (arrowheads). B. The sense control probe displayed no specific hybridization. Scale bar represents 300 μm.

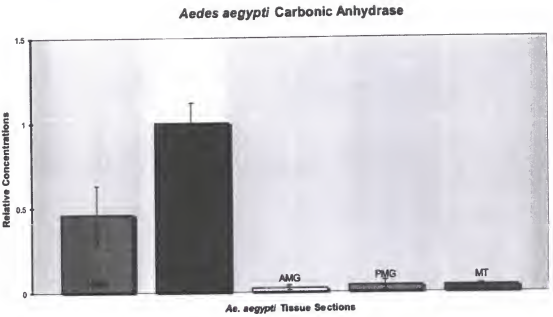

Figure 4-6. Relative quantification of CA IV-like message in *Ae. aegypti* larvae using real time PCR. The gastric caeca tissue displays the greatest amount of CA IV-like message. Data was normalized to the gastric caeca (GC) sample. The anterior and posterior midgut along with the Malpighian tubules display very little CA message. The head section displays roughly half the amount of message found in the gastric caeca.

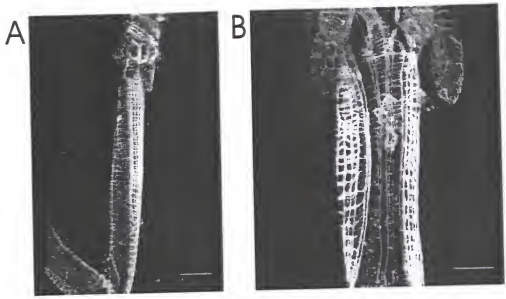

Figure 4-7. *Ae. aegypti* and *An. gambiae* CA protein labeling. The antibody generated against the *Ae. aegypti* CA can also be used to localize the homologous CA isoform within *An. gambiae*. The larvae were incubated with phalloidin (red) and the CA-specific antiserum (green). Colocalization of the red and green signals appears yellow. A. The antibody localization shows the strongest labeling in *Ae. aegypti* for a subset of muscle fibers in the anterior midgut and the proximal portions of the gastric caeca. B. Antibody localization of *An. gambiae* CA is depicted by the yellow muscle fibers, while the red muscle fibers are not recognized by the antibody. The scale bar represents 300 μm in A, 150 μm in B.

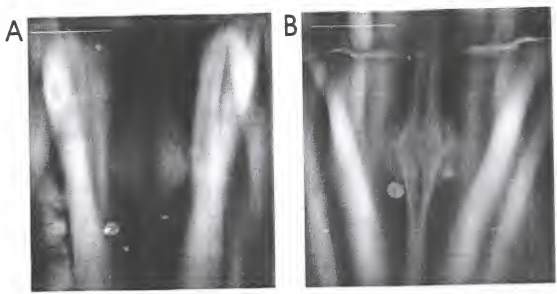

Fig 4-8. The *Ae. aegypti* CNS ganglia express the CA IV-like isoform. A. Pre-immune serum does not show any detectable labeling of the CNS tissue. B. Strong immunolabeling for the mosquito CA IV-like isoform is displayed in the ventral ganglion clusters, as displayed by the fluorescent green coloring as compared to the yellow control (pre-immune) ganglia. The scale bars represent 100 μm.

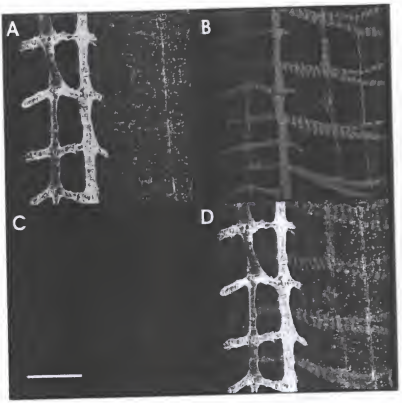

Figure 4-9. Immunolocalization of mosquito CA IV-like enzyme in *Aedes albopictus*. Muscle and nerve fibers within the anterior midgut region are heavily labeled. A. Selective labeling of particular muscle fibers (green). B. Labeled phalloidin (red) was used to localize actin and labels all muscle fibers, including those that were not recognized by the antibody against mosquito CA. C. A nuclear label (blue) was used to distinguish cell numbers present. D. Overlay of all three signals. Colocalization of the green and red signals appear yellow. The CA antibody recognizes only a subset of anterior muscle fibers, and is seen in several different mosquito species. The scale bar represents 50 μm.

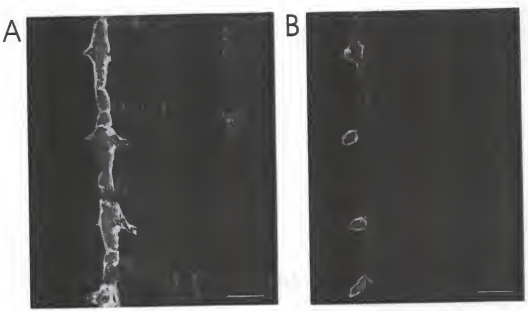

Figure 4-10. High magnification of immunoreactive muscle fibers within the *Aedes albopictus* midgut. A. Labeling of muscle fibers appears to be extracellular. B. Cross section of the same fiber demonstrates that the localization pattern is confined to the extracellular plasma membrane of the midgut muscle fibers. The scale bars represent 25 µm.

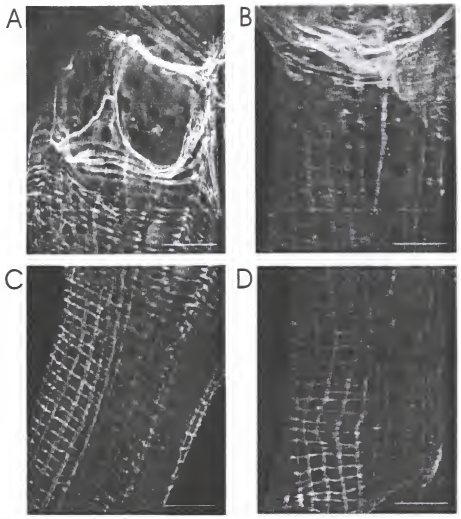

Figure 4-11. Immunoreactivity of *Ae. aegypti* guts for the CA IV-like isozyme. The red labeling is specific for muscle fibers. The green labeling shows localization of the mosquito CA IV-like protein. The yellow labeling shows co-localization of the mosquito CA IV-like isoform and actin. Prior to immunolabeling, the guts were treated with PI-PLC to determine if the CA IV-like isoforms are GPI-linked to the cell membrane. A. Immunolabeling of the gastric caeca, without the PI-PLC treatment, displays heavy yellow labeling of the GPI-linked CA isoform. B. After PI-PLC treatment there is no CA IV-like immunolabeling of the gastric caeca. C. The anterior midgut displays the immunolocalization of the CA IV-like isoform along a subset of muscle fibers. D. After PI-PLC treatment the yellow immunolabeling for the GPI-linked mosquito CA is greatly reduced. The decreased immunolocalization within the gastric caeca and anterior midgut signifies that the PI-PLC was successful in severing the GPI-link and releasing the CA from the membrane association. The scale bars represent 100 μm.

CHAPTER 5
ANION EXCHANGER EXPRESSED WITHIN THE LARVAL *ANOPHELES GAMBIAE* MOSQUITO

Introduction

The larval mosquito gut provides an ideal model for studying epithelial transport due to its cellular simplicity, being only one cell layer thick. The transport of bicarbonate within the larval mosquito gut was prompted by several studies (Boudko et al., 2001a,b; Corena et al., 2002). Bicarbonate is the main pH buffer in most complex organisms (Sterling and Casey, 2002) so it was predicted that de-protonated bicarbonate (ie. carbonate) is necessary for attaining the highly alkaline lumen of the larval mosquito midgut. However, the anterior midgut was found to apparently lack an active CA enzyme (Corena et al., 2002). An alternative to bicarbonate being rapidly produced within the anterior midgut, is the transport of bicarbonate into the anterior midgut. This alternative was supported by a previous study which implicated a chloride/ bicarbonate anion exchanger within the larval mosquito gut through the use of self-referencing ion-selective (SERIS) microelectrodes (Boudko et al., 2001b). However, the molecular identity of the chloride/ bicarbonate anion exchanger (AE) was not determined. We now present the first anion exchanger (AE) to be cloned and characterized from the *An. gambiae* mosquito, in an attempt to unravel the physiology of an extremely alkaline digestive system.

Localizing an AE within the larval mosquito gut is important because intracellular pH is known to be regulated by exchangers of bicarbonate and chloride (Phillips and

Baltz, 1999). AE localization will also distinguish whether the AE is co-expressed within the same epithelial cells as the H^+ V-ATPase and if the polarity of basal or apical expression is also the same. The localization of a H^+ V-ATPase within the larval mosquito gut was found to be apical in the gastric caeca, basal in the AMG, and then apical again in the PMG (Zhuang et al., 1999).

The highly dynamic system of alkaline digestion in the larval mosquito gut does not exist in any known mammalian system. However, mammalian organs such as the kidney are able to perform many parallel functions of the mosquito gut, such as water regulation, filtration, and ionic homeostasis. The CA, AE, and H^+ V-ATPase proteins, in particular, have been extensively studied and localized within the mammalian kidney due to their dynamic roles in acid-base balance (Huber et al., 1999; Schwartz, 2002). The co-localization and polar expression of an AE with a H^+ V-ATPase will define the epithelial cells of the mosquito gut as resembling the mammalian kidney A-intercalated cell type, the B-intercalated cell type, or the non-A non-B intercalated cell type (types as defined by Brown and Breton, 1996 and Kim et al., 1999).

Results

An. gambiae AE Sequence Analysis

The full length *An. gambiae* AE1 (AgAE1) cDNA was cloned from midgut tissue and contains 3309 bases (accession number AY280611) with a molecular weight of 123 kDa for the predicted protein. The NCBI conserved domain search tool (CDD) determined that the protein sequence was part of a family of bicarbonate transporters (BT) and cotransporters (PF00955) as well as sodium-independent chloride/bicarbonate exchangers and related sodium/bicarbonate cotransporters (KOG1172; Geer et al., 2002).

This complex of BTs contains both the solute carrier 4A (SLC4) and solute carrier 26A (SLC26A) proteins. More specifically, the EnsEMBL database places this particular AE cDNA sequence within the anion exchange/ band3 protein family (ENSF00000000189) as 1 of the 8 putative anion exchange band3 transcripts (ENSANGP00000010112) encoded in the *An. gambiae* genome. These 8 transcripts arise from 3 different genes (ENSANGG00000007623, ENSANGG00000004501, and ENSANG00000012483). The gene that gives rise to the cloned AE that we are presenting (ENSANGG00000007623) is located on chromosome 3R. The other 2 genes (ENSANGG00000004501 and ENSANG00000012483) are located on chromosome 2L (Hubbard et al., 2002; Clamp et al., 2003).

The 1102 amino acids comprising the *An. gambiae* AE form a cytosolic framework at the amino terminus while the carboxy terminus is composed of 12 transmembrane spanning domains also with an intracellular cytosolic terminus (hmmtop v.2; Tusnady and Simon 1998; Tusnady and Simon 2001). This hmmtop prediction was generated based on two assumptions: 1), that the CA binding site is within the carboxy terminus; and 2), that the C-terminus is intracellular, as is found for all known AEs. This structure is consistent with the predicted structure of the *Drosophila melanogaster* sodium dependent anion exchanger (NDAE1), which consists of a 12 membrane-spanning pattern with intracellular carboxy and amino termini (Romero et al., 2000). The highly conserved sequence identity of the *An. gambiae* AE1 with respect to the *D. melanogaster* NDAE1 allows the predictive 12 transmembrane-spanning domains of the *D. melanogaster* protein to be superimposed upon the *An. gambiae* protein (Fig. 5-1).

The amino terminus of the AgAE1 protein contains 523 cytoplasmic residues enriched with multiple binding sites for cytoskeletal proteins (Bairoch et al., 1997). The carboxy terminus contains the membrane-spanning domains that are responsible for ion transport. According to the PROSITE motif search and the hmmtop server, sites of potential post-translational modification include 2 cAMP and cGMP-dependent protein kinase phosphorylation sites, 16 protein kinase C phosphorylation sites, 11 casein kinase II phosphorylation sites, 16 N-myristoylation sites, 1 prokaryotic membrane lipoprotein lipid attachment site, and 1 leucine zipper pattern (Bairoch et al., 1997; Gupta et al., 2002). The last 82 amino acids of the *An. gambiae* AE carboxy terminus are predicted to project into the cytosol, the correct orientation that is expected for binding of a cytosolic CA. The CA II binding site comprises a hydrophobic amino acid residue followed by at least two acidic residues within the next four residues (Vince and Reithmeier, 2000). Figure 5-2 displays the CA II binding sites found in several AE proteins along with the putative CA II binding site (LDDIM) in the *An. gambiae* AE.

BT Sequence Comparisons

Following the sequence prediction that this *An. gambiae* BT is an AE, the closest characterized protein sequence is the NDAE1 (accession number AAF98636) from *D. melanogaster*. The *An. gambiae* AE1 shares 72% identity with NDAE1 (Fig. 5-3). However, the greatest similarity is with an uncharacterized splice form of NDAE1 (AAF52497) that contains an inserted sequence that is also found in the *An. gambiae* AE sequence (Fig. 5-4). Other BTs such as the sodium bicarbonate cotransporters (NBCs) and AE4 show 45%-52% identity to AgAE1, AE1-3 exhibits 36% identity, and the BTs

that are also capable of transporting sulfate (SLC26A group) show only 11% amino acid identity (Fig. 5-3).

Anion exchangers, specifically AE2 and AE3, were determined to be pH sensitive. AE3 is stimulated by intracellular alkalization whereas AE1 is not. More specifically, a region of amino acids (WRETARWIKFEE) within the carboxy terminus is responsible for the pH sensitivity seen in AE2 (Vince et al., 2000). The *An. gambiae* AE sequence in this same region contains 14 of the 16 residues found within AE2 while the other two amino acids are conserved (Fig. 5-5). AE1 shares only 8 of the 16 amino acids in this region.

Localization of Anion Exchanger mRNA in *An. gambiae* Larvae

A DIG-labeled antisense cRNA probe comprising the full length AE cDNA was employed to localize the AgAE1 mRNA. A DIG-labeled sense probe was used as a control. The AgAE1 mRNA was found in every region of the larval gut including gastric caeca, anterior midgut, posterior midgut, Malpighian tubules, and rectum (Fig. 5-6). In the gastric caeca and posterior midgut regions, the probe was localized to epithelial cells. Within the gastric caeca the labeling is most intense in the area where the lobes face the lumen. The gastric caeca labeling was confined to the proximal cells, whereas the Cap cells displayed no label (Fig. 5-6A,B). The rectum displayed staining in a small subset of epithelial cells along with tracheoles (Fig. 5-6D).

Muscle, nerve, and trachea cells that traverse the outer plasma membrane of the anterior gut epithelial cells were labeled with the AE antisense probe (Fig. 5-7). Labeled tracheal fibers are displayed in close association with the gastric caeca (Fig. 5-8). These

trachea extend from the gastric caecal region and become incorporated with the anterior midgut where they are intimately associated with nerve fibers (Fig. 5-9).

The third abdominal segment marks the beginning of the posterior midgut and is located by the fourth pair of trachea that connect to this part of the midgut. This junction displays a marked contrast in AgAE1 mRNA transcript expression. Strong staining of the epithelial cells begins here, coinciding with the beginning of the posterior midgut and change in epithelial cell morphology (Fig. 5-10). Along with small epithelial cell labeling, tracheal fibers also display strong label for AgAE1 mRNA within the posterior midgut. The larger type of epithelial cell within the posterior midgut, the columnar cell, shows extensive labeling for AgAE1 mRNA expression, with signal localized near the plasma membranes (Fig. 5-10B). The extreme end of the posterior midgut displays strong labeling within a cluster of small epithelial cells known as cuboidal cells (Fig. 5-11). Cellular processes that extend rostral and lateral from these cells are also labeled. All cells of the Malpighian tubules label positively for AgAE1 transcript expression (Fig. 5-12).

AgAE1 mRNA expression is also localized to the ventral midgut ganglion. Each ventral ganglion displays specific labeling within one or two longitudinally directed neurons that traverse the same plane (Fig. 5-13). No other neuronal cells display signal for AE mRNA expression. The labeling is very specific for precisely one neuronal pathway within each ganglion (Fig. 5-13). The sense (control) DIG probes display no hybridization (Fig. 5-14).

Antibody Localization of AE Protein

Two antigenic peptide sequences (EVRKRPPEKNPKEEIDEE and KPKQQPVTTISVTKVAEQ) were chosen from the cytosolic framework of the amino terminus and the anion exchange carboxy terminus respectively, of the translated AE cDNA (accession number AAQ21364). Chickens were used to produce antibodies against these antigenic peptides. The resultant chicken antisera were used to localize the AgAE1 protein within whole mounts of the *An. gambiae* fourth instar larvae. The AgAE1 protein was localized to the plasma membranes of the gastric caeca (Fig. 5-15) and posterior midgut epithelial cells (Fig. 5-16). A three-dimensional reconstruction of the cellular localization of AgAE1 enabled us to discriminate the immunolabeled basolateral membranes from the non-labeled apical membranes. Antisera for both peptides displayed the same basolateral immunolocalization pattern. Neuronal cells within the AMG displayed immunoreactivity (Fig. 5-17). Pre-immune sera displayed no specific immunoreactivity.

AE Functional Expression in Oocytes

In order to ascertain the functional characteristics of the AgAE1, the protein was expressed in *Xenopus* oocytes. The AgAE1 was subcloned into the pXOOM vector (Jespersen et al., 2002; generous gift from Dr. T. Jespersen) for oocyte expression. The *Xenopus* oocytes were injected with either AgAE1 RNA or water to serve as the control. Three to seven days post-injection the oocytes were tested for AgAE1 expression using two-electrode voltage clamp electrophysiology. Oocytes expressing AgAE1 displayed a decreased volume as compared to the water-injected controls (T. Seron, unpublished observation), which correlates with the AE regulatory functions of cell pH and volume.

The AgAE1 was determined to be a functional protein with the capacity to transport chloride. No sodium ion or potassium ion dependence was determined with the voltage clamp assay. A comparison of current versus voltage (I-V plots) for both the AgAE1 expressing oocytes and the water injected controls are compared when two different bath solutions are applied to the oocytes. The I-V plots for the water-injected controls displayed no transport with or without chloride (Fig. 5-18A). When the solution contains chloride (N98), the AgAE1 expressing oocytes are capable of transporting chloride, as seen by the steep rise in current (Fig. 5-18B). When chloride is replaced by a non-ionic equivalent (N98-Cl) there is no transport (Fig. 5-18B). The transporter blockers, 4,4'-diisothiocyanodihydrostilbene-2,2'-disulfonate (DIDS) and niflumic acid (NA) both inhibited the transport capabilities of the expressed AE1 protein (NA not shown). The application of DIDS inhibited the transport of chloride such that the I-V plot showed an affect similar to the removal of chloride ions from the bath solution (Fig. 5-19A). The likeness of removing chloride and the inhibitory affect of DIDS is easily viewed by comparing the differences in current between the DIDS inhibition and the removal of chloride (Fig. 5-19B). When the difference between chloride and chloride removal are compared to the blocked and chloride removal transport, a large difference can be seen (Fig. 5-19B). Activity of the mosquito AE1 was also inhibited when the CA-specific inhibitor acetazolamide was added to the media (data not shown). Because acetazolamide is known to have no direct inhibitory effect on AEs, unlike other sulfonamides, it can be inferred that the AgAE1 is inhibited by acetazolamide due to its tight coordination and regulation by endogenous CA, as was found to be the case in mammalian systems (Sterling et al., 2001a). Endogenous CA was bound by mammalian

AEs when they were expressed in HEK293 cells, and was shown to increase the rate of bicarbonate transport. Furthermore, co-expression with mutant CA II (non-active) was shown to result in decreased bicarbonate transport due to the displacement of the active endogenous CA. The CA II binding motif found in this mosquito AE could similarly bind the oocyte's endogenous CA, also resulting in an increased transport rate. This may explain the inhibition seen in AE transport when acetazolamide was applied. AgAE1 expression studies in oocytes are presently ongoing to further assess the function and inhibition of this protein.

Discussion

An AE cDNA was cloned from fourth instar, larval *An. gambiae* gut tissue. The translated 123 kDa protein is predicted to consist of intracellular amino and carboxy termini and 12 transmembrane segments. *In situ* hybridization and antibody immunolocalization identified AE mRNA message expression and protein localization within epithelial cells of cardia, gastric caeca, posterior midgut, rectum, and Malpighian tubules as well as tracheal, nerve, and muscle cells. Expression of AgAE1 in *Xenopus* oocytes displayed a reversible transport of chloride.

The most similar characterized protein sequence is the NDAE1 from *D. melanogaster*. *Xenopus* oocyte expression with pH analysis determined that this protein was sodium ion dependent. The *An. gambiae* AE1 protein has 72% sequence identity to the NDAE1 but does not display sodium ion dependence. The carboxy termini of these proteins show little similarity and therefore the carboxy terminus of NDAE1, unlike AgAE1, may contain the necessary domain for sodium ion dependence (refer to Fig. 5-4).

In *Xenopus* oocyte expression tests of AgAE1, activity was decreased with a CA-specific inhibitor, acetazolamide. Bicarbonate, rapidly formed by the hydration of carbon dioxide by CA, is a substrate for the AE. The decreased ability to exchange ions in the presence of acetazolamide leads to the prediction that this mosquito AE is directly regulated by CA activity. There is evidence within the mammalian system for the tethered coordination of anion exchangers with carbonic anhydrase. The mammalian anion exchanger (AE1/ band3) has been shown to interact with and actually bind to CA II at its carboxy terminus (Sterling et al., 2001b). AEs and in fact all bicarbonate transporters (except DRA) identified to date have potential CA II-binding sites at their carboxy termini (Sterling et al., 2002b) including this *An. gambiae* AE. The inhibitory effect of acetazolamide on AgAE1 expressed in *Xenopus* oocytes suggests that this mosquito AE is coupled with an active CA enzyme, speculatively an endogenous *Xenopus* CA protein. A protein complex consisting of a membrane-spanning AE and a cytoplasmic CA has the ability to maintain tight pH homeostasis both inside and outside of the cell at the same time. Furthermore, this complex brings together bicarbonate production and transport in such a way that virtually all lag time is abolished by the tethered coordination of the system (Sterling et al., 2001b). This type of bicarbonate transport metabolon, if found to exist within the mosquito, may explain how the mosquito gut is capable of driving and supporting a pH greater than 10 within the lumen while sustaining a near neutral pH within the adjacent cells. Now that an AE has been localized to CA active regions within the mosquito gut, namely the gastric caeca and posterior midgut, it will be necessary to determine whether they form a bicarbonate metabolon as proposed.

Several acid-base controlling proteins have now been identified within the mosquito gut (Zhuang et al., 1999; Corena et al., 2002). The distribution of these proteins along the length of the mosquito gut is both heterogeneous and discontinuous. Along the length of the gut, non-adjacent regions such as the gastric caeca and posterior midgut display similar protein expression and CA activity, while the region that separates them, the anterior midgut, displays a different pattern of protein expression. This is not surprising as the highly alkaline pH of the anterior midgut also contrasts with the nearly neutral pH of the flanking gut regions. The most intriguing part of the novel expression profile of these mosquito proteins is the parallel expression profile for the same proteins within the mosquito midgut and the well-characterized mammalian kidney. As characteristic of most epithelia, the epithelial cells found in both the mammalian kidney and the mosquito midgut share several specific morphological features. Both populations are mitochondria-rich, display apical microvilli, contain active cytosolic CA activity, and express a proton translocating H^+ V-ATPase on specific domains of their plasma membranes (Clements, 1992; Sterling et al., 2001a). Similarly, cell polarity proteins can also be compared between the A (alpha) intercalated cells of the collecting tubules of the mammalian kidney and the mosquito epithelial cells of the gastric caeca and posterior midgut. The A cell subpopulation of kidney intercalated cells expresses, and is defined by, an apical H^+ V-ATPase, and a basolateral AE (Matsumoto et al., 1994). The epithelial cells of the gastric caeca and posterior midgut also express an apical H^+ V-ATPase (Zhuang et al., 1999), and a basolateral AE. Furthermore, B (beta) intercalated cells of the mammalian kidney are defined by a H^+ V-ATPase expressed within the basolateral plasma membrane and an apical AE. This apical AE is different from AE1,

but has yet to be cloned and characterized (Kim et al., 1999). Like B cells, anterior mosquito midgut cells have been shown to express a basolateral H^+ V-ATPase whereas expression of AgAE1 was absent from this region. The closely associated A and B intercalated cells of the mammalian kidney are known to function in acid secretion and bicarbonate secretion, respectively. Interestingly, the bicarbonate-secreting moiety, for which the function of the B cell is defined, is unknown.

The co-occurrence of these A and B cell types provides for the tight regulatory control of the maintenance of near-neutral pH in the kidney. Perhaps the pH differential of 4 units, as seen in the mosquito anterior midgut, is achieved by the decoupling of these cell types. In the mosquito gut, the A-like cells of the gastric caeca and posterior midgut translocate protons toward the lumen and reduce the alkaline pH to near neutral levels. The B-like cells of the alkaline anterior midgut secrete bicarbonate and protect the cells from the high lumenal pH. Although the presented AgAE1 is not that moiety, the parallels between cells of the mammalian kidney and the mosquito midgut are evident. The similarities between epithelial cells of the mammalian kidney and the mosquito midgut support the use of the mosquito midgut as a simple model in which to study cell polarization, pH balance, protein targeting and trafficking, as well as disease states. The decoupling of A and B intercalated cells, as they may exist in the mosquito midgut, provides an excellent model for studying human diseases such as distal renal tubular acidosis, which is caused by mutations in either the basolateral AE1 or different subunits of the apical H^+ V-ATPase (Alper, 2002).

The simple epithelium of the mosquito midgut may continue to reveal mechanisms and pathways that also function within the complex metabolic network

comprising the mammalian kidney. Many studies have sought to determine specific amino acids responsible for pH sensitivity within the anion exchangers. The sixteen amino acid pH sensitive region of AE2 is almost identical to the comparable region within the AgAE1 sequence (refer to Fig. 5-5). The mosquito midgut provides an excellent model for studying precisely the pH dependent moieties and proteins due to the large pH gradient that it supports. The one cell layer epithelium that divides the alkalinity of the lumen (pH 11) from the neutral pH of 7-8 within the cell cytosol has yet to reveal the cell polarity that is capable of maintaining this system.

The elucidation of such a metabolon within the mosquito gut, in which an AE is directly tethered to one or more CAs, such as in the mammalian system (Sterling et al., 2001a), would provide a mosquito model which could be used as a simple framework for uncovering metabolic networks within complicated mammalian systems such as the kidney.

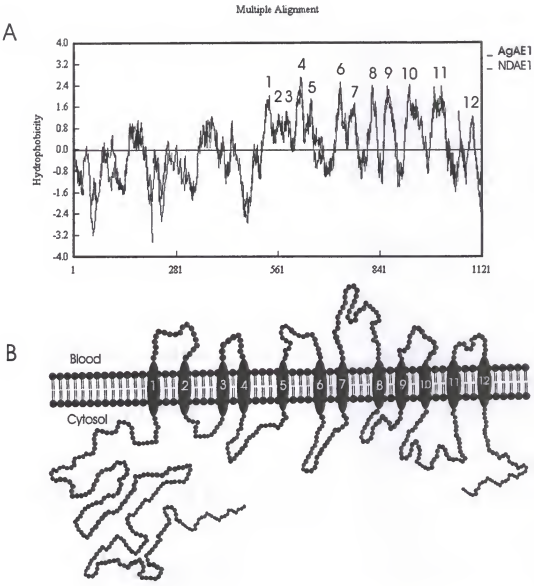

Figure 5-1. Structural prediction of the *An. gambiae* AE1. A. Hydrophobicity plot of the DNAman-aligned *D. melanogaster* NDAE1 and *An. gambiae* AE1 sequences suggests a nearly identical protein topology of 12 membrane-spanning domains in both proteins. B. Illustration depicting the intracellular location of both protein termini as well as the predicted 12 transmembrane domains.

```
AgAE1 [AAQ21364]      LDYIFTKRELKILDDIMPEMTKRARADDLHQLEDGEVG
Human AE1[P02730]     LPLIFRNVELQCLDADDAKATFDEEEGRDEYDEVAMPV
Human AE2[P04920]     LTRIFTDREMKCLDANEAEPVFDEREGVDEYNEMPMPV
Human AE3[NP005061]   LPRLFQDRELQALDSEDAEPNFDE-DGQDEYNELHMPV
Human AE4[Q96Q91]     LERVFSPQELLWLDELMPEEERSIPEKGLEPEHSFSGS
                      *  .*   *.  **
```

Figure 5-2. Putative amino terminus CA II binding motif. The highlighted conserved leucine (L) was shown to be necessary for the specificity of CA binding in AE1 (Vince et al., 2000) and is also present in AgAE1. The motif consists of at least two acidic amino acids within the four residues following the conserved non-polar L. The ability of AEs to bind CA enzymes greatly raises their ability to regulate ionic homeostasis. Identical residues (*) are noted in the alignment as well as conserved residues (.).

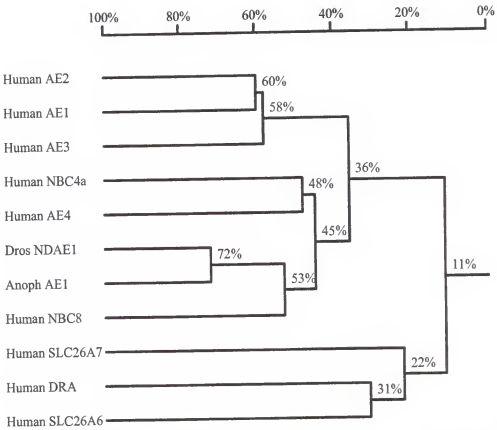

Figure 5-3. Homology tree depicting the amino acid identity between several BTs. The *An. gambiae* AE1 amino acid sequence displays the closest identity to the *D. melanogaster* NDAE1 (AAF98636) and human NBC8 (NP004849) sequences with 72% and 53% identity, respectively. The human AEs display 36% to 45% identity while the sulfate transporters (SLC26 group) display only 11% identity to AgAE1. Accession numbers: human AE2 (P04920), human AE1 (P02730), AE3 (NP005061), NBC4a (NP067019), AE4 (Q96Q91), SLC26A7 (NP439897), DRA (P40879), and SLC26A6 (Q9BXS9).

```
AgAE1 AAQ21364   MMDEGVVDEEAPIDPRLKNRTFTADQD----------FEGHRAHTVFVGVHIPGSSR  47
Dros  AAF52497   -----MAEKNEYIELPWTMNSSSGDDEAPKDPRTGGEDFTQQFTENDFEGHRAHTVYVGVHVPGG-R  61
NDAE1 AAF98636   -----MAEKNEYIELPWTMNSSSGDDEAPKDPRTGGEDFTQQFTENDFE----------  24

AgAE1 AAQ21364   RHSQRRRHKHHQASRENGDKGSTG----------SEAERPVTPPAQRVQFILG  90
Dros  AAF52497   RHSQRRRKHHHSGPGGGGGGGGGGSIGGSGSVGGGAGKDNVSEKQQEVERPVTPPAQRVQFILG  126
NDAE1 AAF98636   ----------VTPPAQRVQFILG  57
```

Figure 5-4. Alignment of carboxy terminus amino acids of *An. gambiae* and *D. melanogaster* AEs. The characterized *D. melanogaster* NDAE1 (AAF98636) is 72% identical to our *An. gambiae* AE1 sequence. The greatest number of amino acid differences occurs at the carboxy terminus, the regulation domain. However, an uncharacterized splice variant of NDAE1 (AAF52497) displays an inserted sequence at the carboxy terminus that the characterized protein does not. This inserted sequence shows similarity to the AgAE1 sequence and therefore is the closest predicted protein to AgAE1.

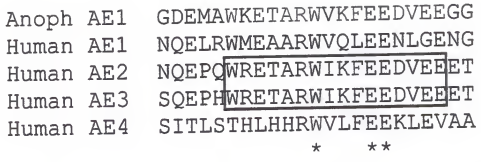

Figure 5-5. Alignment of *An. gambiae* and human AEs. pH sensitivity of AE2 (P04920) and AE3 (NP005061) was mapped to the boxed 16 amino acids shown (Vince et al., 2000). Unlike AE3, AE1 (P02730) was not stimulated by intracellular alkalization (Vince et al., 2000). The *An. gambiae* AE1 (AAQ21364) sequence shows a strong similarity to the identified amino acid sequence and has 14 identical residues. The human AE1 sequence has only 8 identical residues. pH sensitivity of an AE within the mosquito gut would be an important attribute due to the regional compartmentalization of the pH flux. The recently identified AE4 (Q96Q91) was included in this alignment for completeness. It displays the least conservation with only 6 identical residues. Stars indicate identical residues within all aligned sequences.

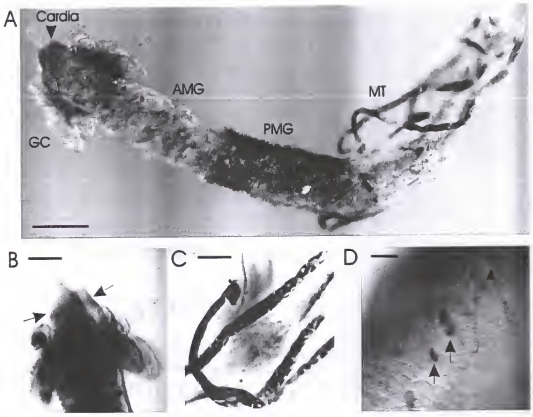

Figure 5-6. Localization of AgAE1 mRNA within whole mount *An. gambiae* larvae. A. Gastric caeca (GC), posterior midgut (PMG), and Malpighian tubules (MT) show extensive expression while other gut regions display more restricted hybridization. B. The gastric caeca as well as the cardia region (arrows) display label. C. Extensive expression of AgAE1 mRNA in the Malpighian tubules. D. Specific cells (arrows) and trachea (arrowheads) of the rectum show expression of AgAE1. Scale bars represent 300 μm in A, 100 μm in B, and 25 μm in C and D.

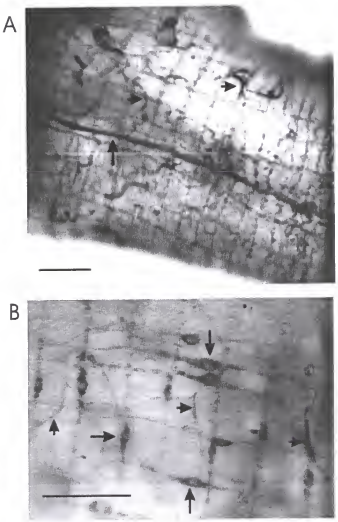

Figure 5-7. Localization of AgAE1 mRNA in muscle, nerve, and trachea in *An. gambiae*. A. The whole mount gut preparation localizes AE message to specific muscle, nerve (long arrow), and trachea (short arrow) fibers of the anterior midgut (AMG). B. A high magnification of the AMG region detailing the tracheal fibers (short arrows) and neuronal cells (long arrow) that express the AgAE1 message. Scale bar represents 75 μm in A and B.

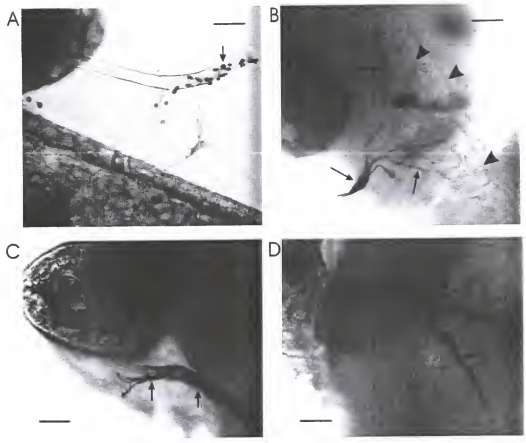

Figure 5-8. *In situ* hybridization of AgAE1 in whole mount *An. gambiae* consistently shows positive labeling of tracheal fibers along the midgut. A. A thick tracheal stalk penetrates the gastric caeca while thinner branches join the AMG. This main tracheal stalk that is closely associated with the gastric caeca consistently displays labeled particles that may be secretory vesicles (arrow). B. Labeled trachea (arrows) traverse the AMG and coincide with labeled nerve fibers (arrowheads) that extend down the midgut. C and D. Labeled trachea (arrows) are randomly associated with the area surrounding the gastric caeca. Scale bars represent 25 μm.

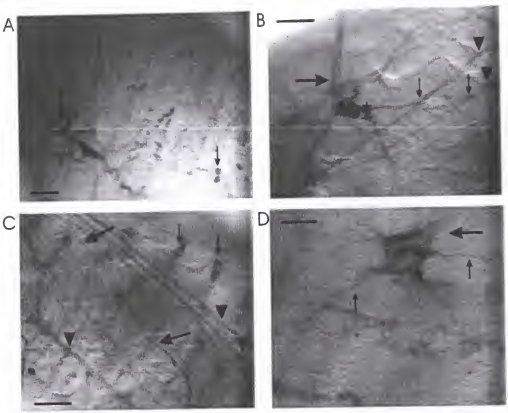

Figure 5-9. Anion exchanger mRNA localization reveals trachea and nerve fibers along with neuronal cell labeling. A. Trachea (large arrow) display a random pattern of distribution on the *An. gambiae* midgut along with pairs of neuronal cells (small arrows). B. A labeled tracheal stalk (large arrow) shows abundant labeling where it joins with the midgut (*). The finer branches of the trachea can be seen joining (small arrow) the parallel nerve fibers (arrowhead) that also display label. C. Neuronal cells (small arrows) scattered over the AMG display AE label along with the nerve (arrowheads) and tracheal fibers (large arrows). D. Strong labeling is consistently seen where the thick trachea connects to the midgut (*) and sends out smaller trachiole fibers (arrows). Scale bars represent 25 μm in A, 50 μm in B, 50 μm in C, and 50 μm in D.

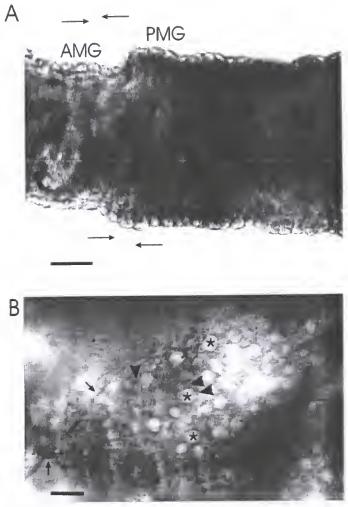

Figure 5-10. Localization of AgAE1 mRNA to the PMG of larval *An. gambiae*. A. The whole mount gut preparation displays the unlabeled AMG on the left side of the photo as compared to the labeled PMG on the right side of the photo. The arrows point to the tracheal stalks that join the gut at the third body segment, corresponding to the beginning of the PMG region. B. Outer margins of large columnar PMG cells display AE mRNA labeling (*) along with labeling of tracheal fibers (arrows) and small cuboidal cells (arrowheads). Scale bar represents 50 μm in A, 25 μm in B.

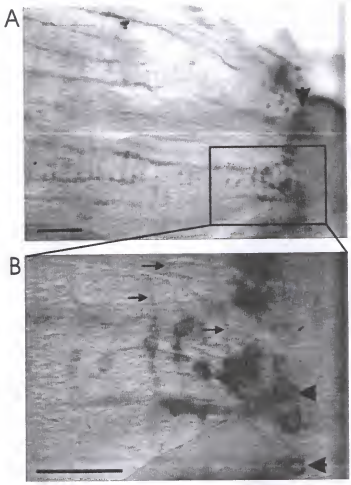

Figure 5-11. Larval *An. gambiae* displays strong AgAE1 expression in the hindgut, the pylorus. A. Distal to the joining of the Malpighian tubules with the gut, the pylorus displays pronounced labeling of small epithelial cells (arrowhead) and closely-associated muscle fibers. B. Higher magnification of the boxed region displays labeled epithelial cells (arrowheads) of the pylorus with closely associated circular muscle fibers (arrows) that form a pyloric sphincter. The pylorus, a part of the hindgut, functions in ionic and osmotic regulation. Scale bars represent 25 μm in A and B.

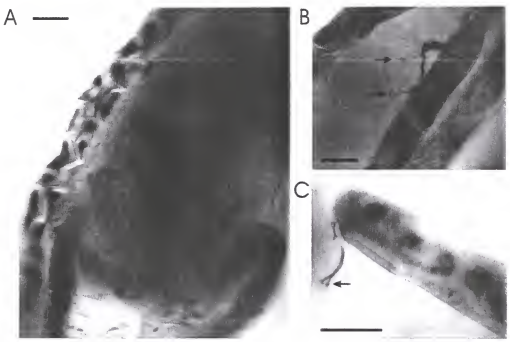

Figure 5-12. Localization of AE mRNA in *An. gambiae* shows abundant labeling of the Malpighian tubules. A. The entire length of the Malpighian tubules displayed labeling of AE mRNA. B. Labeled tracheal fibers are also associated with the Malpighian tubules. C. Labeled tracheal fibers also extend from the tips of Malpighian tubules and may contain secretory vesicles (arrow). Scale bar represents 25 μm in A, B, and C.

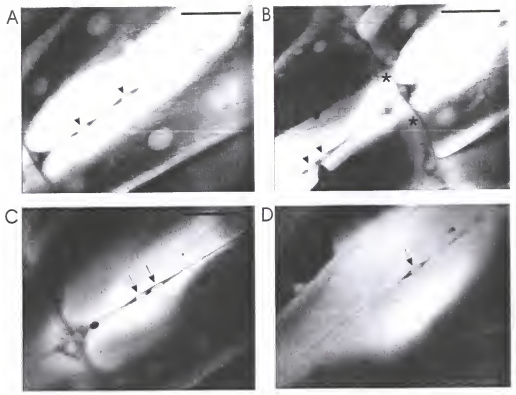

Figure 5-13. Expression of AE mRNA was found throughout the ventral midgut ganglia. Between the ventral midgut and the ventral integument a labeled neuronal pathway connected each ganglia to the next. A. Two neurons (arrows) label positively for the AE mRNA, rendering them highly visible above the other neuronal cells within the unstained ganglia. B. Between each ganglia cluster, a tissue crossbridge (*) passes in a 90° angle between the ganglia and the gut. The neuronal pathway showing AE mRNA expression makes contact with this junction and continues on to the next ganglia cluster on the other side. C. Two neuronal cells within the following ganglia show clear expression of AE mRNA. D. This panel shows an unobstructed view of a single triangular-shaped ganglia cluster. It is clear that the AE mRNA is located within a distinct population of neuronal cells in each ganglion. Scale bars represent 50 μm.

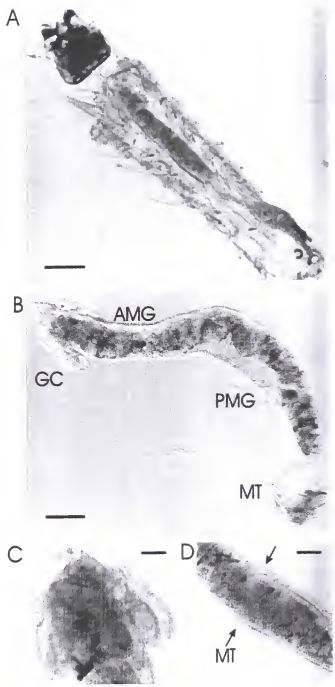

Figure 5-14. Sense AE probes display no specific hybridization. A. These whole mount preparations show no AE sense (control) label in the integument, midgut or hindgut (B). A higher magnification of the gastric caeca (C) and posterior midgut (D) with Malpighian tubules (MT) shows no hybridization with the sense AE probe. These experiments were performed side by side with the antisense probes and therefore length of exposure was identical. Scale bars represent 600 μm in A, 300 μm in B, 100 μm in C, and 100 μm in D.

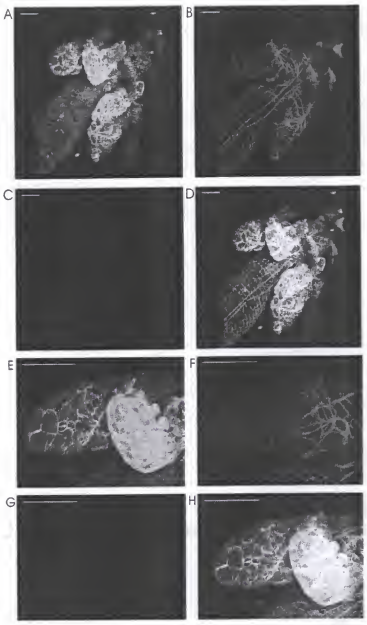

Figure 5-15. Antibody localization of AgAE1 protein to the gastric caeca in *An. gambiae* larvae. A. Our AE specific antibody displays immunoreactivity within the cardia (*) and gastric caeca. B. Phalloidin was used to label the actin-containing muscle fibers throughout the mosquito gut. C. Draq-5 was used to label nuclear DNA. D. Three signal overlay depicting the AE protein in relation to muscles and cell nuclei. E-H shows higher magnification views of the gastric caeca with the same labeling profile as in A-D. AE protein expression can be seen on plasma membranes (arrows) of the gastric caeca (E). Scale bars represent 25 μm in A-D and 100 μm in E-H.

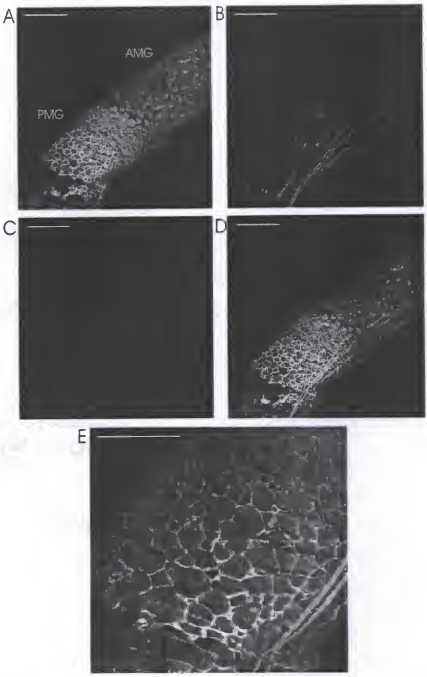

Figure 5-16. Localization of AgAE1 protein within the PMG of *An. gambiae* larvae. A. Our AE specific antibody displayed immunoreactivity within the PMG; most prominantly within a specific band of cells that encircle the PMG region. B. Phalloidin was used to label muscle fibers. C. Draq-5 was used to localize nuclear DNA. D. Overlay of AE labeled cell membranes in relation to muscle fibers and nuclei. E. High magnification of AE protein localization within the PMG. Cell membranes of both large and small cells are clearly labeled with our antibody. Scale bars represent 150 μm in A-D and 75 μm in E.

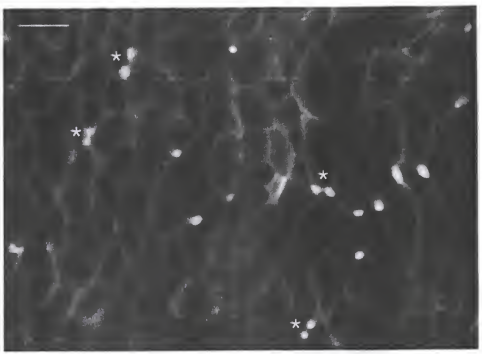

Figure 5-17. Neuronal cells within the AMG display immunoreactivity for our *An. gambiae* AE specific antibody. These neuronal cells also displayed AE mRNA expression (refer to Fig. 5-13A) and are most often seen in pairs (*). Scale bar represents 50 μm.

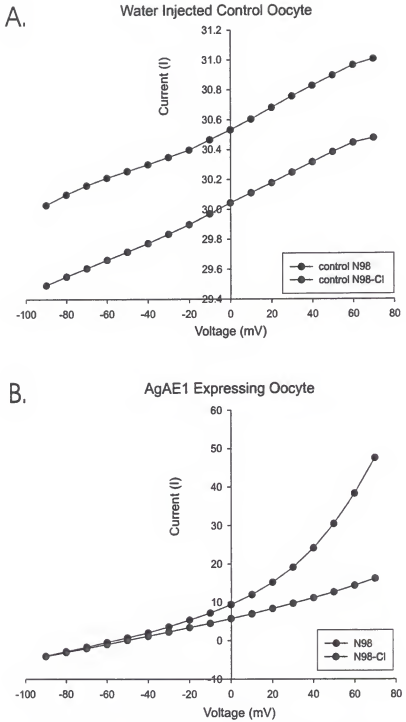

Figure 5-18. Current-voltage (I-V) plots depicting ion transport by the AgAE1 expressing oocytes in contrast to the water injected control oocytes. A. When chloride is removed from the solution bathing the control oocyte and replaced with a nonionic equivalent there is no change in the slope of the curve, signifying no ionic transport. B. When chloride is removed from the media surrounding the AgAE1 expressing oocyte, the ionic transport is eliminated, as seen by the decrease in slope.

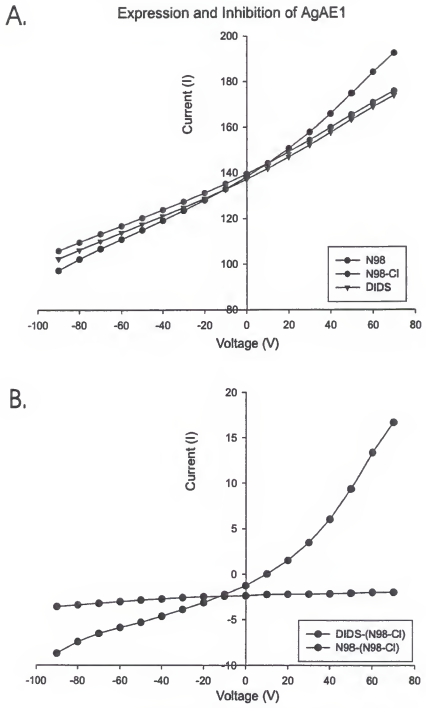

Figure 5-19. Inhibition of AgAE1 mediated chloride transport by DIDS. A. DIDS blocks the transport of chloride by AgAE1. The result is similar to taking chloride out of the bath solution. B. There is almost no difference between blocking chloride transport with DIDS and removing chloride. In contrast, removing chloride from the uninhibited exchanger shows a large difference in chloride transport.

CHAPTER 6
CYTOSOLIC CA EXPRESSION IN LARVAL *ANOPHELES GAMBIAE*

Introduction

Carbonic anhydrase (CA) represents a superfamily of enzymes that reversibly hydrates carbon dioxide to form bicarbonate and a proton. There are three families of CAs (α, β, and γ). Mammals have fourteen different CA isoforms, all belonging to the α CA family. The vast characterizations of the mammalian CAs have revealed cytosolic, membrane-bound, membrane-spanning, and mitochondrial isoforms. Interestingly, it is becoming increasingly apparent with the recent availability of genome sequences, that less complex organisms also contain a large array of CAs. The *Anopheles gambiae* genome contains at least 14 putative CA genes (EnsEMBL protein family ENSF00000000228). Whether the 14 well-characterized mammalian CAs serve the same functions as the 14 mosquito genes is intriguing. This question will remain unanswered until all of the CAs from *An. gambiae* or a similarly distant species are characterized. We can, however, speculate as to their relatedness through sequence identity and conservation.

Carbonic anhydrase is an interesting enzyme to study in the context of the mosquito for several reasons. Unlike most animals, mosquitoes use a highly alkaline digestive strategy instead of an acid environment. Additionally, the functions of the mosquito gut are similar to the mammalian kidney in filtering wastes and maintaining ionic homeostasis. Uncovering the function of CAs in an insect, such as the mosquito,

will lead to evolutionary clues within the family of α CAs. The relationship between the three distinct CA families is believed to represent convergent evolution. The relationship between α CAs from distantly related species is unknown, mostly due to the lack of characterized CAs from non-mammalian species.

We report here the first cytosolic CA that has been cloned and characterized from the *An. gambiae* mosquito, in an attempt to unravel the physiology of an extremely alkaline digestive system. There are at least two different CA isoforms expressed within the larval mosquito gut. One is a GPI-linked CA isoform expressed in a specific subset of muscle and nerve fibers that traverse the anterior midgut and gastric caeca regions (refer to Chapter 4). The other is a cytosolic CA isoform expressed primarily within the gastric caeca and posterior midgut regions.

Results

Anopheles gambiae CA Sequence Analysis

A CA cDNA was cloned from *An. gambiae* gut tissue. The full-length CA cDNA sequence (accession number AY280613) represents 1 of 14 putative CA genes in the *An. gambiae* genome predicted by the Ensembl CA protein family (ENSF00000000228). This CA is comprised of 257 amino acids and is predicted to be a cytosolic isoform (no signal sequence or hydrophobic transmembrane domains; Letunic et al., 2002). The molecular weight is predicted to be 29 kDa (DNAman software). Multiple sites of potential post-translational modification include 5 protein kinase C phosphorylation sites, 4 casein kinase II phosphorylation sites, and 5 N-myristoylation sites (Bairoch et al., 1997). The numerous potential sites for protein modification may contribute to regulatory control.

This CA displays all of the 13 highly conserved residues found in most other active CA proteins, including the three necessary histidine residues required for the binding of a zinc atom (Tashian, 1992; Sly and Hu, 1995; Tamai et al., 1996a). Figure 6-1 shows an alignment of the active sites of *An. gambiae*, *D. melanogaster*, and human CA proteins. The active site region of the cytosolic CA from *An. gambiae* contains one amino acid difference from all of the mammalian isoforms. This particular residue (C-89; *An. gambiae* CA numbering), is replaced by a serine (S) residue in all of the known human CA isoforms (including mouse CA XIII in lieu of the uncharacterized human CA XIII). This C to S amino acid change is also found in 1 of the 14 CA isoforms predicted from the *D. melanogaster* genome (accession number CG11284-PA; Fig. 6-1).

The fourteen CA genes of humans are apparently required to perform the many metabolic functions that complex organisms require. The recent release of the sequenced genomes of two insect species, *An. gambiae* and *D. melanogaster* has revealed that these organisms also have fourteen CAs. Comparisons based on amino acid composition revealed that these 14 dipteran CAs are probably not homologs to each of the fourteen human CAs. A phylogenetic analysis of the CA protein sequences was performed using the Neighbor-Joining method (Saitou and Nei, 1987) as implemented in DNAman software. A rooted tree shows the relationship between the human, mouse, and dipteran CAs (Fig. 6-2). The human and mouse CAs cluster together, and the dipteran CAs cluster together, however the mammalian and the dipteran proteins cluster separately. A bootstrapping test was performed to determine the confidence value of the phylogenetic tree. The *An. gambiae* CA that has the S to C difference within the active site pairs with the *D. melanogaster* CA with the same difference (Fig. 6-2). These two dipteran CAs

appear to be CA homologs. Further studies must be performed to determine whether any differences in the activity or inhibitory profile of these dipteran CA proteins exists due to this active site difference. This conserved amino acid change found in *An. gambiae* and *D. melanogaster,* but not humans, may suggest an evolutionary importance that could be exploited in future mosquito larvacide production. Ongoing efforts aimed at crystallization and x-ray analyses with collaborators at the University of Florida will also reveal the structural identity of this *An. gambiae* cytosolic CA.

Localization of CA Activity in *Anopheles gambiae* Larvae

A modified version of Hansson's CA histochemistry method (Hansson, 1967) was used to localize CA activity within the *An. gambiae* larvae. Precipitated cobalt salts marked the regions of CA activity within the larvae. The regions of CA activity include the cardia, gastric caeca and posterior midgut (Fig. 6-3). A small subset of specific cells within the rectum also stained positively for CA activity (Fig. 6-3E).

Localization of Cytosolic CA mRNA in *Anopheles gambiae* Larvae

A DIG-labeled antisense RNA probe was utilized to localize the CA message. The most intense labeling was consistently viewed within epithelial cells of the gastric caeca and posterior midgut (Fig. 6-4). The localization of cytosolic CA mRNA to the gastric caeca and posterior midgut correlates with the location of CA activity within the *An. gambiae* gut, as determined by CA histochemistry (refer to Fig. 6-3). The cardia was also labeled, as well as a subset of nerve cells and fibers that traverse the AMG longitudinally (Fig. 6-4B,C). Within the posterior midgut, the labeling was confined to the outer edges of a subset of large columnar cells and the small cuboidal cells (Fig.6-5).

Labeling was also seen within the rectum and the last distal cell of the Malpighian tubules (MT; Fig. 6-6).

Antibody Localization of CA Protein

The antigenic peptide sequence QYIRSPDAQTEIDAD was chosen from the *An. gambiae* translated CA cDNA sequence (accession number AAQ21366) to elicit the production of antibody. This peptide was chosen for its antigenic capacity as well as its uniqueness among the 14 putative *An. gambiae* CA genes. The resultant chicken antiserum was used to localize the CA protein within whole mount preparations of fourth instar *An. gambiae* larvae.

Immunoreactivity for the cytosolic CA was predominantly displayed within the gastric caeca (Fig.6-7). The PMG also displayed immunolabeling along the periphery of both the large and small epithelial cells. Immunoreactivity was also evident within a small population of neuronal cells scattered along the midgut, most often seen in pairs (Fig.6-8). The pre-immune antisera displayed no specific immunoreactivity.

Bacterial Expression and Purification of *Anopheles gambiae* Cytosolic CA

The full-length CA cDNA was subcloned into a pET100 directional expression vector (pET100/D-TOPO; Invitrogen) for expression of the recombinant protein with an N-terminal tag containing an Xpress epitope and a polyhistidine (6X His) tag. The 6X His tag was utilized when purifying the CA protein. Antibodies against both the Xpress epitope and the CA peptide recognized a band of the predicted molecular weight (33 kDa) for the recombinant CA protein (Fig. 6-9).

Purified CA fractions were tested for CA activity using ^{18}O isotope exchange experiments (Silverman and Tu, 1986). This technique showed that CA activity was

present within the purified, recombinant CA fractions (data not shown). Activity was partially inhibited by the application of methazolamide, a CA-specific inhibitor (data not shown). These analyses confirmed that this cytosolic CA, cloned from an *An. gambiae* gastric caeca cDNA library, has CA activity and therefore contributes to the CA activity in the gastric caeca and posterior midgut regions, as determined by CA histochemistry.

Discussion

The CA isoform, cloned from the *An. gambiae* midgut, is a predicted cytosolic protein that is expressed in the cardia, gastric caeca and posterior midgut regions. Carbonic anhydrase activity was localized to these same regions through CA histochemistry. The purified recombinant CA was shown to have CA activity through ^{18}O isotope exchange experiments. This CA isoform is therefore responsible, at least in part, for the CA activity displayed within the gastric caeca and posterior midgut regions of the larval mosquito gut.

The one amino acid difference (C instead of S) within the active site of this mosquito CA is not found in any mammalian isoform. The *D. melanogaster* genome however displays an identical (C instead of S) difference in one of its putative CA isoforms. The S residue at this position is present in every mammalian CA and therefore may represent an evolutionary divergence within the α CA family. The phylogenetic analysis of mammalian and dipteran CAs shows a more distant relationship between the Dipteran and mammalian proteins than within the mammalian CA family. The dipteran CA isoforms do not cluster with the mammalian CAs despite common functional characteristics and sequence homology in all known α CAs. Instead, the mosquito CA sequences cluster together, apart from the mammalian CA clusters.

The mammalian anion exchanger (AE1) has been shown to physically bind a cytosolic CA isoform (Sterling et al., 2001a). An AE has been cloned from the *An. gambiae* midgut (refer to chapter 5) and protein expression has been localized to the gastric caeca and posterior midgut regions. This AE also has a putative CA binding site within its intracellular carboxy terminus. The membrane localization of this predicted cytosolic CA may be caused by its interaction with a membrane protein such as an AE. Future experiments will reveal if this cytosolic CA is indeed coupled to an AE within the gastric caeca and posterior midgut regions of the mosquito gut, forming a bicarbonate transport metabolon. The existence of such a metabolon within gut regions flanking the highly alkaline anterior midgut may be the mechanism through which cellular homeostasis is maintained.

```
AAQ21365 CAIV-like    QMHFHWG---------SEHTLDDTRYGLELHLVH
AAQ21366 CAII-like    QLHFHWGIGDGS--GSEHTLEGSTYSMEAHAVH
ENSANGP00000001812    QFHFHAP---------SENLIEGHSYPLEGHLVH
ENSANGP00000018999    QLHFHWGLSALD--GSEHTIDGYRLPLELHVIH
ENSANGP00000029518    QFHCHWGCSDSR--GSEHTVDGESFAGELHLVH
ENSANGP00000011908    EIHVHYGLHDQF--GSEHSVEGYTFPAEARHIQ
ENSANGP00000001574    EIYFHYGTDNNQ--GSEHHIHGYSFPGEIQLYG
ENSANGP00000011013    QLHFHWGDNDTF--GSEDMIDNERFPMELHVVF
ENSANGP00000012957    GLHFHWGDKNNR--GAEHVLNDIRYPLEMHIIH
ENSANGP00000016412    QFHCHWGCSDSR--GSEHTVDGESFAGELHLVH
ENSANGP00000010017    QLHFHWGPDDAV--GSEHLLDGRAHSMEAHLVH
ENSANGP00000014948    QLHFHWGADNGR--GSEHTFDGVAMEAHFVF
ENSANGP00000014919    QFHFHWGVNSTV--GSEHVYDYQRYPMEIHLVF
ENSANGP00000001278    QMHFHWGPNNSE--GSEHRINGERFPLEVHLVF
CG9235-PA Dros        EISFRWSWASSL--GSEHTLDHHHSPLEMQCLH
CG18672-PA Dros       GLHFHWGSYKSR--GSEHLINKRRFDAEIHIVH
CG10899-PA Dros       QLHFHWGSALSK--GSEHCLDGNYYDGEVHIVH
CG11284-PA Dros       QLHFHWSDCDES--GSEHTLEGMKYSMEAHAVH
CG12309-PA Dros       ELRFHWGWCNSE--GSEHTINHRKFPLEMQVMH
CG3940-PA Dros        QIHMHWW---------SEHTINDIRYPLEVHIVH
CG32698-PA Dros       EIHMHYGLHDQF--GSEHSVEGYTFPAEIQFFG
CG6074-PA Dros        GLHFHWGDKNNR--GSEHVINDIRYTMEMHIVH
CG18673-PA Dros       SVHFHWGSREAK--GSEHAINFQRYDVEMHIVH
CG1402-PA Dros        EIYIHYGTENVR--GSEHFIQGYSFPGEIQIYG
CG3669-PA Dros        AFHFHWGSPSSR--GSEHSINQQRFDVEMHIVH
CG6906-PA Dros        QFHFHWGENDTI--GSEDLINNRAYPAELHVVL
CG5379-PA Dros        AVHFHWGSPESK--GSEHLLNGRRFDLEMHIVH
CG7820-PA Dros        QFHCHWGCTDSR--GSEHTVDGVSYSGELHLVH
P00915 CA-I           QFHFHWGSTNEH--GSEHTVDGVKYSAELHVAH
P00918 CA-II          QFHFHWGSLDQQ--GSEHTVDKKKYAAELHVVH
P07451 CA-III         QFHLHWGSSDDH--GSEHTVDGVKYAAELHLVH
P22748 CA-IV          QLHLHWSDLPYK--GSEHSLDGEHFAMEMHIVH
AAB47048 CA-V         QFHFHWGAVNEG--GSEHTVDGHAYPAELHLVH
CAC42429 CA-VI        QMHFHWGGASSEISGSEHTVDGIRHVIEIHIVH
P43166 CA-VII         QFHFHWGKKHDV--GSEHTVDGKSFPSELHLVH
JN0576 CA-VIII        EVRFHWGRENQR--GSEHTVNFKAFPMELHLIH
AAH14950 CA-IX        QLHLHWGAAGRP--GSEHTVEGHRFPAEIHVVH
Q9N585 CA-X           EIRLHFGSEDSQ--GSEHLLNGQAFSGEVQLIH
AAH02662 CA-XI        ELRLLFGARDGA--GSEHQIHHQGFSAEVQLIH
AAB23981 CA-XII       QLHLHWGNPNDPH-GSEHTVSGQHFAAELHIVH
AAK16672 mCA-XIII     QFHLHWGSADDH--GSEHVVDGVRYAAELHVVH
BAA85002 CA-XIV       QLHLHWGQKGSPG-GSEHQINSEATFAELHIVH
                                    *
```

Figure 6-1. Clustal alignment of active sites within *An. gambiae, D. melanogaster,* and human CA proteins. All active α CAs are tethered to a zinc molecule by the coordination with three histidine (H) residues. There are three human CAs which do not possess H residues in this orientation and have been shown to lack CA activity. Within the active site region, some of the *An. gambiae* CAs display novel differences, as compared to the tightly-conserved human CAs. Without exception in the human isoforms, a conserved glutamine (E; marked with *) always follows a serine (S). In contrast, the *An. gambiae* alignment shows a change from the S to a cysteine (C) in one of their 14 putative isoforms. The *An. gambiae* alignment also displays a gap within the active site regions of two of the CAs. One of these sequences (AAQ21365) was cloned and determined to be a GPI-linked CA IV-like isoform that was discussed in a previous chapter. These novel active site differences may be exploited in the formulation of a specific mosquito larvacide. The same active site differences are also displayed within the *D. melanogaster* genome and therefore may also provide clues to the evolutionary mechanism of these proteins.

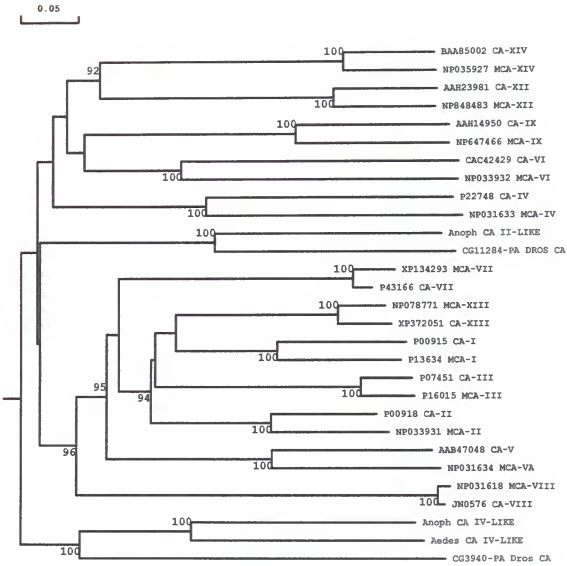

Figure 6-2. Phylogenetic analysis between mammalian (human and mouse) and dipteran (*An. gambiae* and *D. melanogaster)* CAs. This phylogenetic tree was assembled using the Neighbor-Joining method. The tree has been rooted and the bootstrapping confidence values are shown. The mammalian sequences are shown in blue, MCA designates the mouse, while the dipteran sequences are shown in green. The mammalian CAs cluster separately from the dipteran CA clusters, signifying a high divergence between mammalian and dipteran CAs. There is also a high divergence between the dipteran CA II-like sequences and the dipteran CA IV-like sequences.

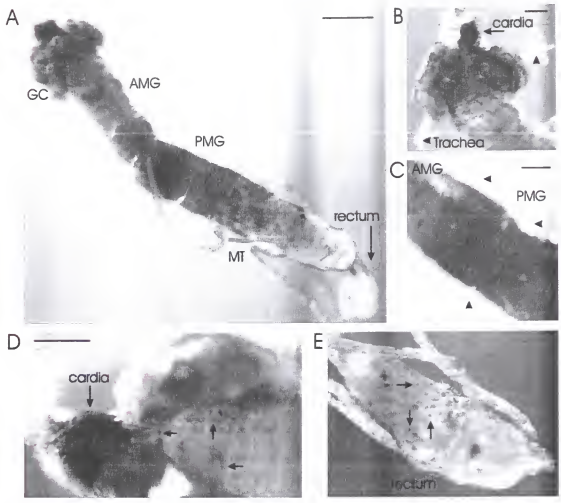

Figure 6-3. Localization of *An. gambiae* CA activity. Using CA histochemistry, CA activity was localized to the cardia, gastric caeca, and posterior midgut regions. A. A whole mount view of the entire gut region. B. A higher magnification view of the gastric caeca and cardia regions that displayed CA activity. Trachea are indicated with arrowheads. C. A higher magnification view of the AMG to PMG boundary. The PMG displayed epithelial CA activity while the AMG does not. The trachea are indicated by arrowheads. D. Specific cells of the cardia along with cells of the AMG (arrows) displayed CA staining. E. Small cells within the rectum also displayed CA activity (arrows). Scale bars represent 300 μm in A, 100 μm in B and C, and 150 μm in D and E.

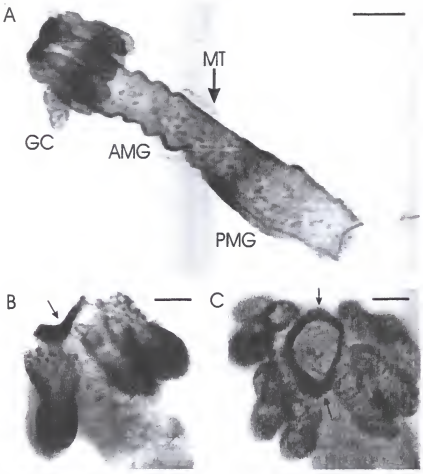

Figure 6-4. Localization of CA mRNA expression within *An. gambiae* whole mounts. A. A view of the entire gut region hybridized with the CA cRNA probe. The most prominent hybridization was found in the gastric caeca and posterior midgut. B. A higher magnification view of the gastric caeca. Both the proximal cells and distal cap cells of the gastric caeca show CA mRNA expression. Rostral to the gastric caeca the cardia region also displayed intense label (arrow). C. Top view of the cardia displays consistent labeling around the circumference of the cardia region (arrows). Scale bars represent 300 μm in A, 75 μm in B and C.

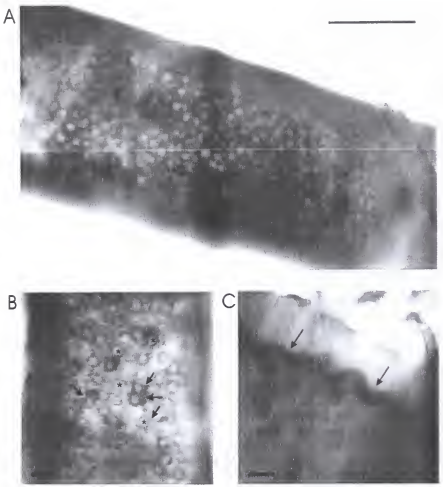

Figure 6-5. Localization of CA mRNA expression within the posterior midgut of *An. gambiae*. A. The PMG displays staining for CA mRNA within the peripheral borders of both the large and small epithelial cells. B. Higher magnification of the PMG shows the stained large columnar cells (*) and the labeled small cuboidal cells (arrows). C. Side view of the PMG reveals CA mRNA expression near the plasma membranes (arrows) and not throughout the cytoplasm. Scale bars represent 150 μm in A, 25 μm in B, and 50 μm in C.

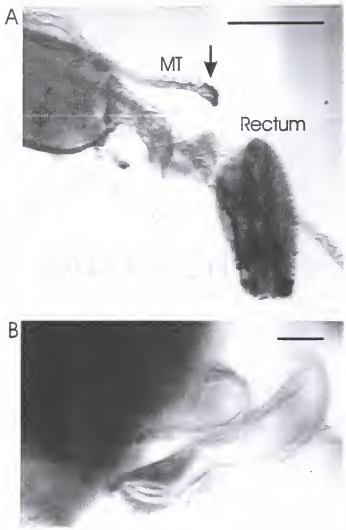

Figure 6-6. Localization of CA mRNA expression within the hindgut. A. The hindgut displays CA label within the Malpighian tubules (MT, arrow) and the rectum. B. Higher magnification of the Malpighian tubules shows staining for CA expression confined to the most distal one or two cells. All other cells of the MT show no hybridization. Scale bars represent 300 μm in A and 25 μm in B.

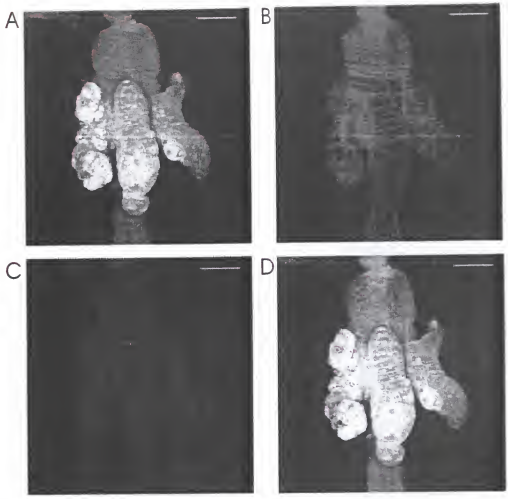

Figure 6-7. Localization of CA protein within gastric caeca of *An. gambiae* larvae. A. The CA specific antibody prominently labels cells of the gastric caeca. B. Phalloidin was used to localize muscle fibers. C. Draq-5 was used to localize nuclear DNA. D. Overlay of the three signals shows the location of CA in relation to muscle fibers and nuclei. Scale bars represent 100 μm.

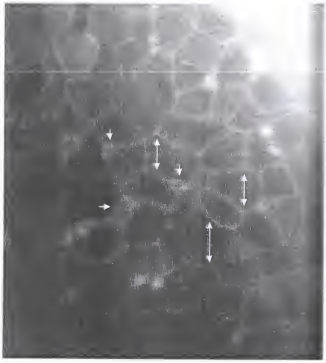

Figure 6-8. Localization of CA protein within the PMG of *An. gambiae*. The CA-specific antibody labels cell membranes of both large (double arrows) and small cells (small arrows), mimicking the protein localization pattern for the AgAE1 protein. Since this particular CA isoform is predicted to be a cytosolic isoform, its localization to cell membranes suggests an interaction with a membrane protein. The AgAE1 protein, known to be a membrane protein, capable of binding CA II, and the localization of the AE1 protein to the same cells supports the hypothesis of a bicarbonate metabolon within the mosquito gut. Scale bar represents 25 μm.

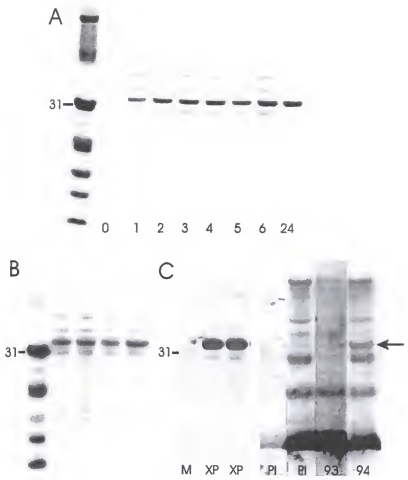

Figure 6-9. Protein gels and western blots of recombinantly expressed CA protein. A. Brilliant blue staining of CA protein induction (33 kDa) from 0 to 24 hours. B. Fast green staining of recombinant CA protein expression (33 kDa). C. The XPRESS (XP) antibody detected a 33 kDa band. Pre-immune sera from two chickens inoculated with a conjugated CA peptide (PI) did not detect a band at 33 kDa. The antisera collected from one of the inoculated chickens, detects a visible protein band at the expected 33 kDa (94; red arrow). The antisera collected from the other chicken (93), does not recognize the 33 kDa protein band on the western blot. The lane containing the molecular weight standard is marked with an M.

CHAPTER 7
CONCLUSIONS AND FUTURE DIRECTIONS

Conclusions

Molecular cloning techniques using isolated mosquito guts from *Aedes aegypti* and *Anopheles gambiae* resulted in the full-length cDNA cloning of three carbonic anhydrase (CA) genes. Our study of CA(s) within the mosquito gut began with a simple understanding that the anterior midgut lumen has a pH of 11. The ability of CA to greatly enhance the production of bicarbonate (and carbonate), a strong buffer, made it a likely candidate for buffering the mosquito gut. Mammalian CA isoforms have been studied extensively throughout the past several decades. However, the relationship between α CAs from mammals, and those of less complex species such as mosquitoes, is unknown. This is partly due to the lack in characterization of multiple CA isoforms from a single non-mammalian species.

Fourteen different α CA isoforms from mammals have been characterized. The *An. gambiae* and *D. melanogaster* genomes also display fourteen CAs. However, a phylogenetic analysis of amino acid sequences has shown that the fourteen mammalian CA isoforms and the fourteen dipteran CA isoforms are not direct homologs. When more CA isoforms are characterized from insects it will be extremely interesting to determine which isoforms are represented or omitted from the insect divergence of CAs.

Before the fourteen CA isoforms in mammals and mosquitoes can be truly compared, every mosquito CA isoform must be characterized to determine their

functional identities. Two different CA isoforms from larval mosquitoes were partially characterized within this study. One GPI-linked CA isoform was found in both *An. gambiae and Ae. aegypti*, and the other cytosolic CA isoform was found in *An. gambiae*. The additional characterization of more mosquito CAs in the future, will present a great opportunity for studying the evolution of CAs within the same α CA family.

A GPI-linked CA isoform, similar to the mammalian CA IV isoform was localized to the gastric caeca and a specific subset of muscle fibers in the anterior midgut region of both *Ae. aegypti* and *An. gambiae*. This isoform is different from the other α CA isoforms (characterized in mammals) in that the entire CA protein is located extracellularly, with only the GPI-link maintaining an association to the plasma membrane. These GPI-linked CA isoforms from two different mosquito species also have a direct homolog in the *D. melanogaster* genome database. These three dipteran CA IV-like isoforms all display a shortened active site region. How this novel active site affects the activity of the CA protein is unknown. However, it is known that mammalian CA IV proteins are oriented by the GPI attachment so that the active site is directed away from the membrane, thereby affording the greatest accessibility of substrate to the active site. The GPI-linked CA of the anterior midgut muscle fibers would be in the prime location and conformation for taking up substrate from the hemolymph.

The other full-length CA cDNA isolated from *An. gambiae* gut tissue is a cytosolic CA isoform. The expression of mRNA was localized to the cardia, gastric caeca and posterior midgut epithelial cells. These regions were also shown to contain an active CA enzyme through CA histochemistry. Recombinant expression of this *An. gambiae* CA protein in bacteria, produced a purified CA-active eluate, as measured by

^{18}O exchange. The activity was shown to be sensitive to the CA-specific inhibitor, methazolamide. This cytosolic CA isoform therefore contributes to the CA activity present within the cardia, gastric caeca and posterior midgut epithelial cells.

A full-length anion exchanger (AE) cDNA was also cloned from the gut tissue of *An. gambiae*. The AEs are a small group within a large bicarbonate transporter (BT) superfamily. Studies of mammalian BTs are ongoing and many new forms are still being discovered and characterized to date. AEs reversibly transport chloride for bicarbonate in a 1:1 electroneutral exchange. Cloning and localizing an AE within the mosquito gut was therefore a direct progression from localizing the CAs, relating the production and transport of bicarbonate within the alkaline gut.

The larval mosquito AE was expressed in *Xenopus* oocytes and was shown to have electrophysiological characteristics of known AEs (i.e. chloride transport and DIDS inhibition). The AE contains an intracellular carboxy terminus that is predicted to moderate ion exchange and an amino terminus that performs ion exchange via the twelve membrane-spanning domains.

The antibodies we produced, specific to carboxy and amino terminal peptides, label the membranes of both gastric caeca and posterior midgut epithelial cells. To maximize ion exchange, the *An. gambiae* AE contains an amino terminus CA binding motif. If indeed the AE binds a cytosolic CA, the gastric caeca and posterior midgut regions would have control over cellular pH, via both intracellular and extracellular means. Since both of these regions contain active cytosolic CA enzyme(s), we propose that the AE spans the membrane in the GC and PMG and binds a cytosolic CA, forming a bicarbonate transport metabolon to transport the bicarbonate that is made by the CA(s).

To further regulate ion exchange, the AE has a particular region of amino acids with similarity to mammalian AEs 2 and 3. This region was found to confer pH sensitivity through intracellular alkalization. The ability of a mosquito AE to detect intracellular alkalization may be the underlying mechanism through which the alkalinity remains confined to the anterior midgut region. The AE- and CA-containing regions (gastric caeca and posterior midgut) flank the anterior midgut and could possibly modulate their transport rates in response to the encroaching or retreating alkaline pH. This bicarbonate metabolon could have the ability to maintain a large pH gradient as is displayed in the larval mosquito gut. Discovering the proteins involved in the production and maintenance of such an alkaline pH could define a fundamental metabolon that is critical for pH homeostasis.

New Model

The cloning and localization of CAs and an AE within the larval mosquito gut has uncovered an unpredicted model of physiology. Our original model, based on *Manduca sexta* (refer to Fig. 1-3), has evolved considerably due to our new findings within larval mosquitoes. The most unexpected finding, was the failure to detect a CA within the anterior midgut. Carbonic anhydrase histochemistry, ^{18}O isotope exchange, *in situ* hybridization, immunohistochemistry, and real time PCR all failed to give evidence for a CA within the AMG region. Although these data did not support our original model of anterior midgut alkalization, our new model describes a system in which CA is not necessary within the AMG epithelial cells. Furthermore, our new data, including the localization of AE within the mosquito gut, has provided insight as to why our new model of AMG alkalization is more efficient in the absence of CA.

Although CA is a reversible enzyme, the mammalian CA IV is even faster than CA II at bicarbonate dehydration. This ability, along with prior studies that have found a very low concentration of bicarbonate in the hemolymph surrounding the mosquito anterior midgut, have led to a prediction of the role of the CA IV-like enzyme in the mosquito midgut. The high alkalinity of the AMG lumen is energized by a H^+ V-ATPase, which pumps protons from the epithelial cells into the hemolymph surrounding the anterior midgut. Only the AMG contains a basally-oriented H^+ V-ATPase, whereas the other regions of the midgut (gastric caeca and PMG) express an apically-oriented H^+ V-ATPase (Zhuang et al., 1999). The CA IV-like enzymes that are suspended in the hemolymph are in the perfect position to provide a sink for these protons. Through the action of the CA IV-like enzyme in the hemolymph, protons are combined with bicarbonate to form carbon dioxide and water. Due to this coordinated effort, the H^+ V-ATPase can keep pumping protons out into the hemolymph without creating a concentration gradient. The CA activity on the hemolymph side of the AMG therefore allows the H^+ V-ATPase to function more efficiently.

In contrast to the benefit that the CA IV-like enzyme provides to the H^+ V-ATPase, the existence of CA within the epithelial cells of the AMG would actually hinder the H^+ V-ATPase. The benefits of not having a CA in the AMG are twofold, due to the reversibility of CA. First, because there is no CA to dehydrate bicarbonate, there is no competition with the H^+ V-ATPase for protons. Secondly but most importantly, because there is no CA to hydrate carbon dioxide to provide protons to the H^+ V-ATPase, the protons must come into the cell from the lumen to replace the protons that are being pumped out to the hemolymph. This need for proton replacement may be the driving

force that pulls the proton from bicarbonate in the lumen to leave a carbonate ion. The proton may enter the cell through a channel or be exchanged for a cation, such as potassium. This carbonate or potassium carbonate could then drive the pH up to the high alkalinity. The absence of an anion exchanger in the AMG would also contribute to the alkalinity in the lumen by not providing a route for bicarbonate to leave the AMG lumen.

The localization of the AE to the basolateral membranes in both gastric caeca and posterior midgut correlates with the localization of a cytosolic CA isoform to the same regions. This AE brings bicarbonate into the cell in exchange for dumping chloride into the hemolymph. This AE could account for the high levels of chloride and low levels of bicarbonate that have been measured in the hemolymph (Boudko et al., 2001a). The bicarbonate that enters the cell provides a substrate for the cytosolic CA. Due to the CA binding motif at the amino terminal of the AE, the binding of these two proteins would form a bicarbonate transport metabolon. This complex would maximize bicarbonate transport due to the elimination of diffusion, normally relied upon to get substrate from one protein to the next.

Our new model reflects the absence of CA within the AMG epithelial cells and instead shows a GPI-linked CA bound to specific muscle fibers traversing the AMG and GC, as well as a cytosolic CA within epithelial cells of the cardia, GC and PMG (Fig. 7-1). The AE is found in regions that express CA and flank the alkaline anterior midgut. Therefore, the cloned AE is shown in the GC and PMG. This AE has the ability to bind a cytosolic CA, whereby the coordinated efforts of producing and transporting bicarbonate are enhanced. The new model reflects a bicarbonate transport metabolon within the gastric caeca and posterior midgut regions.

Future Directions

There are fourteen predicted CA isoforms in *An. gambiae*; however, this dissertation research only dealt with the cloning and characterization of two. Although both were found to have expression in the larval midgut, there may be more that can influence our model. However, if any additional active CAs are localized within the larval mosquito midgut, they most likely will also be localized to the gastric caeca and/or PMG. All of our CA studies failed to show any evidence for a CA in the AMG epithelial cells. An apically expressed CA in the AMG may have avoided the CA histochemical staining but the ^{18}O isotope exchange assay should have uncovered any CA activity present within this gut region.

The hypothesis that a bicarbonate transport metabolon exists within the regions flanking the alkaline anterior midgut needs to be investigated. If indeed the AE is found to bind CA, then the putative CA binding sequence located within the intracellular carboxy terminus needs to be examined. The amino acids necessary for binding should be studied to determine whether the binding motif of mammalian AEs is valid for the binding of mosquito CA(s) to the mosquito AE, as proposed.

The localization of two different CA isoforms and an AE within the larval mosquito gut has established a new model upon which to build. Preceeding this investigation, only a H^+ V-ATPase was localized within the larval mosquito gut. Other channels and transporters need to be identified and localized, such as chloride channels and sodium/ hydrogen exchangers.

The results of these studies may be used to formulate specific mosquito larvacides. Both of the cloned mosquito CA isoforms display novel active site regions.

CA inhibitors can be manufactured to potentially block only CAs containing this novel active site. Although these novel active sites are not found in any mammalian CA, they are also found in other insects such as *D. melanogaster*. A larvacide specific for mosquitoes can still be made due to the incorporation of an alkaline pH trigger. Species that do not have a highly alkaline digestive strategy, such as *D. melanogaster,* will therefore not be exposed to the specific CA inhibitor(s).

The larval mosquito gut provides a simple model for kidney epithelial transport. An important finding was that the mosquito epithelial cells resemble the α and β intercalated cells of the mammalian kidney. The addition of more ion transporters and exchangers to our mosquito model will enable further comparisons between the mosquito gut and the mammalian kidney. Diseases related to anion exchangers and V-ATPases can also be studied using the mosquito gut due to the one cell layer epithelium that allows for easier tracking of ions, as compared to the complex kidney.

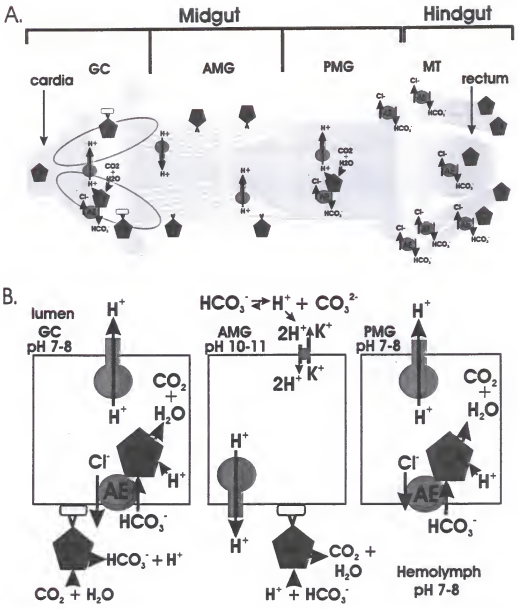

Figure 7-1. New larval mosquito model. A. The larval mosquito gut is divided into the foregut, midgut, and hindgut. The gastric caeca (GC) and anterior midgut (AMG) express a GPI-linked CA isoform on muscle fibers (shown in yellow). The cardia, GC, posterior midgut (PMG), rectum, and last distal cell of Malpighian tubules (MT) express a cytosolic CA isoform. The GC, PMG, MT and rectum express a chloride/ bicarbonate anion exchanger (AE). In the GC, and PMG, the AE may bind a cytosolic CA isoform forming a metabolon. A V-ATPase is expressed in GC, AMG, and PMG. B. Diagram of a representative cell from GC, AMG, and PMG displaying the cell polarity. The V-ATPase is expressed apically in GC and PMG, and basally in AMG. The AE is expressed basally in the GC and PMG. The GPI-linked CA isoform is expressed extracellularly on muscle fibers in the GC and AMG.

REFERENCES

Alper, S. L. (2002). Genetic diseases of acid-base transporters. *Annu. Rev. Physiol.* **64**, 899-923.

Alper, S. L., Chernova, M. N. and Stewart, A. K. (2001). Regulation of Na+-independent Cl-/HCO3- exchangers by pH. *Jop.* **2**, 171-175.

Altschul, S. F., Gish, W., Miller, W., Myers, E. W. and Lipman, D. J. (1990). Basic local alignment search tool. *J. Mol. Biol.* **215**, 403-410.

Baird, T. T., Jr., Waheed, A., Okuyama, T., Sly, W. S. and Fierke, C. A. (1997). Catalysis and inhibition of human carbonic anhydrase IV. *Biochemistry* **36**, 2669-2678.

Bairoch, A., Bucher, P. and Hofmann, K. (1997). The PROSITE database, its status in 1997. *Nucleic Acids Res.* **25**, 217-221.

Berenbaum, M. (1980). Adaptive significance of midgut pH in larval Lepidoptera. *Am. Nat.* 115, 138-146.

Boudko, D. Y., Moroz, L. L., Harvey, W. R. and Linser, P. J. (2001a). Alkalinization by chloride/ bicarbonate pathway. *Proc. Natl. Acad. Sci.* USA **98**, 15354-15359.

Boudko, D. Y., Moroz, L. L., Linser, P. J., Trimarchi, J. R., Smith, P. J. S., Harvey, W. R. (2001b). In situ analysis of pH gradients in mosquito larvae using non-invasive, self-referencing, pH-sensitive microelectrodes. *J. Exp. Biol.* **204**, 691-699.

Brown, D. and Breton, S. (1996). Mitochondria-rich, proton-secreting epithelial cells. *J. Exp. Biol.* **199** (Pt 11), 2345-2358.

Brown, D. and Waneck, G. L. (1992). Glycosyl-phosphatidylinositol-anchored membrane proteins. *J. Am. Soc. Nephrol.* **3**, 895-906.

Chegwidden, W. R. and Carter, N. D. (2000). Introduction to the carbonic anhydrases. *Exs.* 14-28.

Clamp, M., Andrews D., Barker, D., Beven, P., Cameron, G., Chen, Y., Clark, L., Cox, T., Cuff, J., Curwen, V., et al. (2003). Ensembl 2002: accommodating comparative genomics. *Nucleic acids res.* **31** (1), 38-42.

Clark, T. M., Koch, A. and Moffett, D. F. (1999). The anterior and posterior "stomach" regions of larval *Aedes aegypti* midgut: regional specialization of ion transport and stimulation by 5-hydroxytryptamine. *J. Exp. Biol.* **202** (Pt 3), 247-252.

Clements, A. N. (1992). The biology of mosquitoes. Chapman & Hall, London, UK.

Corena, M. P., Seron, T. J., Lehman, H. K., Ochrietor, J. D., Kohn, A., Tu, C. and Linser, P. J. (2002). Carbonic anhydrase in the midgut of larval Aedes aegypti: cloning, localization and inhibition. *J. Exp. Biol.* **205**, 591-602.

Dadd, R. H. (1975). Alkalinity within the midgut of mosquito larvae with alkaline-active digestive enzymes. *J. Insect Physiol.* **21**, 1847-1853.

Darsie, R. F., Jr. and Morris, C. D. (2000). Keys to the adult females and fourth instar larvae of the mosquitoes of Florida (Diptera, Culicidae). Bull. Fla. Mosq. Control Assoc.

Dodgson, S. J. (1991). Why are there carbonic anhydrases in the liver? *Biochem. Cell Biol.* **69**, 761-763.

Donaldson, T. L., and Quinn, J. A. (1974). Kinetic constants determined from membrane transport measurements: carbonic anhydrase activity at high concentrations. *Proc. Natl. Acad. Sci.* USA **71**, 4995-4999.

Dow, J. A. (1984). Extremely high pH in biological systems: a model for carbonate transport. *Am. J. Physiol.* **24**, (4 Pt 2), R633-636.

Eisenhaber, B., Bork, P. and Eisenhaber, F. (1999). Prediction of potential GPI-modification sites in proprotein sequences. *J. Mol. Biol.* **292**, 741-758.

Fernley, R. T. (1988). Non-cytoplasmic carbonic anhydrases. *Trends Biochem. Sci.* **13**, 356-359.

Frohman, M. A. and Zhang, Y. (1997). Using rapid amplification of cDNA ends (RACE) to obtain full-length cDNAs. *Methods Mol. Biol.* **69**, 61-87.

Geer, L. Y., Domrachev, M., Lipman, D. J. and Bryant, S. H. (2002). CDART: protein homology by domain architecture. *Genome Res.* **12**, 1619-1623.

Gubler, D. J. (1997). in: Dengue and dengue hemorrhagic fever. (ed. Gubler, D. J. & Kuno, G.), CAB International, Wallingford, U.K. pp. 1-22.

Gupta, R., Jung, E., and Brunak S. (In preparation 2002) Prediction of N-glycosylation sites in human proteins.

Halstead, S. B. (1997). in: Dengue and dengue hemorrhagic fever. (ed. Gubler, D. J. & Kuno, G.), CAB International, Wallingford, U.K. pp. 23-44.

Hansson, H. P. J. (1967). Histochemical demonstration of carbonic anhydrase activity. *Histochemie* **11**, 112-128.

Harvey, W. R. (1992). Physiology of V-ATPases. *J. Exp. Biol.* **172**, 1-17.

Haskell, J. A., Clemons, R. D. and Harvey, W. R. (1965). Active transport by the Cecropia midgut. I. Inhibitors, stimulants and potassium-transport. *J. Cell. Comp. Physiol.* **65**, 45-56.

Hewett-Emmett, D. (2000). Evolution and distribution of the carbonic anhydrase gene families. *Exs.* **90**, 29-76.

Hewett-Emmett, D. and Tashian, R. E. (1996). Functional diversity, conservation, and convergence in the evolution of the alpha-, beta-, and gamma-carbonic anhydrase gene families. *Mol. Phylogenet. Evol.* **5**, 50-77.

Holt, R. A. Subramanian, G. M. Halpern, A. Sutton, G. G. Charlab, R. Nusskern, D. R. Wincker, P. Clark, A. G. Ribeiro, J. M. Wides, R. et al. (2002). The genome sequence of the malaria mosquito Anopheles gambiae. *Science* **298**, 129-149.

Hogue, C. W. (1997). Cn3D: a new generation of three-dimensional molecular structure viewer. *Trends Biochem. Sci.* **22**, 314-316.

Hubbard, T., Barker, D., Birney, E., Cameron, G., Chen, Y., Clark, L., Cox, T., Cuff, J., Curwen, V., Down, T. et al. (2002). The ensembl genome database project. *Nucleic Acids Res.* **30**, 38-41.

Huber, S., Asan, E., Jons, T., Kerscher, C., Puschel, B. and Drenckhahn, D. (1999). Expression of rat kidney anion exchanger 1 in type A intercalated cells in metabolic acidosis and alkalosis. *Am. J. Physiol.* **277**, F841-849.

Jespersen, T., Grunnet, M., Angelo, K., Klaerke, D. A. & Olesen, S. P. (2002). Dual-function vector for protein expression in both mammaliancells and Xenopus laevis oocytes. *Biotechniques* **32**, 536-538, 540.

Jungreis, A. M., Barron, D. N. and Johnston, J. W. (1981). Comparative properties of tobacco hornworm *Manduca sexta*, carbonic anhydrases. *Am. J. Physiol.* **241**, R92-99.

Kim, J., Kim, Y. H., Cha, J. H., Tisher, C. C., and Madsen, K. M. (1999). Intercalated cell subtypes in collecting tubule and cortical collecting duct of rat and mouse. *J. Amer. Soc. Nephrol.* **10**, 1-12.

Letunic, I., Goodstadt, L., Dickens, N. J., Doerks, T., Schultz, J., Mott, R., Ciccarelli, F., Copley, R. R., Ponting, C. P. and Bork, P. (2002). Recent improvements to the SMART domain-based sequence annotation resource. *Nucleic Acids Res.* **30**, 242-4.

Lindskog, S. (1997). Structure and mechanism of carbonic anhydrase. *Pharmacol. Ther.* **74**, 1-20.

Marchler-Bauer, A., Panchenko, A. R., Shoemaker, B. A., Thiessen, P. A., Geer, L. Y. and Bryant, S. H. (2002). CDD: a database of conserved domain alignments with links to domain three-dimensional structure. *Nucleic Acids Res.* **30**, 281-283.

Martin, M. M., Martin, J. S., Kukor, J. J. and Merrit, R. W. (1980). The digestion of protein and carbohydrate by the stream detritivore, *Tipula abdominalis* (Diptera, Tipulidae). *Oecologia* **46**, 360-364.

Matsumoto, T., Winkler, C. A., Brion, L. P. and Schwartz, G. J. (1994). Expression of acid-base-related proteins in mesonephric kidney of the rabbit. *Am. J. Physiol.* **267**, F987-997.

Matz, M., Shagin, D., Bogdanova, E., Britanova, O., Lukyanov, S., Diatchenko, L. and Chenchik, A. (1999). Amplification of cDNA ends based on template-switching effect and step-out PCR. *Nucleic Acids Res.* **27**, 1558-1560.

Meldrum, N. U. and Roughton, F. J. W. (1933). Carbonic anhydrase: Its preparation and properties. *J. Physiol.* London **80**, 113-142.

Osborne, W. R. A. and Tashian, R. E. (1975). An improved method for the purification of carbonic anhydrase isozymes by affinity chromatography. *Anal. Biochem.* **64**, 297-303.

Parkkila, S., Rajaniemi, H., Parkkila, A. K., Kivela, J., Waheed, A., Pastorekova, S., Pastorek, J. and Sly, W. S. (2000). Carbonic anhydrase inhibitor suppresses invasion of renal cancer cells in vitro. *Proc. Natl. Acad. Sci.* USA **97**, 2220-2224.

Phillips, K. P. and Baltz, J. M. (1999). Intracellular pH regulation by HCO3-/Cl- exchange is activated during early mouse zygote development. *Dev. Biol.* **208**, 392-405.

Ridgway, R. L. and Moffett, D. F. (1986). Regional differences in the histochemical localization of carbonic anhydrase in the midgut of tobacco hornworm (Manduca sexta). *J. Exp. Zool.* **237**, 407-412.

Rockstein, M. (1964). The physiology of insecta. (ed. Rockstein, M.), Academic Press, New York, NY. pp. 380-387.

Romero, M. F., Henry, D., Nelson, S., Harte, P. J., Dillon, A. K. and Sciortino, C. M. (2000). Cloning and characterization of a Na+-driven anion exchanger (NDAE1). A new bicarbonate transporter. *J. Biol. Chem.* **275**, 24552-24559.

Saitou, N. and Nei, M. (1987). The neighbor-joining method: a new method for reconstructing phylogenetic trees. *Mol. Biol. Evol.* **4**, 406-25.

Schwartz, G. J. (2002). Physiology and molecular biology of renal carbonic anhydrase. *J. Nephrol.* **15** Suppl 5, S61-74.

Shahabuddin, M. and Pimenta, P. F. (1998). Plasmodium gallinaceum preferentially invades vesicular ATPase-expressing cells in Aedes aegypti midgut. *Proc. Natl. Acad. Sci.* USA **95**, 3385-3389.

Silverman, D. N. and Tu, C. K. (1986). Molecular basis of the oxygen exchange from CO2 catalyzed by carbonic anhydrase III from bovine skeletal muscle. *Biochemistry* **25**, 8402-8408.

Sly, W. S. (2000). The membrane carbonic anhydrases: from CO2 transport to tumor markers. *Exs.* 95-104.

Sly, W. S. and Hu, P. Y. (1995). Human carbonic anhydrases and carbonic anhydrase deficiencies. *Annu. Rev. Biochem.* **64**, 375-401.

Spielman, A. and D'Antonio, M. (2001). Mosquito: A natural history of our most persistent and deadly foe. Hyperion Press, New York, NY.

Sterling, D., Alvarez, B. V. and Casey, J. R. (2002a). The extracellular component of a transport metabolon. Extracellular loop 4 of the human AE1 Cl-/HCO3- exchanger binds carbonic anhydrase IV. *J. Biol. Chem.* **277**, 25239-25246.

Sterling, D., Brown, N. J., Supuran, C. T. and Casey, J. R. (2002b). The functional and physical relationship between the DRA bicarbonate transporter and carbonic anhydrase II. *Am. J. Physiol. Cell Physiol.* **283**, C1522-1529.

Sterling, D. and Casey, J. R. (2002). Bicarbonate transport proteins. *Biochem. Cell Biol.* **80**, 483-97.

Sterling, D., Reithmeier, R. A. and Casey, J. R. (2001a). A transport metabolon. Functional interaction of carbonic anhydrase II and chloride/bicarbonate exchangers. *J. Biol. Chem.* **276**, 47886-47894.

Sterling, D., Reithmeier, R. A. and Casey, J. R. (2001b). Carbonic anhydrase: in the driver's seat for bicarbonate transport. *Jop.* **2**, 165-170.

Stobbart, R. H. (1971). Evidence of Na^+/H^+ and Cl^-/HCO_3^- exchanges during independent sodium and chloride uptake by the larvae of the mosquito *Aedes aegypti*. *J. Exp. Biol.* **54**,19-27.

Sun, M. K. and Alkon, D. L. (2002). Carbonic anhydrase gating of attention: memory therapy and enhancement. *Trends Pharmacol. Sci.* **23**, 83-89.

Tamai, S., Cody, L. B. and Sly, W. S. (1996a). Molecular cloning of the mouse gene coding for carbonic anhydrase IV. *Biochem. Genet.* **34**, 31-43.

Tamai, S., Waheed, A., Cody, L. B. and Sly, W. S. (1996b). Gly-63-->Gln substitution adjacent to His-64 in rodent carbonic anhydrase IVs largely explains their reduced activity. *Proc. Natl. Acad. Sci.* USA **93**, 13647-13652.

Tashian, R. E. (1969). in: Biochemical methods in red cell genetics. (ed. Yunis, J. J.), Academic Press, New York, NY. pp. 307-336.

Tashian, R. E. (1992). Genetics of the mammalian carbonic anhydrases. *Adv. Genet.* **30**, 321-356.

Tashian, R. E., Hewett-Emmett, D., Carter, N. and Bergenhem, N. C. (2000). Carbonic anhydrase (CA)-related proteins (CA-RPs), and transmembrane proteins with CA or CA-RP domains. *Exs.* 105-120.

Thompson, J. D., Higgins, D. G. and Gibson, T. J. (1994). CLUSTAL W: Improving the sensitivity of progressive multiple sequence alignment through sequence weighting, position-specific gap penalties and weight matrix choice. *Nucleic Acids Res.* **22**, 4673-4680.

Tong, C. K., Brion, L. P., Suarez, C. and Chesler, M. (2000). Interstitial carbonic anhydrase (CA) activity in brain is attributable to membrane-bound CA type IV. *J. Neurosci.* **20**, 8247-8253.

Turbeck, O. B. and Foder, B. (1970). Studies on a carbonic anhydrase from the midgut epithelium of larvae of lepidoptera. *Biochim. Biophys. Acta.* **212**, 139-149.

Tusnady, G. E. and Simon, I. (1998). Principles governing amino acid composition of integral membrane proteins: application to topology prediction. *J. Mol. Biol.* **283**, 489-506.

Tusnady, G. E. and Simon, I. (2001). The HMMTOP transmembrane topology prediction server. *Bioinformatics* **17**, 849-50.

Vince, J. W. and Reithmeier, R. A. (2000). Identification of the carbonic anhydrase II binding site in the Cl(-)/HCO(3)(-) anion exchanger AE1. *Biochemistry* **39**, 5527-5533.

Vince, J. W., Carlsson, U. and Reithmeier, R. A. (2000). Localization of the Cl-/HCO3- anion exchanger binding site to the amino-terminal region of carbonic anhydrase II. *Biochemistry* **39**, 13344-13349.

Volkmann, A. and Peters, W. (1989a). Investigations on the midgut caeca of mosquito larvae I. Fine structure. *Tissue & Cell* **21**, 243-251.

Volkmann, A. and Peters, W. (1989b). Investigations on the midgut caeca of mosquito larvae II. Functional aspects. *Tissue & Cell* **21**, 253-261.

Waheed, A., Okuyama, T., Heyduk, T. and Sly, W. S. (1996). Carbonic anhydrase IV: purification of a secretory form of the recombinant human enzyme and identification of the positions and importance of its disulfide bonds. *Arch. Biochem. Biophys.* **333**, 432-438.

Westerfield, M. (1994). The zebrafish book: A guide for the laboratory use of zebrafish (*Brachydanio rerio*). (ed. Westerfield, M.), University of Oregon Press, Eugene, OR. pp. 9.16-9.21.

Wieczorek, H., Gruber, G., Harvey, W.R., Huss, M. and Merzendorfer, H. (1999). The plasma membrane H^+-V-ATPase from tobacco hornworm midgut. *J. Bioenerg. Biomembr.* **31**, 67-74.

Wieczorek, H., Gruber, G., Harvey, W. R., Huss, M., Merzendorfer, H. and Zeiske, W. (2000). Structure and regulation of insect plasma membrane H(+)V-ATPase. *J. Exp. Biol.* **203** (Pt 1), 127-135.

Zhang, Y. and Frohman, M. A. (1997). Using rapid amplification of cDNA ends (RACE) to obtain full-length cDNAs. *Methods Mol. Biol.* **69**, 61-87.

Zhuang, Z., Linser, P. J. and Harvey, W. R. (1999). Antibody to H(+) V-ATPase subunit E colocalizes with portasomes in alkaline larval midgut of a freshwater mosquito (Aedes aegypti). *J. Exp. Biol.* **202** (Pt 18), 2449-2460.

BIOGRAPHICAL SKETCH

Theresa J. Seron was born and raised in Connecticut with her older sister and younger brother. She enjoyed the outdoors and wildlife from a very young age and continues to pursue activities such as scuba diving and kayaking. She received her Bachelor of Science degree from the University of Connecticut in 1995. She then ventured off to Saint Thomas in the U.S. Virgin Islands, where she lived for twelve months to satisfy her enthusiasm for traveling and diving. Upon returning to the United States, she was employed by Boehringer-Ingelheim Pharmaceuticals in Danbury, Connecticut, where she was introduced to the world of scientific research and discovery. This path was strengthened by a relocation to Miami, Florida, and a second research position at Noven Pharmaceuticals. In 1997, she moved to Gainesville, Florida, to pursue an advanced degree at the University of Florida. She became acquainted with The Whitney Laboratory in Saint Augustine, Florida, when she was chosen to participate in a summer research program. The following fall she was admitted to the University of Florida graduate school in the Department of Fisheries and Aquatic Sciences. Here she was able to combine her research background with her enthusiasm for aquatic animals. Her research project was carried out at The Whitney Laboratory under the direction of Dr. Paul Linser. The project focused on the enzyme carbonic anhydrase and its unknown role in larval mosquito physiology. Upon completion of her doctorate degree she plans to continue scientific research within the aquatic realm.

I certify that I have read this study and that in my opinion it conforms to acceptable standards of scholarly presentation and is fully adequate, in scope and quality, as a dissertation for the degree of Doctor of Philosophy.

Edward J. Phlips, Chair
Professor of Fisheries and Aquatic Sciences

I certify that I have read this study and that in my opinion it conforms to acceptable standards of scholarly presentation and is fully adequate, in scope and quality, as a dissertation for the degree of Doctor of Philosophy.

Paul J. Linser, Cochair
Professor of Anatomy and Cell Biology

I certify that I have read this study and that in my opinion it conforms to acceptable standards of scholarly presentation and is fully adequate, in scope and quality, as a dissertation for the degree of Doctor of Philosophy.

Leonid L. Moroz
Assistant Professor of Neuroscience

I certify that I have read this study and that in my opinion it conforms to acceptable standards of scholarly presentation and is fully adequate, in scope and quality, as a dissertation for the degree of Doctor of Philosophy.

Shirley M. Baker
Assistant Professor of Fisheries and Aquatic Sciences

I certify that I have read this study and that in my opinion it conforms to acceptable standards of scholarly presentation and is fully adequate, in scope and quality, as a dissertation for the degree of Doctor of Philosophy.

Robert M. Greenberg
Associate Professor of Neuroscience

This dissertation was submitted to the Graduate Faculty of the College of Agricultural and Life Sciences and to the Graduate School and was accepted as partial fulfillment of the requirements for the degree of Doctor of Philosophy.

May 2004

Dean, College of Agricultural and Life Sciences

Dean, Graduate School